DESIGN AND CONSTRUCTION OF A GUARDED HOT BOX FACILITY FOR EVALUATING THE THERMAL PERFORMANCE OF BUILDING WALL MATERIALS

A Thesis

by

CLAIRE RENEE MERO

Submitted to the Office of Graduate Studies of
Texas A&M University
in partial fulfillment of the requirements for the degree of

MASTER OF SCIENCE

May 2012

Major Subject: Mechanical Engineering

DESIGN AND CONSTRUCTION OF A GUARDED HOT BOX FACILITY FOR EVALUATING THE THERMAL PERFORMANCE OF BUILDING WALL MATERIALS

A Thesis

by

CLAIRE RENEE MERO

Submitted to the Office of Graduate Studies of
Texas A&M University
in partial fulfillment of the requirements for the degree of

MASTER OF SCIENCE

Approved by:

Chair of Committee,	Michael Pate
Committee Members,	Bryan Rasmussen
	Pavel Tsvetkov
Head of Department,	Jerry Caton

May 2012

Major Subject: Mechanical Engineering

ABSTRACT

Design and Construction of a Guarded Hot Box Facility for Evaluating the Thermal Performance of Building Wall Materials. (May 2012)

Claire Renee Mero, B.S., Texas A&M University

Chair of Committee: Dr. Michael Pate

The focus of this study was to design and build a guarded hot box to test the R-Value of building materials. The Riverside Energy Efficiency Laboratory is looking to expand their testing capabilities by including this service. Eventually, the laboratory will become energy star certified.

A guarded hot box facility consists of two boxes maintained at specific temperatures and a guard box around each one that is maintained at the same temperature as the box it surrounds. The ASTM C1363 standard was used as guide for the construction and testing of sample specimen. This standard called for an air velocity profile uniform within 10% of the average. Velocity tests were performed with various different configurations to give a uniform velocity. Although the velocity did not meet standards, the configuration chosen included a piece of ¼" pegboard placed 2" away from the top and the bottom of the inner box.

By using the known overall heat added and removed from the system, as well as all the heat losses the heat transferred through the specimen and its R-Value can be calculated. The uncertainty of the R-Value and the accuracy of the testing facility gave conflicting results. Future experiments will use improved testing methods that include differential thermocouples to obtain better uncertainty for the R-Value calculations.

ACKNOWLEDGEMENTS

I would like to thank my committee chair, Dr. Pate, and my committee members, Dr. Rasmussen, and Dr. Tsvetkov for their combined time and guidance throughout my graduate career.

I would like to thank Josh Kading, Kathy Wadle, and James Sweeney for their guidance in the design, time managements, budget management, and electrical expertise. Thanks also to Matthew Daugherty for writing all necessary LabVIEW programs as well as aiding in thermocouple calibrations, test runs, as well as ductwork and heater construction. Thanks to Jennifer Rees, Grant Wheeler, Sean Eliston, Angel Morales, and Solomon for their aid in constructing wooden structures, running tests, setting up the testing facility, and their knowledge in calibration and sensors.

I would also like to thank Orcun Inam and Hongjin Wang for theoretical modeling of air flow patterns in Fluent, and Texas A&M Riverside Architecture for constructing the wooden frame and cutting the insulation board for the frame for the guarded hot box.

NOMENCLATURE

Symbol/ Name	Definition
Hot Box, Hot Side, or Heat Source	Refers to the side of the testing apparatus that is only heated
Cold Box, Cold Sink, or Heat Sink	Refers to the side of the testing apparatus that is chilled and has a heater for finite temeprature control
B	The bias is 1/2 the smallest increment on the device, or half of the accuracy if an accuracy is given. If the device is calibrated the bias also includes the difference between the measurement the device reads and the standard
$\mathbf{P_x}$	The precision limit is the standard deviation mulitplied by the ζ. Z depends on the confidence interval and the number of samples recorded. This can be found in Z-table. X is the measurement, such as temperature, or pressure in this paper.
$\mathbf{T_i}$	T stands for temperature. The index i refers to ith location of a set.
$\mathbf{P_i}$	This P stands for pressure. The index i refers to ith location of a set.
ρ	This is the symbol for density. In this paper I used density as a function of temperature based on three temperatures and densities from a standard gas table.
U	U is uncertainty. Therefore if there is a subscript on U, it is the uncertainty of that variable/symbol.
V	V is Velocity
ṁ	ṁ is the mass flowrate of air through the ductwork at a given location.
D	D is the diameter of the ductwork
π	π is approximatley 3.14. It is the ratio of the circumference to the diameter
Q	Q is heat transfer. The subscript refers to where the heat transfer is occuring.
$\mathbf{Q_{wall,i}}$	There are 5 walls per the hot and cold side where heat transfer is occuing: the back, near side, far side, top, and bottom.

Symbol/ Name	Definition
A	A is the area
R	R is R-Value, which is defined as the thermal conductivity divided by the thickness.
$Q_{fl,frame}$	This is the flanking loss through the frame. It is heat transfer from the heat source to the heat sink through the frame surrounding the specimen to the cold side.
T_{inner}	Refers to the wall temperature on the side facing the inner box nearest the specimen.
T_{outer}	Refers to the wall temperature on the side facing the outer box furthest away from the specimen.
$T_{H, avg}$	The average temperature of the hot surface temperature of the specimen
$T_{C,avg}$	The average temperature of the cold surface temperature of the specimen
$T_{spec, avg}$	The average of $T_{H,avg}$ and $T_{C,avg}$
T_{room}	The room temperature
$Q_{fl, air}$	The flanking loss to the air. This is the heat transferred from the sides of the specimen through the frame surrounding the specimen outward to the air.
k	Thermal conductivity
n	# of frames needed to surrround the inner and outer boxes.
Cp	Cp is the specific heat of the air.
Q_{duct}	This is the heat transfer added or removed between the exit and the entrance of the inner box through the ductwork.
T_{inlet}	The temperature of the inlet to the inner box in the ductwork
T_{exit}	The temperature of the exit to the inner box in the ductwork.
$Q_{hot, specimen}$	The heat transfer that must be occuring through the specimen by summing all heat transfers on the hot side of the testing apparatus.
$Q_{cold, specimen}$	The heat transfer that must be occuring through the specimen by summing all heat transfers on the cold side of the testing apparatus.

TABLE OF CONTENTS

CHAPTER Page

Page

LIST OF FIGURES

FIGURE Page

FIGURE Page

FIGURE Page

FIGURE Page

LIST OF TABLES

TABLE Page

TABLE Page

TABLE Page

TABLE Page

TABLE Page

CHAPTER I
INTRODUCTION

Background

Most houses in the United States have some form of air conditioning for heating or cooling. In order to minimize the amount of conditioning that is needed, insulation is used to prevent heat from transferring into or out of houses. Insulation is used even in areas of moderate climates to allow for more accurate temperature control

There are three main forms of heat transfer that can either warm or cool a house; conductive, convective, and radiation. Conductive heat transfer is the easiest to reduce. Simply adding an air gap prevents conductive heat transfer, however, if the air gaps are too large, and then air movement within the gap will increases the heat transfer due to convection. Convective heat transfer refers to how the movement of air helps increase the heat transfer into a surface. A vacuum is the perfect insulation for these two types of heat transfer. [1] In real life, in order to break up the air movement, the best insulations are materials that trap many little pockets of air, with smaller air pockets working better.

The third type of heat transfer is due to radiation, which is electromagnetic wave energy and has the largest temperature differences. During winter nights, the atmospheric temperature can be well below freezing even when the ambient temperature is above freezing, this effect is what causes ice to appear on cars even when the outside air temperature is not below freezing. This type of heat transfer will occur even in a vacuum. Low emissivity materials will prevent this form of heat transfer by reflecting most the electromagnetic waves, preventing them from being absorbed and heating the house.

Housing codes have standards for the minimum allowable R-Value, or the resistance to heat transfer, which is how well the insulation works. The minimum standard only refers to conductive and convective heat transfer, but the International Energy Conversation Code, or EICC, continues to increase the strictness of the standards [2]. Some housing builders will include insulation with higher R-values, or even a radiant

---

This thesis follows the style of ASHRAE Journal.

barrier as a benefit because it will decrease the amount of air conditioning needed and consequently the cost of maintaining comfortable conditions. In areas with extreme temperatures, such as Arizona, where the summers are over 100°F and the winters are below freezing, it is common for the buildings to also use low emissivity materials to prevent radiation heat transfer.

A more recent trend in housing insulation is "superinsulated." A 2,000sq.ft. home retrofitted to be a superinsulated home in a case study presented by Appelfeld & Svendsen saved a little over $2,000/year in gas and electricity. A superinsulation home is one that uses multiple types of insulation to reduce heat transfer in the home to nearly nothing and completely seals any air leaks.

Sealing all air leaks makes it more difficult to meet minimum fresh air requirements per room, which means that in order to meet these requirements the intake air must be increased. More intake air means that more air must be conditioned, which can be costly. In addition to conditioning costs, older homes that are being retrofitted must incur costly renovations to increase the intake ducts. [3]

In order to accomplish the required insulation through exterior walls, an R-value of 36°F-ft^2-hr/BTU, they must either be thick, use insulation on the exterior of the house, or block thermal bridging. [4] Thermal bridging is defined as a path for heat transfer with less thermal resistance than areas surrounding it. The most noticeable example of thermal bridging is typically around windows, where the insulation may not be flush to the edge of the frame or at a metal window frame. Although not as significant as metal window frames, studs in walls are also thermal bridges, since the thermal resistance of wood is much less than the insulation surrounding them. [5]

In order to block thermal bridging, either exterior insulation or Aerogel stud strips can be used. [4]. Most exterior insulation works well if sealed properly, but the seal commonly leaks around doors and windows, where the sealant is rarely installed properly. Water can destroy the insulation and if not planned for, it will sit against the wall and deteriorate the wall components. [6]

Aerogel is a silica based nano-scale structure originally developed by NASA and used on the Mars Rover that is 98% air [7], [8]. Until recently aerogel has been far too expensive to even consider using in homes, however recent innovations have made it possible to sell it for nearly $4-6/sq. ft. [9], [10]. This product is still too costly for the average home buyer, and ripping out walls to install it is even more costly.

The client developed a low emissivity paint to combat radiation heat transfer called the Durable Finish Coat, or DFC. Although the DFC excels at reflecting light, the client acknowledges that a low emissivity outer coating will not completely insulate a building and there are still two forms of heat transfer that are not combated with this paint. The client developed a derivation of this paint in hopes that it would have a low thermal conductivity and be a cheap aid to the standard home insulation.

The client is looking for an inexpensive method of improving the R-Value of a given wall segment by reducing the thermal bridging, not to superinsulation standards, but as a way for home builders to save consumers money inexpensively. The client developed a paint with a low thermal conductivity intended to aid standard insulation in preventing the transfer of heat. The idea is that painting the inside of a building before the insulation and drywall are installed on a house will increase the R-value of the wall. If the paint does increase the R-value, then it can be used in collaboration with the standard insulation and cost less than the higher quality insulations, such as the foam board insulations and aerogel. The client has contracted the Riverside Energy Efficiency Laboratory to test the R-value of the paint, and comparatively test the paint in collaboration with base standard insulations against other methods of insulation, and study the effects of thermal bridging to determine the effect the paint has on heat transfer and thermal bridging.

Project Scope

In order to perform the tests, a guarded hot box will be used. Originally, a guarded hot plate apparatus was considered because it offers better temperature control, no convection analysis, and more accurate results, [11] however, this method is not

applicable to non-homogeneous materials per standards [12]. A guarded hot box is a method of determining the amount of heat transfer through a given material by controlling the temperature on both sides of the material and minimizing the extraneous heat transfers other than those through the given material. Knowing the total amount of heat transfer through the material and the temperature of each surface of the material, the R-value can be determined.

There are three main standards that can be used to analyze the data from a guarded hot box. Although the Russian Standard GOST 26602.1-99 is the most accurate method of measuring the U-value of non-homogeneous materials, ASTM 1363-05 standards were attempted because they require less analysis of each individual component of each specimen and a simple calibration of the hot box as an overall system to be performed once. These requirements make the ASTM standards more suitable for a wide range of non-homogenous samples. EN ISO 8990 is similar in methodology to the ASTM standards [13]. The ASTM standard has been used in various research papers and was selected due to its practicality.

Hot Box Principle

In order to test thermal bridging a hot box must be used to measure the R-vale for non-homogeneous materials. The hot box consists of two boxes each with an open side facing the other. The material to be tested or specimen is located between the two open faces. One box is the heat sink and the other the heat source. Since each specimen is supposed to represent a segment of wall, the heat source and the heat sink are used to simulate a house in an average summer or winter climate when insulation is most needed.

In order to calculate the R-value, the heat transfer through the specimen needs to known. To minimize any extraneous heat loss through the walls of the boxes, the walls need to be insulated. To further minimize the heat loss through the walls, the temperature difference across the walls is minimized by surrounding each box with a larger guard box. The guard box is maintained at the same temperature as the box inside

it. To approximate the heat loss or gain through the walls, the surface temperatures of the walls need to be measured.

The temperature needs to be conditioned and controlled. The only requirements are that the temperature and air velocity within the box remain uniform and steady. ASTM standards define uniform as being within 2K, or 2%, whichever is larger for the temperature and within 10% for the air velocity.

A temperature controller is used at the entrance of the inner box to ensure the entering air is controlled properly. Calibrated thermocouples are used to monitor the surface temperature on each side of the specimen. Additional thermocouples are used to measure the air surrounding both sides of the specimen to ensure temperature uniformity. The following diagram, Figure 1, shows a general schematic and location of the inner and outer boxes of the heat sink and the heat source, the air conditioning systems, and the location of the RTD used by the controller.

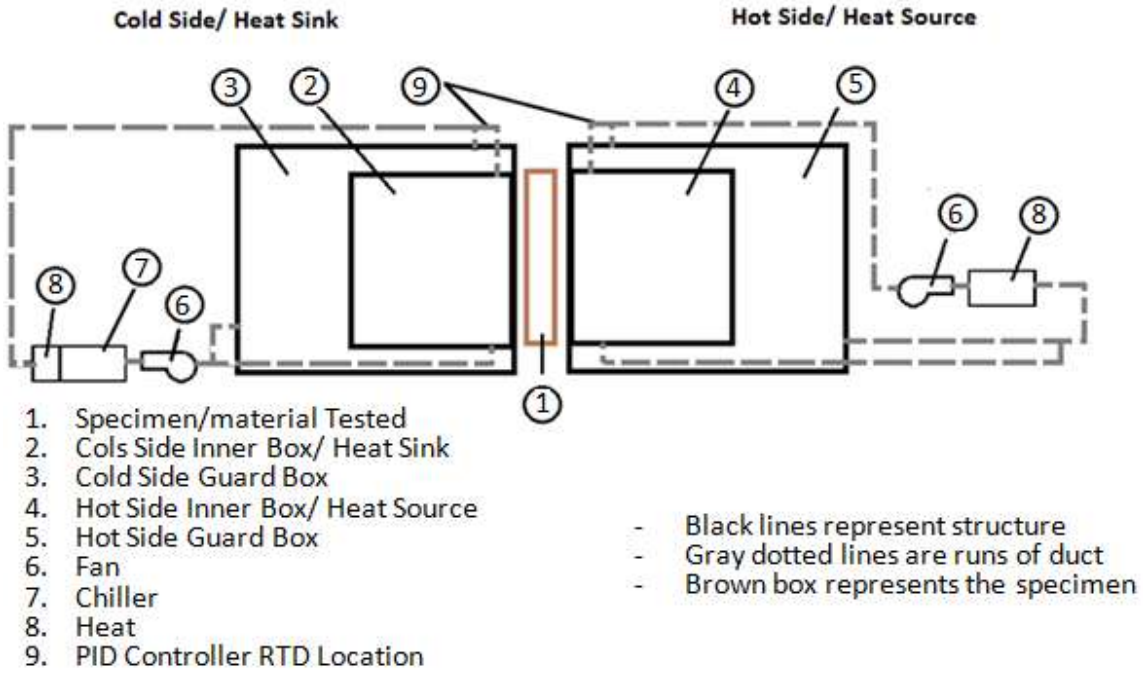

Figure 1. General hotbox schematic including ductwork, air conditioning systems, and the RTD location read by the controller

Testing

In order to evaluate the validity of the testing facility and the effectiveness of the paint, a 2ft by 4ft section of each of the following samples will be tested:

- ¾" Uncoated Oriented Strand Board (OSB)
- ¾" Paint Coated OSB
- ¾" Solar Board Coated OSB
- Uncoated Standard Wall Segment with R-13
- Paint Coated Standard Wall Segment with R-13
- Paint Coated Standard Wall Segment with R-13, where the studs are not painted
- Uncoated 2x6 Wall Segment with R-13
- Uncoated Standard Wall Segment with Spray Foam
- Paint Coated Standard Wall Segments with Spray Foam

Since OSB is not homogeneous, in order to ensure the accuracy of the R-value of the paint, two specimens of the first two samples will be tested. Testing two of the same material will also provide a validity check because the R-Values should be similar. A Standard Wall Segment is a piece of OSB with 3 equidistant 2x4 studs screwed to it, insulation in between, and a piece of $^{3}/_{8}$" drywall nailed to the other side of the 2x4's. The R-Value of these samples should be greater than the R-Value of the OSB.

CHAPTER II

TEST FACILITY

Hot Box Construction Details

For the construction of the hot box, two identical frames were created from 2x4s for the inner boxes of both the heat sink and heat source. The top and bottom of the frame are made from ¾" plywood resulting in a structure that is 48 ½" tall, 62" long, and 21" deep. The frames are lined with RMAX Thermasheath-3 1½" polyisocyanurate for the walls. Figure 2 shows the construction details of the inner box.

Holes in the top and bottom of each box allow for air to enter the inner box. 4x4 lumber was used to elevate the inner box and another sheet of ¾" plywood was used to distribute the weight of the inner box, so that holes were not punctured in the insulation board of the outer box. Figure 3 shows the top and bottom views of the inner box to show the locations of the holes for air to enter and exit.

The heat source and heat sink outer boxes are also identical to one another and constructed similarly to the inner boxes, but more than 6" larger in every direction. This structure is 66 ¼" tall, 68" long, and 30" deep. Again, identical holes were cut on both the heat sink and the heat source outer box to allow air to enter and exit the outer and inner boxes. Figure 4 shows the construction details of the outer box.

Once each box was constructed the inner box for both the heat sink and the heat source was placed inside of the outer box for each side. They were positioned such that the fronts of both the inner and outer box were aligned. Since the inlets and exits are shaped differently on the inner box than the corresponding inlet or exit on the outer box, unusually shaped ductwork needed to be created to connect them without allowing air to mix. Figure 5 and Figure 6 show the construction details of the bottom and top ductwork created to connect the two boxes.

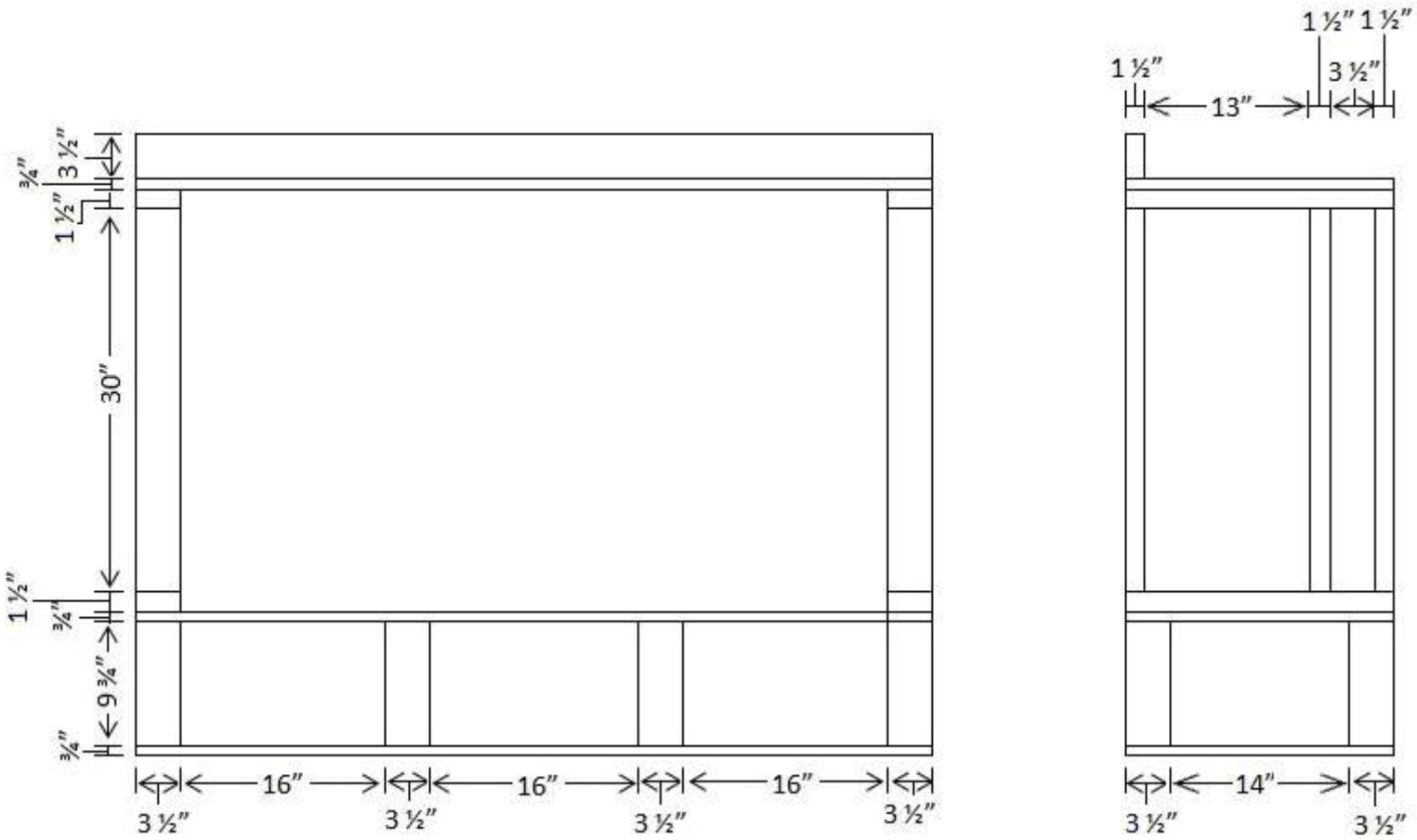

Figure 2. The front and side view of the inner box at 1/16 scale

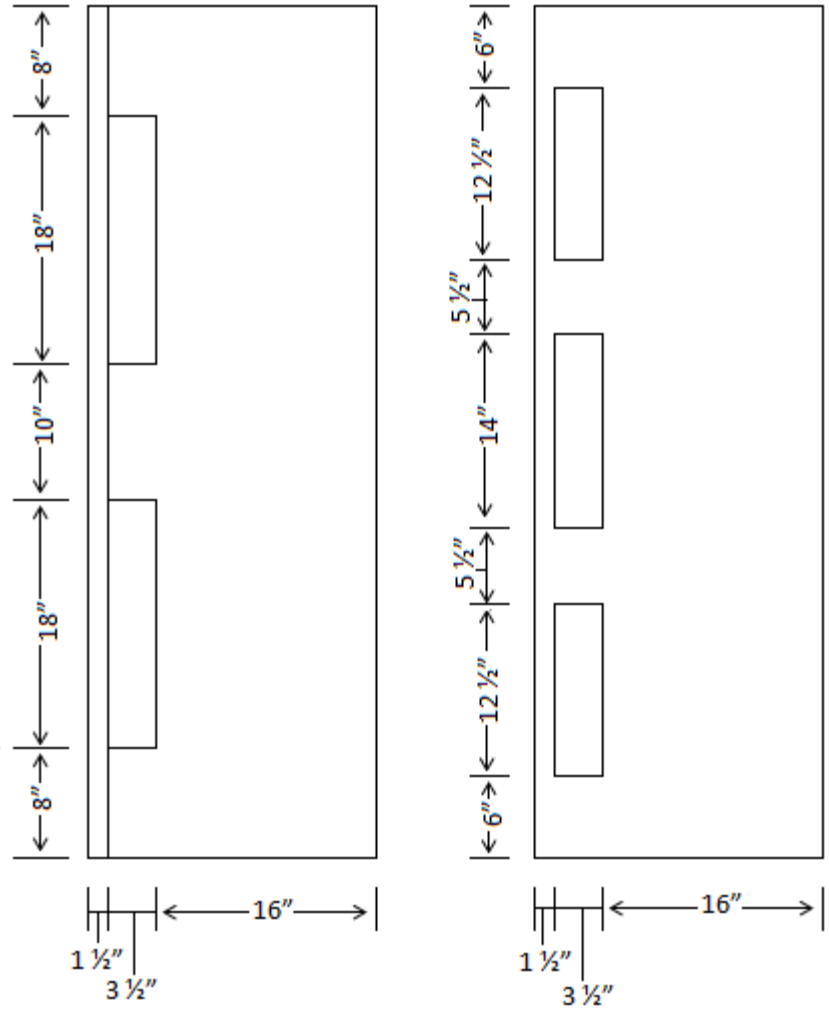

Figure 3. Left: top view of the holes in inner box right: bottom holes in inner box

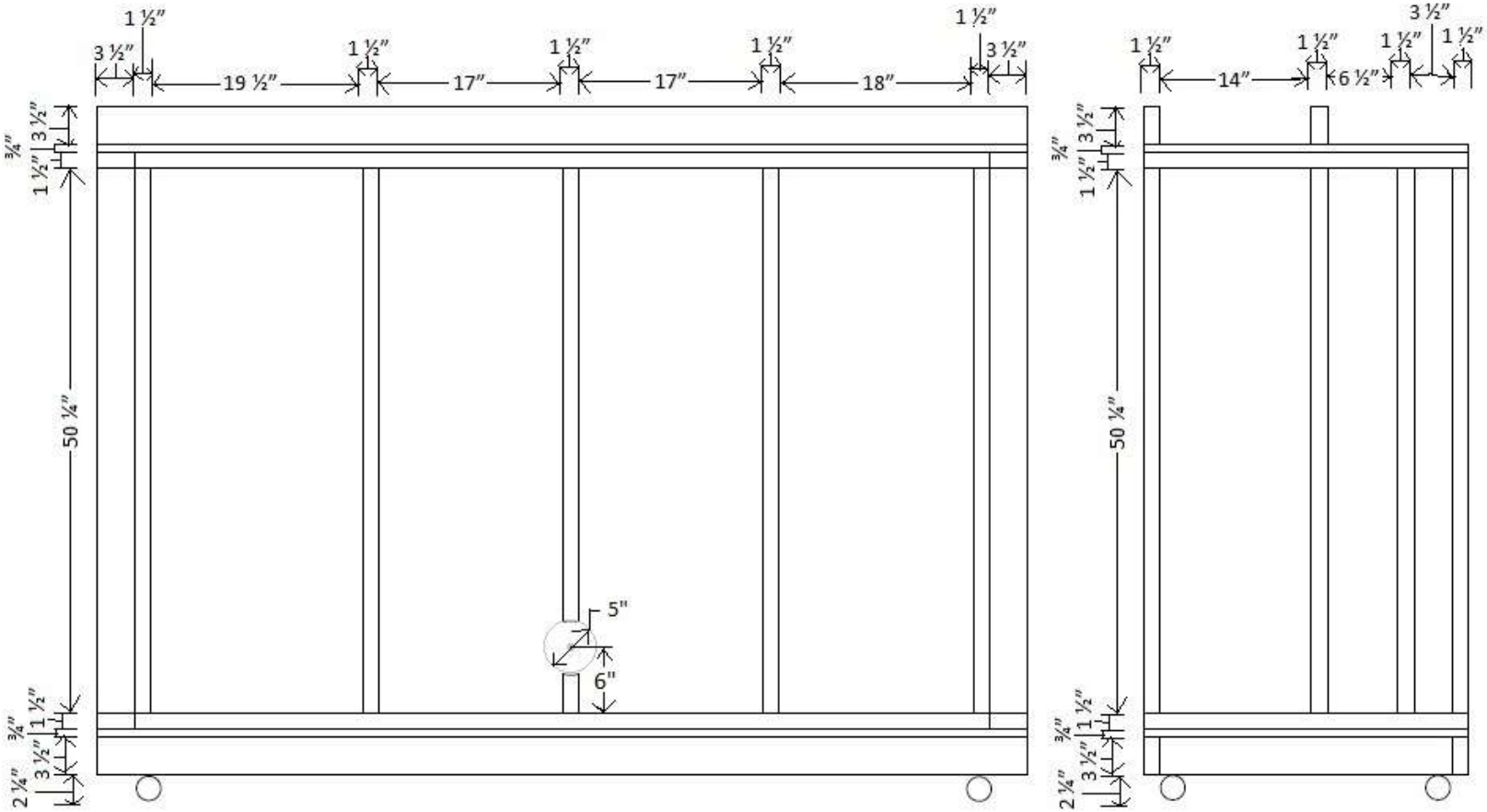

Figure 4. Back and side view of the outer box construction details

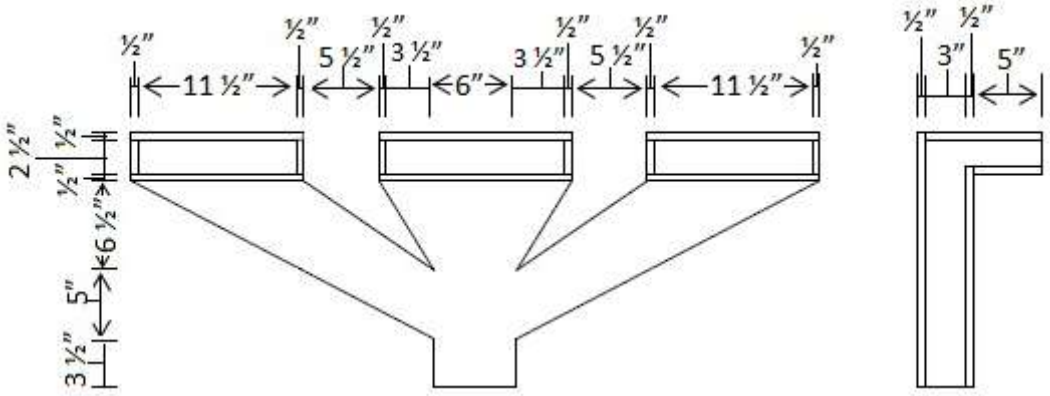

Figure 5. The bottom ductwork

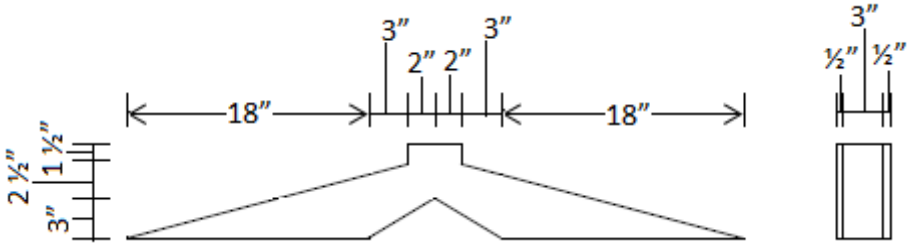

Figure 6. The top ductwork

Temperature Control and Settings

For the heat sink side, 4"x48"x14 ½" heat exchanger and a Tecumseh 30,000BTU cooling capacity AWG4530EXNXM condensing unit was used to remove heat from the system. To ensure better accuracy of the temperature control, a small heating coil and Watlow ¼ DIN SD series PID control system, or a proportional-integral-derivative controller were used. A Fantech FG10XL fan was used to push the air through the

ductwork. The construction details of the closed loop system of the heat sink is shown in Figure 7 and Figure 8 below.

For the heat source side, a heater made by Matt had resistance heating coils in it and was designed to provide a maximum of 1.3kW of heating power. A Fantech FG12XL fan was used to push the air through the system and the same Watlow PID controller was used for temperature control. Figure 9 and Figure 10, below, shows the construction details of the ductwork for the heat source side.

The location of the RTD connected to the PID for both controllers is just before the entrance to the inner box. The ASTM standard requires that the inlet air be with 2K, or 2%, whichever is larger. Locating the RTD directly at the entrance of the inner box, which is the only temperature required to be steady, allows for better temperature control by removing any possibility of heat loss through ductwork after the RTD sensor.

For each specimen, two tests are run; one hot test and one cold test. The hot test is designed to represent a standard hot summer day, so the heat source is maintained at120°F, or 46°C, and the heat sink is maintained at approximately 70°F, or 21°C. For a cold test, designed to represent a cold winter day, the heat source is maintained at 86°F, or 30°C and the heat sink is maintained at 41°F, or 5°C. Although these are not quite the typical cold day temperatures, the chiller could not cool the box lower than 5°C and the code requires a 25°C temperature difference, so the “indoor” temperature needed 30°C, which is warmer than most people will tolerate given the option.

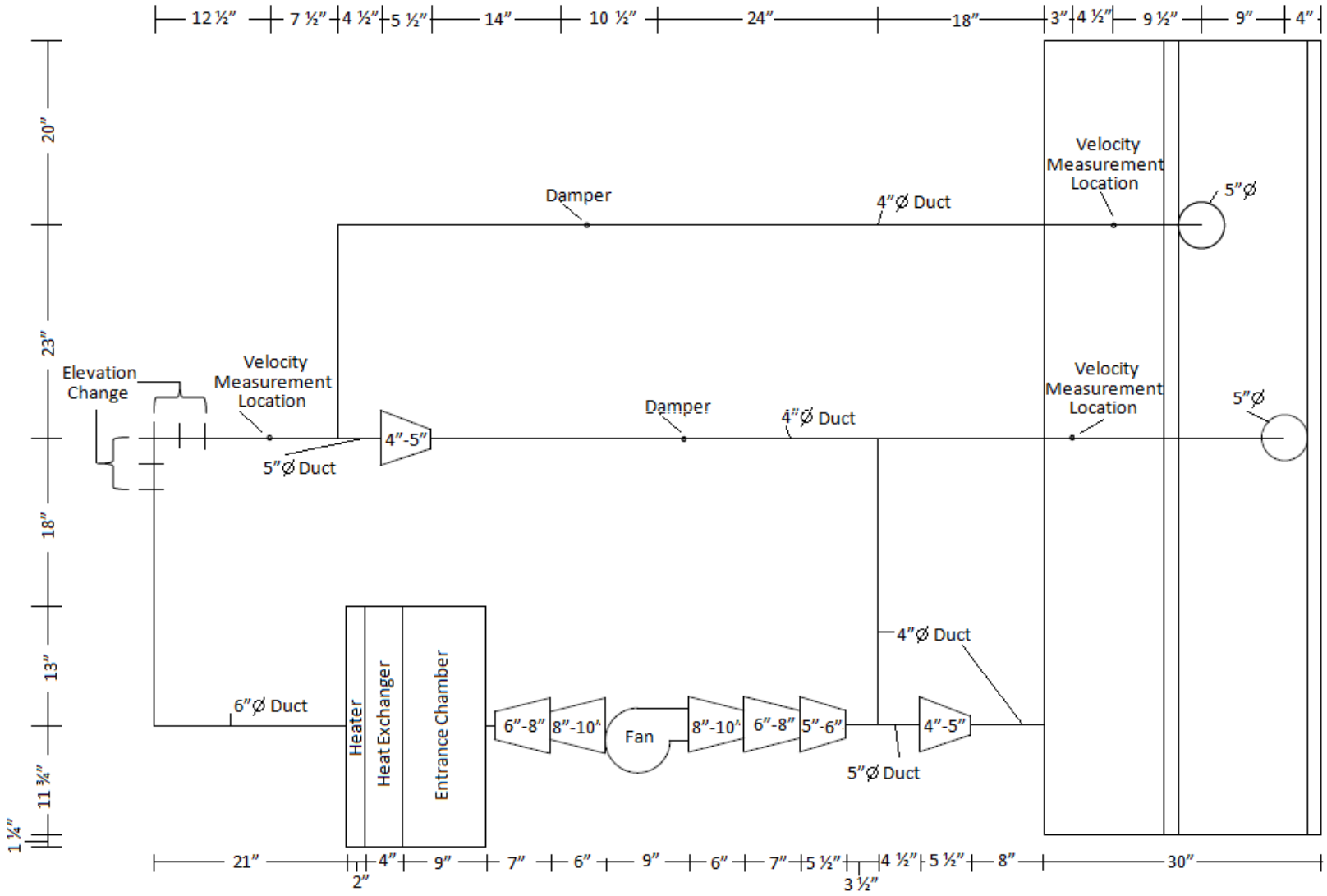

Figure 7. Drawing of the top view of ductwork for the heat sink

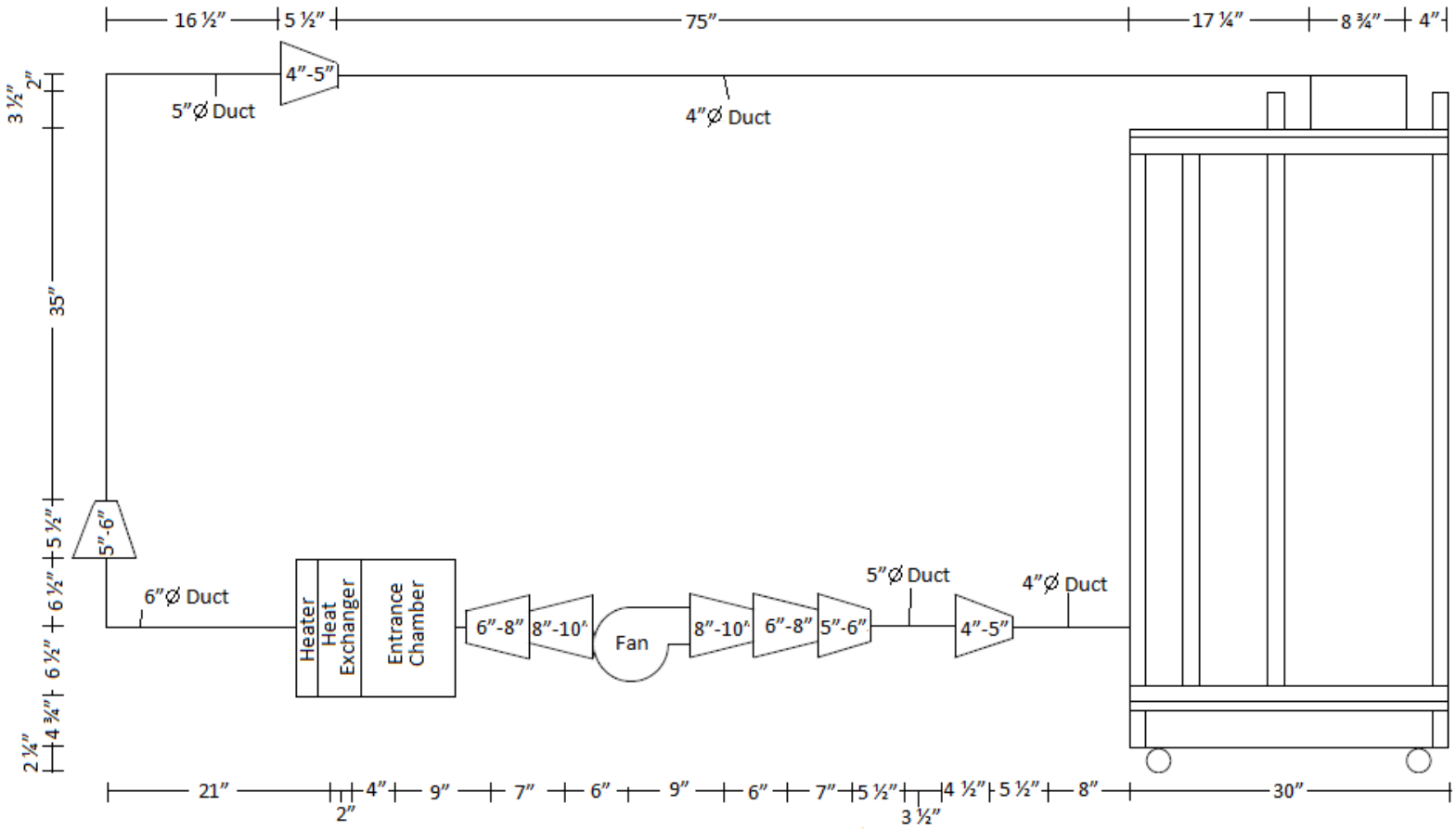

Figure 8. Drawing of the side view of the ductwork for the heat sink

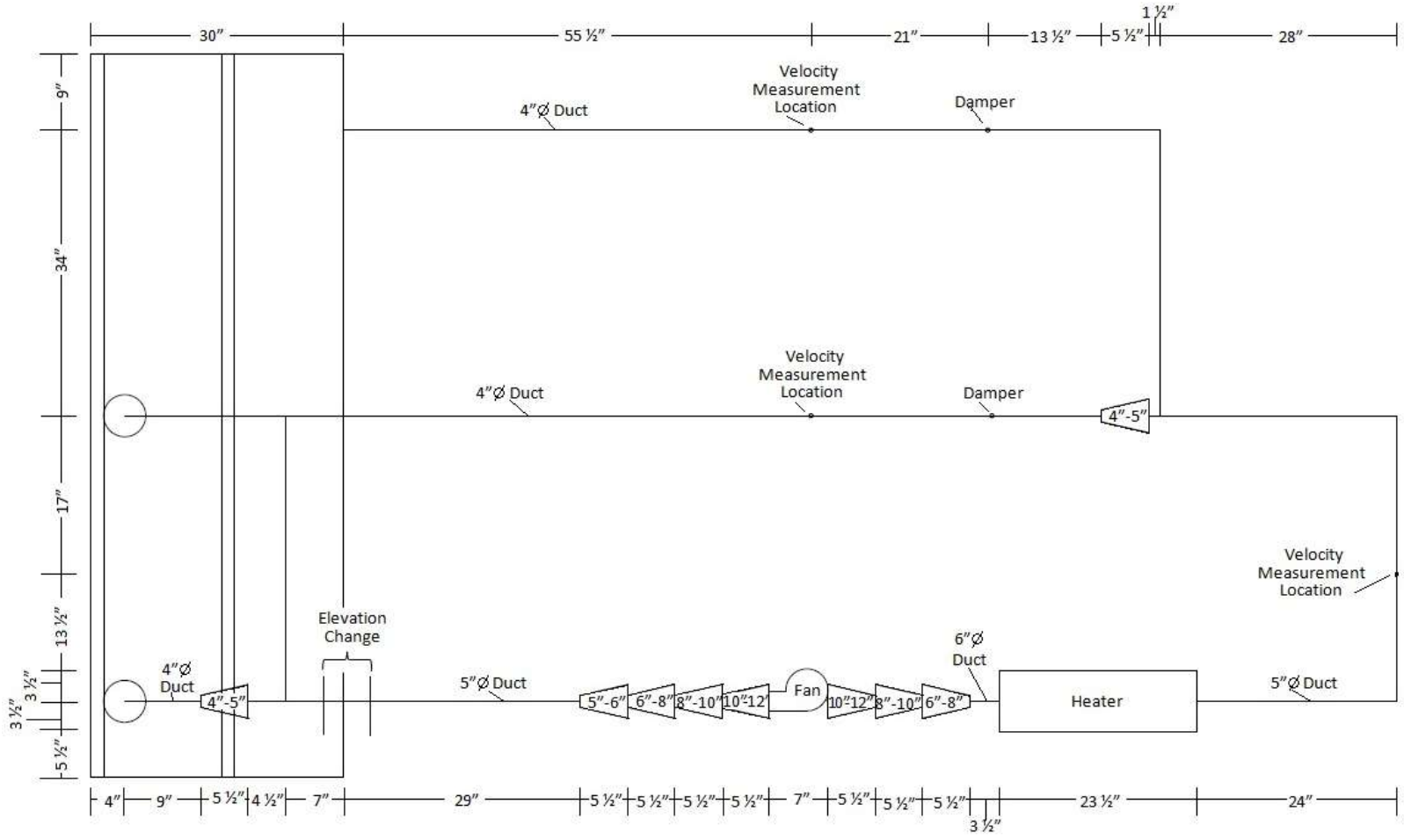

Figure 9. top view of the ductwork for the heat source

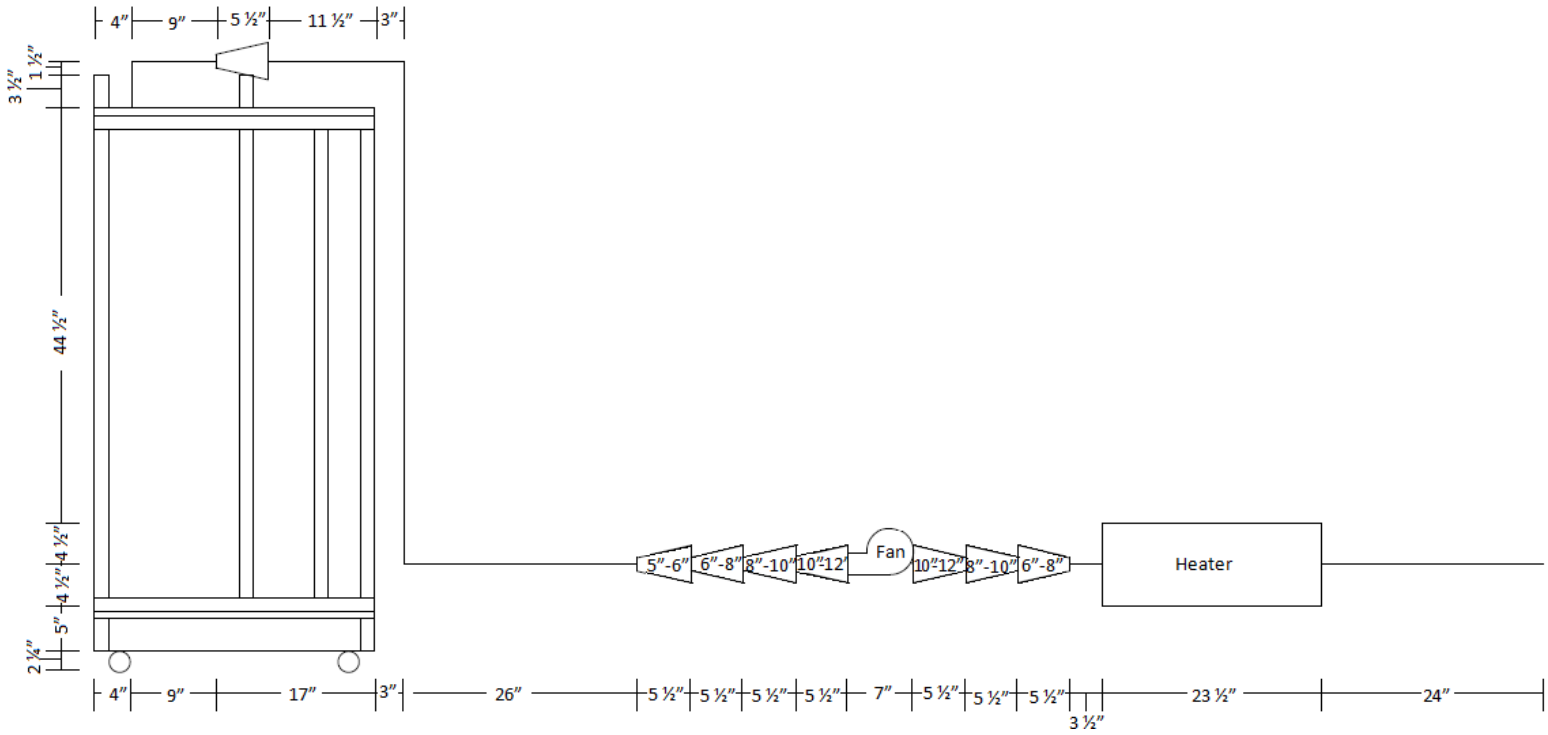

Figure 10. Drawing of the side view of the ductwork for the heat source

Sensor Locations

To approximate the heat loss or gain through the walls, a grid of 9 thermocouples is located along the inside and the outside of each wall of each inner box, totaling to 20 thermocouple grids. The location of each thermocouple is carefully placed such that there is a thermocouple placed directly across from it on the other side of the wall. Using this thermocouple placement, allows for a flux to be determined at that location. Essentially, the average flux of nine difference locations along each wall can be measured in this manner.

The specific locations for both back walls are the same, just as all the sides have the same locations, and the tops and the bottoms have the same thermocouple locations. The following diagrams show the exact thermocouples locations for each wall type. For the most part the thermocouple locations form a 3x3 evenly spaced grid with the exception of the sides, which were too narrow for the grid to be feasible. The following diagrams, Figure 11-Figure 13, show the thermocouple grid pattern along each wall.

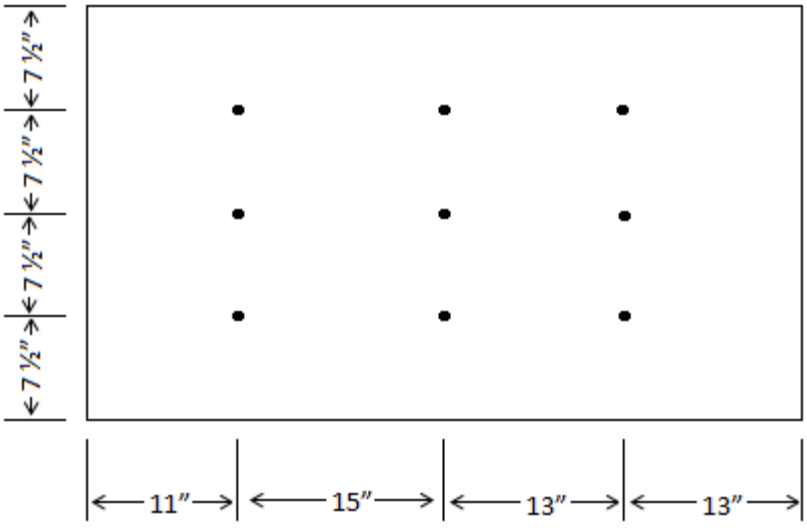

Figure 11. Thermocouple location for the back walls, air and specimen profiles

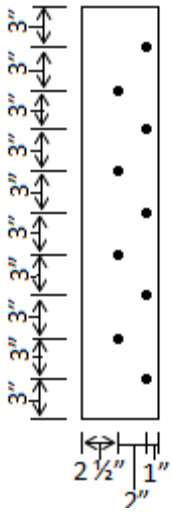

Figure 12. Side walls thermocouple locations

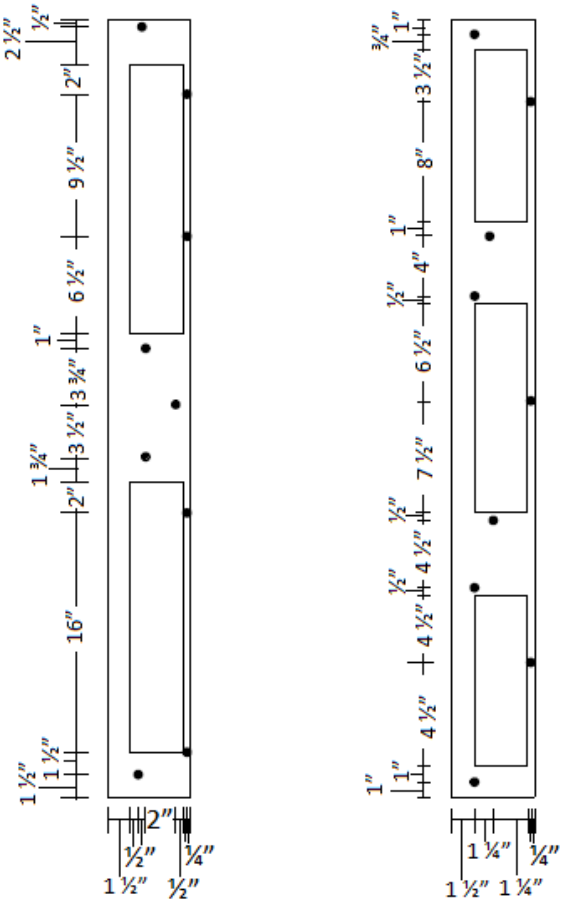

Figure 13. Thermocouples locations of the bottom and top of the inner box, respectively. The right side is the back wall

Nine calibrated thermocouples are used to monitor the surface temperature of the surface of each side of the specimen. Another nine thermocouples are used to measure the air surrounding both sides of the specimen. Since these temperatures are required to be uniform and steady, with 2K (2°C) as required by the ASTM standard, these thermocouples are individual measurements and not grids. These thermocouples follow the same thermocouple grid pattern of the back wall shown in Figure 11.

In order to determine the inlet and outlet temperatures of each inner box, RTD's are placed along the line of duct just outside the outer box. Since the outer box is maintained at the same temperature as the inner box, there is no heat transfer, and consequently no temperature change in the actual entrance to the inner box. Another RTD, which is used by the PID controller, is located at the entrance to the inner box just outside the outer box.

Data Acquisition

The hot box configuration contains 20 thermocouple grids, 36 individual thermocouples, five RTDs and a flux sensor that need to be recorded. Riverside Energy Efficiency Laboratory already had a compact Field Point data acquisition system consisted of the cFP-BP-8, which is the backplane the terminal boards are plugged into, the cFP-2000 which allows the data acquisition system to connect to the network, two cFP-RTD-122 which allows the data acquisition system to read RTDs and three cFP-CB-1 which allow the RTDs to be plugged into the data acquisition system. This component allowed for a computer on the network to read 16 RTDs, which were used to obtain inlet and exit temperatures as well as room temperature, and the coolant bath temperature.

On a tight budget, it was decided that four cFP-CB-3 boards that allow thermocouples to be connected to the data acquisition system, and four cFP-TC-125 boards that allow the data acquisition system to read the thermocouples would be sufficient giving a total of 32 thermocouple reading devices. Since the air and surface

temperatures needed to be measured separately, a configuration of 9 terminal blocks was set up to read multiple thermocouples depending on which connection was made. (Each thermocouple was calibrated against a single RTD and the LabVIEW program HOTBOX, developed by a co-worker had multiple settings so that the calibration factors changed correctly as long as the terminal block setting matched the LabVIEW setting. A brief voltage check was performed to ensure that using terminal blocks had no effect on the voltage reading from the thermocouple to the computer.) The terminal block configuration used is in Figure 14.

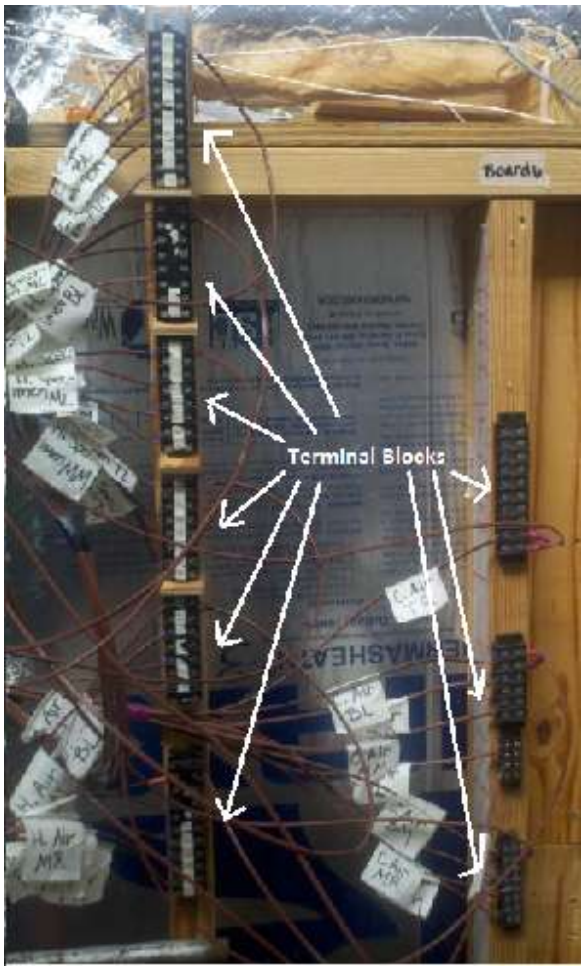

Figure 14. Terminal box configuration: allows various thermocouple readings to be collected from the same port on the terminal board at different times

Once the cFP-2000 was connected to the network the computer was connected too, a connection was made between the cFP-2000 and Measurement Automation Explorer, or MAX. MAX is the program that reads all of the measurements and in MAX the output unit can be set. For example, for the flux sensor, the output unit was mV, but for the thermocouples the output unit was degrees Celsius and T-Type thermocouple was selected. The MAX program had to be standard and run prior to opening LabVIEW to ensure everything is properly connected each time the program is run.

Once MAX was set up, LabVIEW was set to record the data read by MAX every second. The HOTBOX program read and adjusted the temperatures by the calibration factors collected during the thermocouple calibration, and saved the data into four different excel files; one containing the ten heat sink thermocouple grid measurements, one containing the ten heat source thermocouple grid measurements, one containing all of the RTDs and the flux sensor, and the last containing all of the temperature measurements for one setting. Due to limitations in the hardware, the last file does not contain all of the temperature measurements required, so the connected thermocouples had to be switched through the five settings and recorded separately, giving five different setting files. Since it takes approximately 30 minutes to cycle through all of the setting, the first three excel files were also recorded five times to ensure that a consistent steady state condition was maintained throughout the entire test.

CHAPTER III

TEST PROCEDURE

Installation of a Specimen

- Determine the direction of the indoor side of the specimen. (For the uncoated OSB there is no directionality to the specimen. For the coated OSBs, the coated side and for the wall segments, the drywall is subjected to the indoor conditions.) Picture of three sizes of specimen with arrows showing indoor conditions.

Figure 15. Indoor and outdoor conditions of the three specimen sizes

- Determine if the test run should be a hot test or a cold test. (If it is a hot test, then the indoor conditions are on the cold side of the box. If it is a cold test, then the indoor conditions are on the hot side of the box.)
- Ensure the proper number of inner frames is placed on the cold box in between the outer frames. (If the specimen is ¾", a Standard Wall Segment, or a 2x6 Wall Segment the proper number of inner frames is 2, 4, or 5, respectively) The picture

below shows all five inner frames installed. When the two inner frames are installed properly, only one inner frame can be seen.

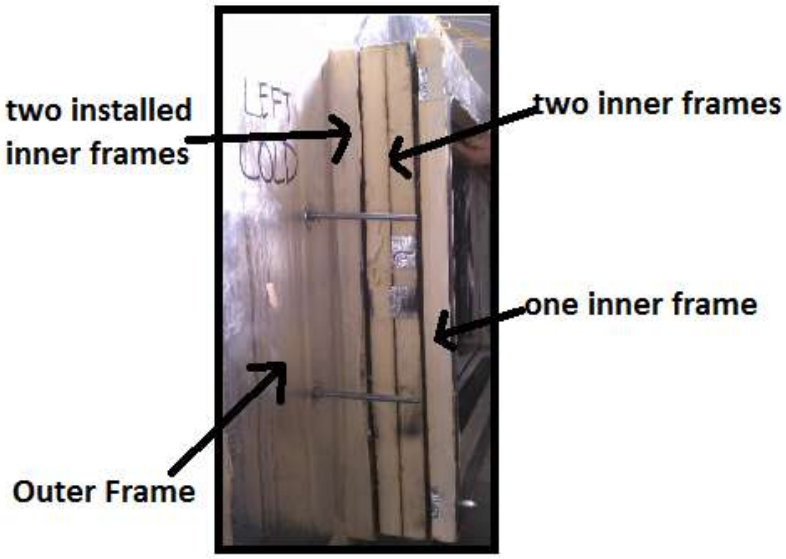

Figure 16. Two sets of two inner frames, and a single inner frame. One set of two is properly installed.

- Use masking tape to seal off air leaks between the inner frames on the inside and the outside of the inner frames.
- Attach the Hot Box outer frame over the last inner frame, with the all-thread rods going through the holes.

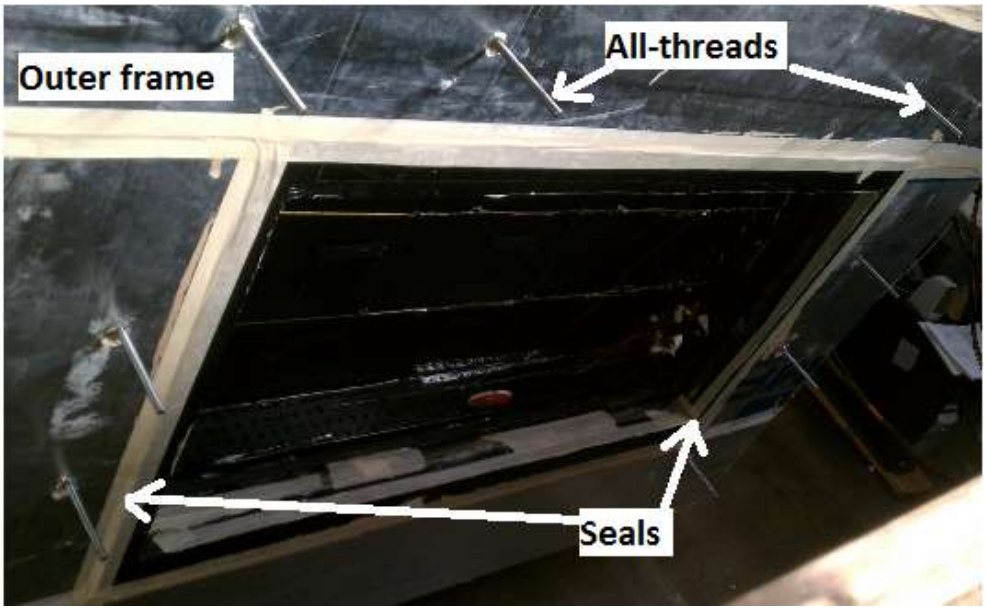

Figure 17. Two inner frames and both outer frames installed and sealed

- Use masking tape to seal off any air leaks between the last inner frame and the outer frame.
- Place the specimen in the inner frames and lean the specimen back.
- Use small squares of double-stick tape to secure the 9 cold-side thermocouples to the specimen and at least four inches of masking tape (since the masking tape has about the same thermal conductivity and emissivity as the all of the specimens) to press down the 9 thermocouples as shown in the picture below.

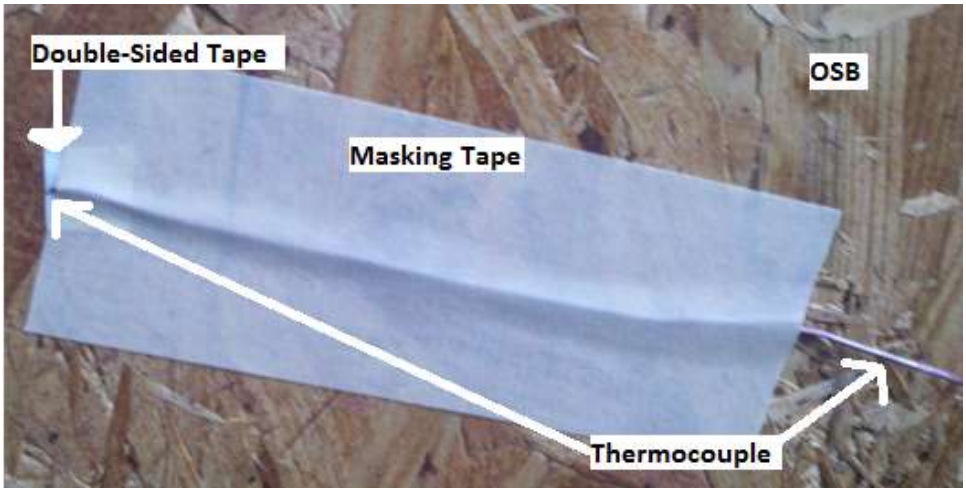

Figure 18. Proper thermocouple installation on specimen

- Use the double-stick tape to secure the hot side of the flux sensor to the center of the specimen, and then use masking tape to secure the cord to the specimen.
- Press the specimen firmly until it is against the stop on the inside of the first inner frame.
- Seal any air leaks by using masking tape around the specimen and the inner frames.
- Use small squares of double-stick tape to secure the 9 hot-side thermocouples to the specimen and at least four inches of masking tape (since the masking tape has about the same thermal conductivity and emissivity as the all of the specimens) to press down the 9 thermocouples.

Assembling the Box

- Once the specimen has been properly installed, the box can be pushed together. Two people are needed for this process.
- With one person on either side of the box push the hot box toward the cold box making sure to line the holes on the hot box with the all-thread rods on the cold box.
- Use the clamps to seal the outer boxes together.
- Use a nut and bolt on the all-threads to seal the inner boxes.

- Place the insulation pads over the all-threads.
- Place the three panels into the holes in the outer box walls and seal off any air leaks with masking tape.

Panels 1 and 2 installed Panel 3 installed

Figure 19. The three panels that allow access to the inner hot box

- Set the controls on the hot box, cold box, and chiller to the proper settings. For a cold test: hot box-30°C, cold box-5°C, chiller-12°C. For a hot test: hot box-46°C, cold box-21°C, chiller-55°C)

Running the Test

The hot tests take a minimum of 2 hours to reach steady state. The cold tests need to be run in the evening/morning so that the ambient air temperature of the lab does not prevent the cold side from reaching the temperature of the set temperature.

Taking velocity measurements

- Start the same MAX program and start a LabVIEW program called Pressures. The program is shown in Figure 20.

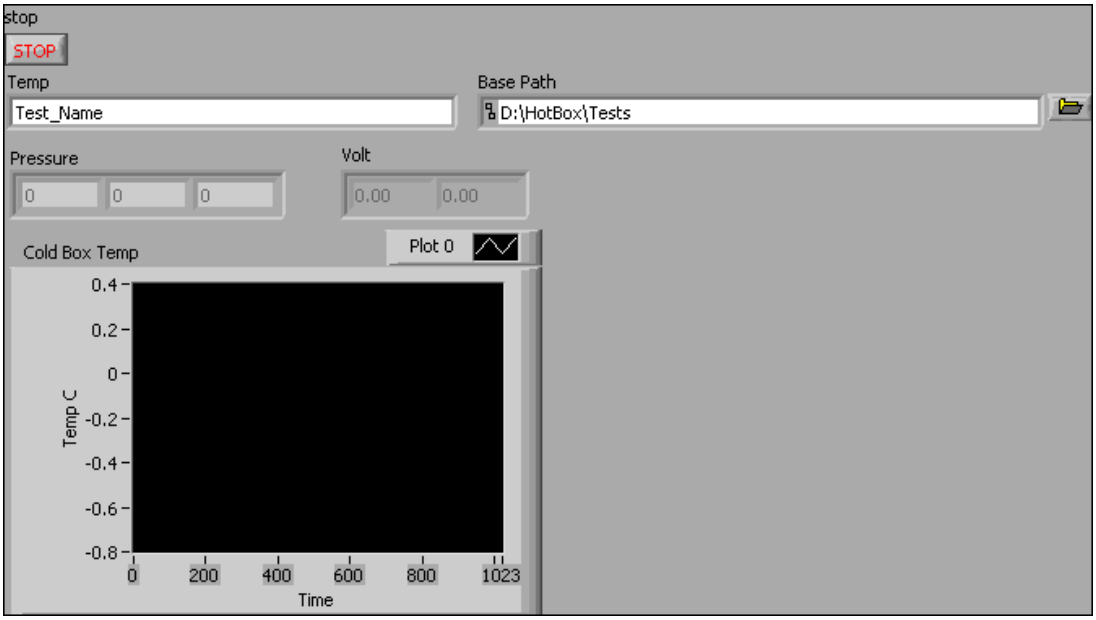

Figure 20. Screenshot of the Pressure Program

- Then set the 4” wooden structure on the on inner line of ductwork for either the hot or the cold side. The picture below shows the 4” and 5” wooden structures

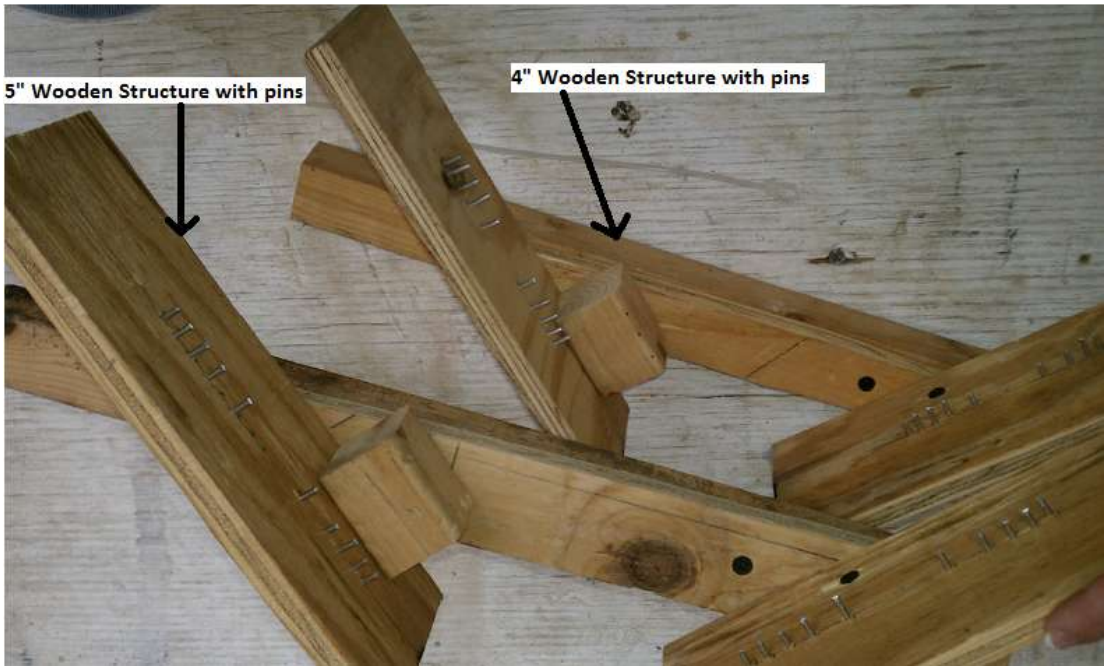

Figure 21. Wooden structures and depths for pressure measurements on the 4”and 5” duct diameter

- Use a small level to ensure that the cross structure stays level and the axis is consistent through the tests.
- Put the pitot tube above pin 1. This depth is approximately 1/16” from the edge of the duct on axis 1. The picture below shows the wooden structure and proper placement with the pitot tube on pin one.
- Label the LabVIEW something that indicates the depth of the pitot tube, which test (hot or cold test) is being run, and which side of the box the pitot tube is measuring (hot or cold side).
- Press the start button (It is a grey button with a white arrow pointing to the right).
- Let it run for approximately 2 minutes (can be longer, but try to keep them consistent). Then hit the red stop sign button to stop the recording.

- Change the depth of the pitot tube by lowing the pitot tube to rest on pin 2. Change the depth indicator part of the title and repeat the previous 3 steps until all 20 depths have been recorded. The following diagram, Figure 23, shows the depth of each pin.

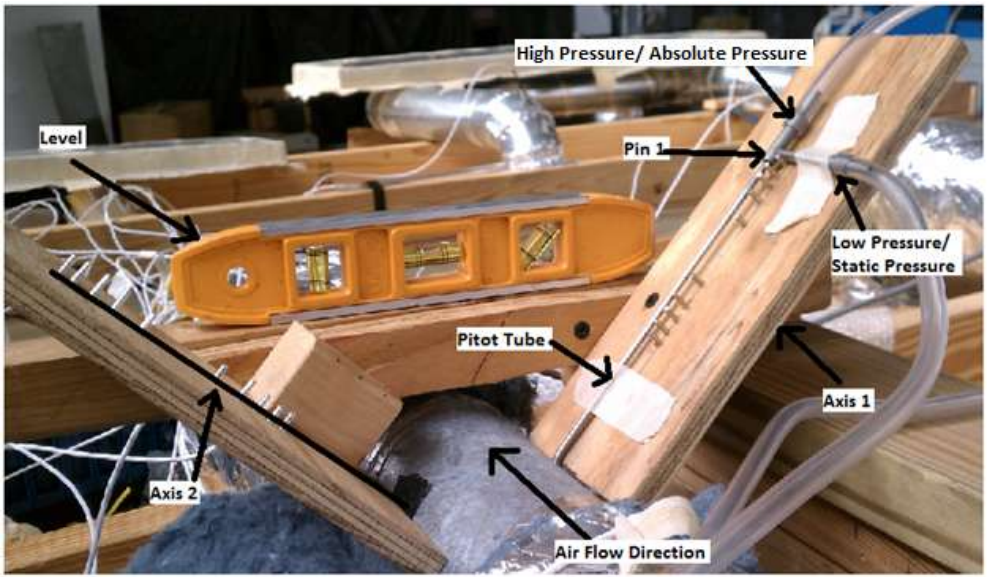

Figure 22. Proper placement of the wooden structure and the pitot tube on the 4" line of duct.

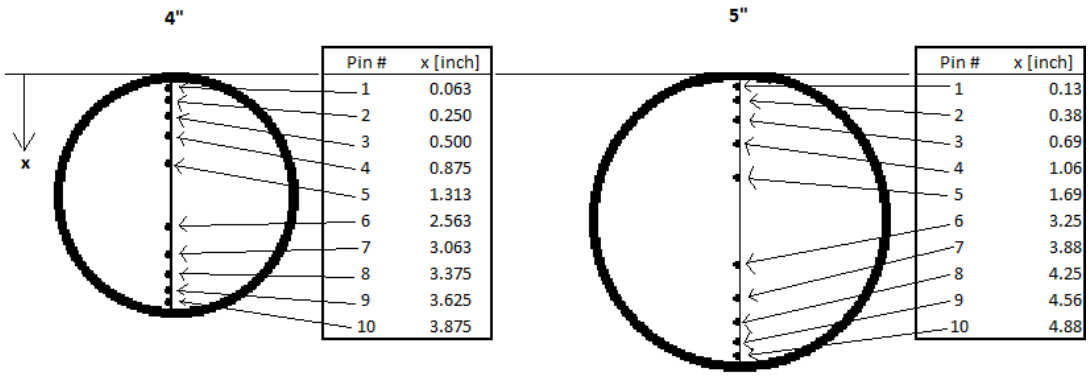

Figure 23. Location of velocity pressure measurements for the 4” and 5” duct diameter

Taking the temperature measurements

- Turn the computer on and open the D drive. This drive is public to all users on the computer.
- Start the program called HotBox_config that looks like a wrench in the screenshot in Figure 24. This icon opens a Measurements Automation Explorer (MAX) program that allows the DAQ system to communicate with the computer.
- Then start the program called HotBox shown in Figure 24. This program opens a LabVIEW program that collects the data and saves them to comma separated value files (.csv)

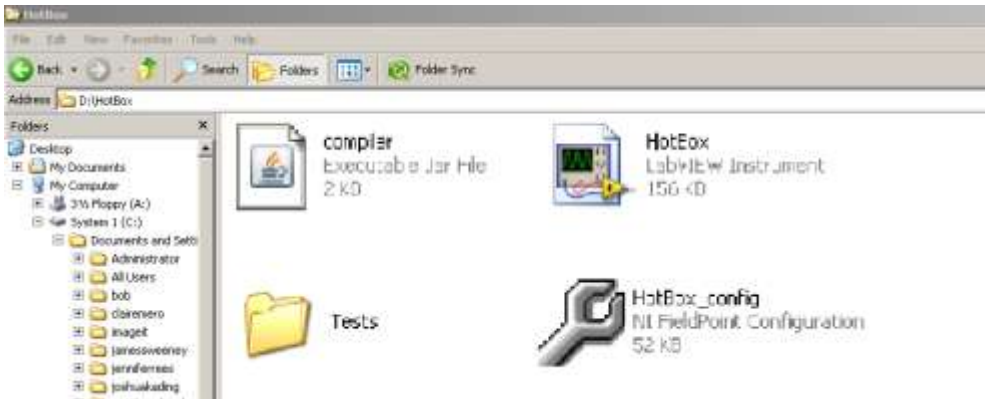

Figure 24. A Printscreen of the icons for the two programs needed to run a test. All the files recorded are saved into the folder called Tests.

- Ensure that all of the terminal blocks are set to setting 1. The figure below, Figure 25, shows all of the terminal blocks on setting 1.

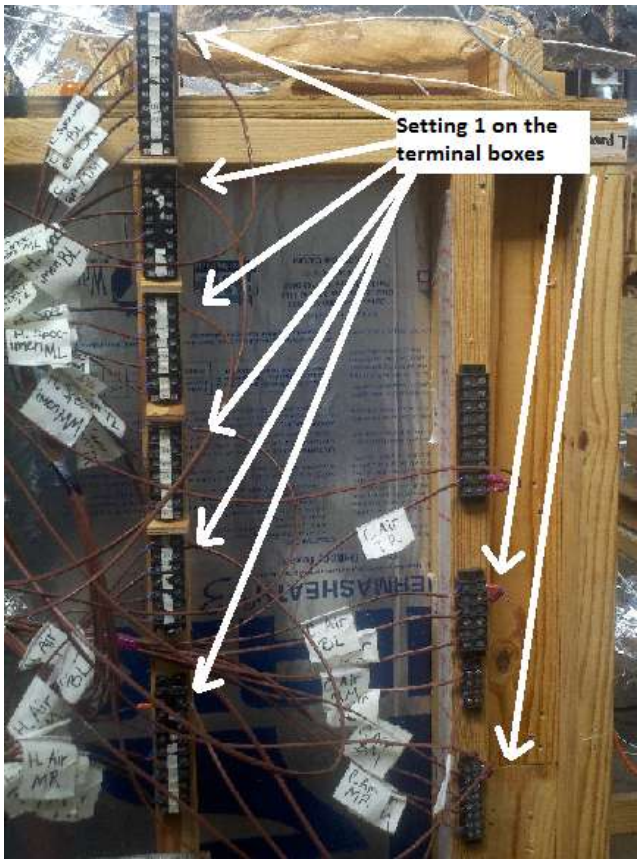

Figure 25. Setting 1 on each of the terminal blocks

- Ensure that the LabVIEW computer program is set to setting 1. Also, be sure to set the type of test run, either hot or cold. The program requires initials, and a test a name indicative of which specimen is in the box. The figure below, Figure 26, shows the program.

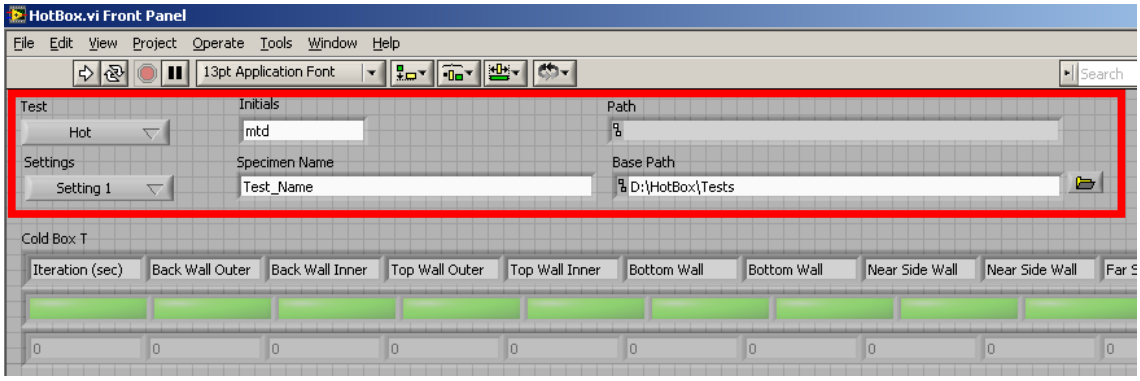

Figure 26. Printscreen of the HotBox program showing the fields that need to be filled out to properly name the file

- Once everything is properly set up hit the start button. This button is grey with a white arrow pointing to the right.
- Let the program run for 2 minutes. Then hit the stop button that looks like a red stop sign.
- Then change the setting on all of the terminal blocks and the computer and restart the program. Repeat the previous until all five settings have been recorded.

Disassembling the Box

- Remove the 3 panels from the hot outer box walls.
- Remove the bolts and washers that seal the inner boxes.
- Remove the clamps sealing the outer boxes.
- Have two people push the outer hot box open slowly so as not to rip the thermocouples on the hot side of the specimen.

Removing the Specimen

- Gently remove the masking tape from each of the thermocouples, making sure to separate the double-stick tape from the masking tape so that the joint of the thermocouple is not damaged.
- Gently remove each of the thermocouples and place out of the way where they will not be damaged.
- Remove the tape surrounding the specimen.
- Gently pull the specimen out of the frame. Multiple tools could be used here, such as a flat head screw driver or the small tool shown below. Be careful not to damage the specimen and pull one side out slightly, then the other or it will get stuck.
- Once the specimen is loose, place the bottom back in the frame and lean it toward so the flux sensor can be reached.
- Gently remove the thermocouples, using the same procedure listed above and the flux sensor trying not to damage the specimen.
- Remove the specimen completely from the frame.
- If running another test is desired follow all of the procedures again.

CHAPTER IV

FLOW STRAIGHTENING

According to ASTM standards, the velocity inside the inner box should be steady and uniform, such that the velocity at any given point in the box is within 10% of the average velocity. The standard also recommends the velocity be under 0.5m/s or 98ft/min so that natural convection assumptions could be made. Additionally, the air temperature profile across the face of the specimen must be with 2K. The higher velocities allow for less time for heat transfer in the air to occur and therefore allows for a more uniform overall temperature distribution. Hence, 98ft/min was chosen as the target velocity.

The code requires that in order to prove the velocity requirements are met; the velocity should be measured at 1 foot increments in a row across the face of the specimen, directly below the air inlet. Since the goal was to understand the flow patterns, the row of velocity measurements were taken at 3 different heights. The following diagram in Figure 27 shows the location of each of the velocity measurement.

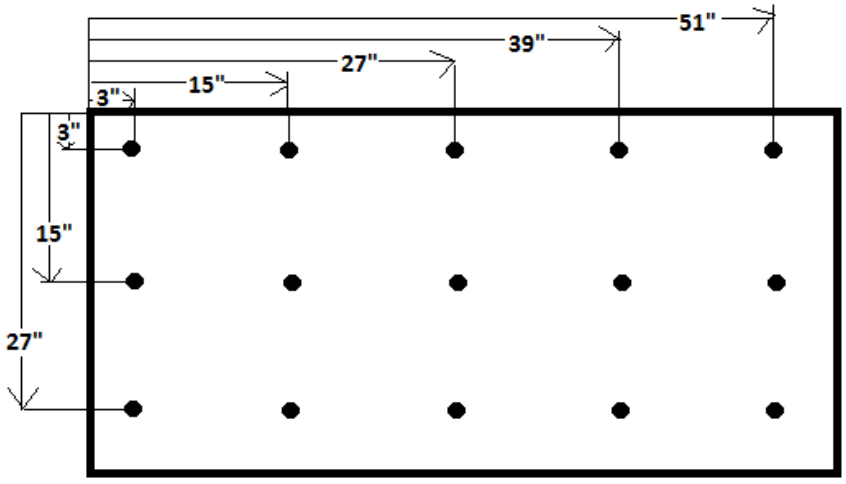

Figure 27. The original cover panel hole locations

In order to perform the velocity tests, the hot box was separated and a cover panel was placed in the outer frame of either the heat sink or source. The cover panel is another piece of 1 ½" polyisocyanurate with holes cut out in certain locations deep enough to allow the probe of the velocity sensor to be directly in the air flow. The picture below, Figure 28, shows the cover panel with masking tape to cover the holes and labeled where the hole location is.

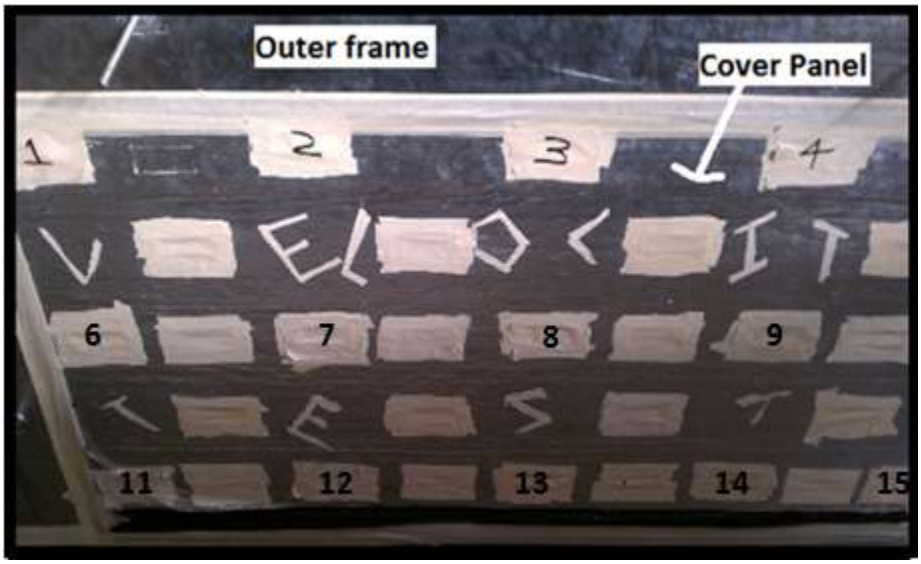

Figure 28. The original cover panel holes labeled with the numbers 1-15, number 5 and 10 are not shown

As various types of flow straightening techniques were attempted, the top and bottom rows could no longer be measured leaving only 5 locations along the middle row for velocity testing. Throughout the testing, the velocity was unsteady and therefore it was difficult to determine the actual flow patterns only given discrete measurement locations of one-directional velocity. To ease this problem, more holes were cut out 6"

between the previous columns of holes. The cover panel with the new hole locations numbered is shown below in Figure 29.

Figure 29. The cover panel with the second set of holes locations marked by numbers. hole number 10 is not shown, but located to the right of 9 ½.

Although the cover panel above helped, there were still problems understanding flow patterns. Since the specimens to be tested are 3" shorter than the height of the inner box and 2" narrower than the inner box, the first and last columns were not in the area across the face of the specimen. Consequently, a new cover panel configuration was created. The new holes were cut halfway, or 6", in between the previous holes vertically and some of the other holes were disregarded leaving a 3x4 grid left. The new cover panel and hole locations are shown in Figure 30, below.

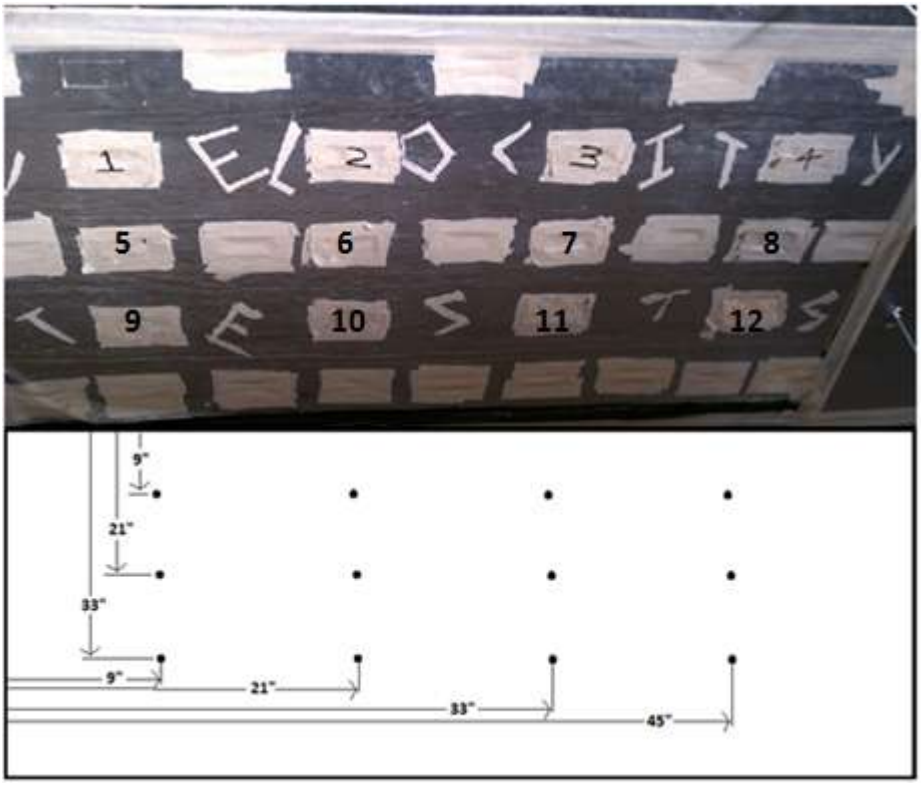

Figure 30. The last cover panel configuration and the location of each hole for velocity measurements

Since the velocity profile tests are arranged by obstruction type and not chronologically, all three configurations can be found in each category. The velocity was measured using an Alnor 9880 velocity sensor shown below in Figure 31. The velocity sensor averages the current velocity with the readings from the 12 previous seconds and can be used from 25-2000fpm with an accuracy of ±5% or 5fpm, whichever is larger. The velocity sensor was monitored for 30 seconds to ensure that it was not changing, or in some cases that the entire range of velocities is recorded.

Figure 31. The velocity sensor used in velocity testing

Throughout the testing the fan type and the air flow through the inner and outer boxes were changed in each category. The fans were switched as needed to overcome increasing pressure drops. The airflow through the inner and outer boxes was controlled with a variable voltage supply and dampers.

The ductwork to the inner and outer boxes for both the heat sink and the heat source were initially equipped with make-shift dampers. Due to the small diameter of the ducts leading to the inner and outer boxes, dampers could not be purchased. If the diameter of the ductwork leading to the inner and outer boxes were 8", then the damper could have been purchased at the local hardware store, but since it was 4" it would have to be special ordered..

Each of the "control" dampers used in this case was made from non-return dampers, a semi-malleable wire, and ducting tape. A small hole was punctured on opposite sides of where the disk or damper component attaches slightly below the small section of ductwork. Then the wire was bent to form a "V" shape in the middle, and the outer edges of the middle shape were pushed through the holes. The "V" was then taped to the disk. The diagram below, Figure 32, shows the bottom view of the created damper.

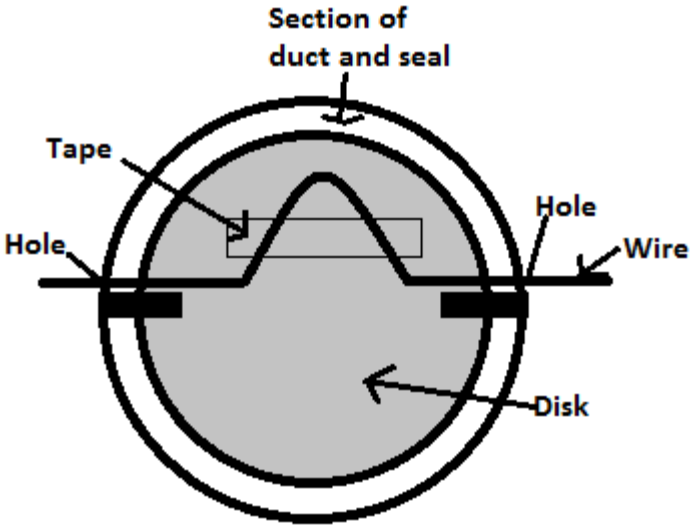

Figure 32. Diagram of the damper construction

To ensure that the dampers worked properly, centerline velocity testing was performed. These tests involved running the fan at full power and the opening and closing of the inner damper. Each damper position was tested twice, once as the damper was being opened and again as the damper was being closed. The table below, Table 1, shows the results of the damper testing.

Conditions		Centerline Velocity [ft/min]			
inner damper	outer damper	inner box supply	inner box return	outer box supply	outer box return
closed	open	112	153	680	900
mostly closed	open	370	425	580	790
mostly open	open	470	530	570	670
open	open	590	560	490	720
open	open	520	570	500	630
mostly open	open	465	520	520	720
mostly closed	open	375	400	620	720
closed	open	190	190	710	890

Table 1. Centerline velocity supply and return of the inner and outer boxes when varying the inner damper position

When looking strictly at the centerline velocities, the dampers appear to be working properly. Throughout the velocity profile tests, various configurations for flow straightening were attempted, most of them involving a large pressure drop. The tests can be split into the following categories: no pressure drop, straw flow straightener, mesh screens, pegboards, a PVC pipe configuration, and any combination of the previous configurations.

No Pressure Drop

The first set of tests performed was on the cold box with no overall pressure drop. As fans were switched, more tests with no overall pressure drops were performed on the hot side. The table below, Table 2, shows all of the tests that fit into this category and how to read the velocity profile testing tables for this section.

Description	Box	Case	Fan	Inner Box	Outer Box	Voltage	Obstructions	Locations
A No overall Pressure drops	Cold	1	Soler And Palau PV100x	damper open	damper open	120		
		2		damper open	damper open	120	3 3/4" fin	6" from the inside of the inlet
		3		damper open	damper open	120	3 3/4" fin	4" from the inside of the inlet
		4		damper slightly closed	damper open	120	3 3/4" fin	5" from the inside of the inlet
		5		damper closed	damper open	120	3 3/4" fin ply of mesh	5" from the inside of the inlet covering both entrances
		6		damper open	damper closed	90	3 3/4" fin ply of mesh	5" from the inside of the inlet covering both entrances
		7		damper open	damper closed	95	3 3/4" fin ply of mesh	4" from the inside of the inlet covering both entrances
	Hot	1	Wells 12"	damper open	damper open	120		
		2	Soler And Palau TD250x	damper open	damper open	30		
		3		damper open	damper open	40		
		4		damper open	damper open	50		
		5		damper open	damper open	60		
		6		damper open	damper open	80		
		7		damper open	damper open	120		
		8		damper open	damper closed	120		
		9		damper open	damper open	120	coke can	at the entrance where the duct splits into three ducts

Table 2.List of all velocity profile tests using no pressure drop

The initial velocity profile, shown below in Table **3** was actually steady, but not uniform and not nearly the target velocity. In order to create a more uniform flow, three variables were added; directional fins made out of ½" insulation boards 3 ¾" long and 4" wide, single plies of mesh, and aluminum can, or coke can. Several tests were performed along these lines.

	1	2	3	4	5
A	27	22	3	29.5	13
B	108	2	37.5	8	89.5
C	93	7.5	15.5	57.5	79.5

	1	2	3	4	5
A	43%	16%	84%	56%	31%
B	120%	96%	23%	84%	83%
C	84%	85%	69%	14%	57%

Table 3. Velocity profile of configuration A, cold box, case 1

The first two cases for the cold box show the velocity and the percent difference between the velocity at that location and the average velocity of the row. The flow was relatively stable, however the percent difference across each row ranged up to 120%, not within 10% of the average that the standard requires. The results show that the air is flowing toward the outer sides of the box. An obstruction should be used to direct flow toward the center.

The best case scenarios for the hot and cold tests are shown in Table 4 and Table 5, respectively. The remaining tests can be seen in Appendix 2: Qualifying Tests on page 89- 93. For the remaining tests in every category, the top left table shows the minimum velocity profiles, top right table shows the maximum velocity profiles, the bottom left table shows the percent difference between the minimum and the maximum velocity at that location, and the bottom right table shows the percent difference between the average velocity at that location and the average velocity of the corresponding row.

	1	2	3	4	5
A	1	42	15	39	1
B	30	6	82	30	33
C	65	29	144	40	73

	1	2	3	4	5
A	1	44	19	45	3
B	38	17	88	38	44
C	69	35	150	42	78

	1	2	3	4	5
A	0%	5%	27%	15%	200%
B	27%	183%	7%	27%	33%
C	6%	21%	4%	5%	7%

	1	2	3	4	5
A	95%	105%	19%	100%	90%
B	16%	72%	109%	16%	5%
C	8%	56%	103%	43%	4%

Table 4. Velocity profile of configuration A, hot box, case 5

	1	2	3	4	5
A	39	28	50	30	25
B	37	170	80	65	104
C	42	72	38	65	17

	1	2	3	4	5
A	43	28	50	30	25
B	70	205	160	160	104
C	76	99	53	98	34

	1	2	3	4	5
A	10%	0%	0%	0%	0%
B	89%	21%	100%	146%	0%
C	81%	38%	39%	51%	100%

	1	2	3	4	5
A	18%	20%	44%	14%	28%
B	54%	62%	4%	3%	10%
C	1%	44%	23%	37%	57%

Table 5. Velocity profile of configuration A, cold box, case 3

These tests again show a velocity profile that is too high in some locations, almost nonexistent in other locations, and has velocity varying up to 110%. The velocity varies up to 200% at any given location. This test failed to meet velocity uniformity and steadiness standards.

Straw Flow Straighteners

The second category of tests performed included a straw flow straightener, which was created by cutting nearly 100 straws into 2” sections. A small wooden box was built such that the interior would fit inside each of the entrances of the cold inner box. The wooden box also had a base such that as all the 1” pieces of straws were put in, the end

would stay level. The straws were then glued around the circumference, such that the air flows through all of the straws.

Two of these straw flow straighteners were created, one for each of the two entrances on the cold box. They were pushed into the entrances, either 1” into the entrance or completely into the entrances, such that they were flush with the top of the box. Table 6 shows all of the tests performed along these lines and how to read the velocity profile table captions for this configuration.

Description	Box	Case	Fan	Inner Box	Outer Box	Voltage	Locations
B Straw Flow Straight-ener	Cold	1	Soler And Palau PV100x	damper closed	damper open	60	1" sticking out of the entrance
		2		damper closed	damper open	70	1" sticking out of the entrance
		3		damper open	damper open	60	1" sticking out of the entrance
		4		damper open	damper open	70	1" sticking out of the entrance
		5		damper open	damper open	80	1" sticking out of the entrance
		6		damper closed	damper open	50	Flush with the entrance
		7		damper closed	damper open	60	Flush with the entrance
		8		damper closed	damper open	70	Flush with the entrance
		9		damper open	damper open	50	Flush with the entrance
		10		damper open	damper open	60	Flush with the entrance
		11		damper open	damper open	70	Flush with the entrance
		12		damper open	damper open	80	Flush with the entrance
		13		damper open	damper open	90	Flush with the entrance

Table 6. List of all tests run using the straw flow straightener

Several tests were performed along these lines. The two tables below, Table 7 and Table 8 show an example of a set from this section. The velocity profile was unsteady, so the minimum and maximum velocity profiles were actually taken. The top left table is the minimum velocity profile, the top right table is the maximum velocity profile, the bottom left table is the percent difference between the minimum and the maximum velocity profile, and the bottom right table is the percent difference between the average velocity at that location and the average velocity of the row of that location. The remainder of the tests using this configuration can be seen in Appendix 2: Qualifying Tests on page 94- 97.

	1	2	3	4	5
A	18	4	42	3	8
B	32	30	20	37	0
C	4	30	60	19	159

	1	2	3	4	5
A	36	7	52	3	10
B	44	60	30	44	0
C	8	30	65	37	164

	1	2	3	4	5
A	100%	75%	24%	0%	25%
B	38%	100%	50%	19%	N/A
C	100%	0%	8%	95%	3%

	1	2	3	4	5
A	48%	70%	157%	84%	51%
B	28%	52%	16%	36%	100%
C	90%	48%	9%	51%	180%

Table 7. Velocity profile of configuration B, cold box, case 2

	1	2	3	4	5
A	3	0	0	5	0
B	3	16	2	22	0
C	0	2	26	15	20

	1	2	3	4	5
A	13	0	3	5	10
B	24	36	14	31	0
C	9	23	33	40	29

	1	2	3	4	5
A	333%	N/A	N/A	0%	N/A
B	700%	125%	600%	41%	N/A
C	N/A	1050%	27%	167%	45%

	1	2	3	4	5
A	105%	100%	62%	28%	28%
B	9%	76%	46%	79%	100%
C	77%	37%	50%	40%	24%

Table 8. Velocity profile of configuration B, cold box, case 4

These two tests have the exact same conditions, except that Table 8 has the inner damper open. These tests do not make much sense because Table 7shows higher overall velocities. The set shown are one of five sets that show this same trend. These results lead to the conclusion that the dampers cause more turbulence, which makes the dampers function more like a nozzle than a damper, but Table 1 shows that the dampers were functioning properly. Varying the voltage of the power supply is the more predictable method of controlling airflow.

Mesh Screens

The third category involved using mesh screens, which were made from window screen wrapped twice around a ½"x ½" wooden dowel rod frames at angles off-set by 45°. The frame was assembled using wood glue, and the screens were attached to the frame one at a time, one side at a time using staples and black duct tape. Figure 33 shows an example of the mesh screen.

Figure 33. An Overall, a close-up view, and a side view of the mesh screen

The mesh screens were intended to create a more uniform air flow by only allowing some air through each hole and forcing the remaining air around to a different hole. With the 2 plies off-set by a 45° angle, the holes are small, and the ½" in between the two sets of mesh should allow the flow to equalize and steady. The table below, Table 9 shows all of the tests performed along these lines and how to read the velocity profile table captions for this section.

Description	Box	Case	Fan	Inner Box	Outer Box	Voltage	Obstructions	Locations
D Mesh Screens	Hot	1	Soler And Palau TD250x	damper open	damper open	60		Flush on Bottom
		2		damper open	damper open	60		Flush on Top and Bottom
		3		damper open	damper open	60		2 Flush on Top and Bottom
		4		damper open	damper open	60		1" away from the Bottom
		5		damper open	damper open	60		1" away from the Top and Bottom
		6		damper open	damper open	60	Mesh Screen 1/2" Insulation Board	Flush on Top and Bottom Partially Covering the Middle Entrance
		7		damper open	damper open	60	Mesh Screen 5 plys of Mesh	Flush on Top and Bottom Covering Middle Entrance

Table 9. List of velocity profile tests performed for the mesh screen configurations

The location and quantity of the mesh screens were varied. Case 1 of these tests is shown below in Table 10. The top left table shows the minimum velocity profile, the top right shows the maximum velocity profile, the bottom left shows the percent difference between the minimum and the maximum, and the bottom right shows the percent difference between the average velocity at a given location and the average velocity of its corresponding row.

	1	2	3	4	5
A	0	44	2	48	3
B	23	14	19	21	2
C	27	17	40	21	29

	1	2	3	4	5
A	0	44	4	49	4
B	26	15	21	22	4
C	28	20	43	25	30

	1	2	3	4	5
A	N/A	0%	100%	2%	33%
B	13%	7%	11%	5%	100%
C	4%	18%	8%	19%	3%

	1	2	3	4	5
A	100%	122%	85%	145%	82%
B	47%	13%	20%	29%	82%
C	2%	34%	48%	18%	5%

Table 10. Velocity profile of configuration D, hot box, case 1

This velocity profile remained unsteady and varied by well over 100%. Theoretical modeling in Fluent, provided by a coworker, showed that the air was actually entering

through the middle entrance, flowing straight, and then hitting the top wall, circling down and exiting the outer entrances at the bottom of the box. These results are likely due to the ductwork. At the entrance to the box, the air is spiraled through the spiral ductwork, which likely makes the air turbulent, and then forced through a 90 degree bend causing the air to hit the specimen in certain locations. The air is never evenly dispersed, so instead of exiting the exits, it hits the top wall directly above the center entrance between the two intended exit holes and is deflected back to the bottom on the outside causing it to exit the two outer bottom intended entrance holes.

For this reason, some of the tests performed had various types of obstructions on the center hole of the three inlets. If the air could be forced to separate and enter into all three holes, perhaps the backflow would be eliminated. Screens were also placed at the top of the box, just before the exit, to try to reduce the effects of the top wall segment between the exits causing the air to flow back down. The best and worst case scenarios are shown in the tables below, Table 11and Table 12.These tests can be seen in the Appendix 2: Qualifying Tests on pages 97- 98.

	1	2	3	4	5
A	9	30	0	36	8
B	29	4	34	15	33
C	27	0	54	42	17

	1	2	3	4	5
A	12	30	0	37	10
B	29	9	38	16	34
C	28	0	57	43	18

	1	2	3	4	5
A	33%	0%	N/A	3%	25%
B	0%	125%	12%	7%	3%
C	4%	N/A	6%	2%	6%

	1	2	3	4	5
A	39%	74%	100%	112%	48%
B	20%	73%	49%	36%	39%
C	4%	100%	94%	49%	39%

Table 11. Velocity profile of configuration D, hot box, case 2

	1	2	3	4	5
A	8	48	0	43	8
B	41	32	1	18	50
C	0	6	0	0	7

	1	2	3	4	5
A	12	50	1	44	12
B	42	35	2	23	51
C	0	8	0	0	8

	1	2	3	4	5
A	50%	4%	N/A	2%	50%
B	2%	9%	100%	28%	2%
C	N/A	33%	N/A	N/A	14%

	1	2	3	4	5
A	56%	117%	98%	92%	56%
B	41%	14%	95%	31%	71%
C	100%	141%	100%	100%	159%

Table 12. Velocity profile of configuration D, hot box, case 7

From the tables above, the velocities at any given location vary up to 125%. The velocity of any given row will vary any from 73% to 159%. Although these tables represent the best and the worst, respectively, it is difficult to distinguish between them. They both fail the velocity tests, indicating these configurations should not be used.

Pegboard

None of the previous parameters tested showed steady and uniform flow. If the critical velocity is reached at each location across the area at the entrance, the velocity should be uniform. These conditions would require a large pressure drop. In order to create a large pressure drop, the fourth category, pegboard was used.

The pegboard was ¼" thick with ¼" diameter holes spaced 1" apart. In some cases the pegboard was wrapped in masking tape and nails or screws were used to create "reduced" sized holes. The pegboard with "reduced" sized holes is shown in the figure below. In other cases the masking tape was used to cover all of the holes except for one row, or all but only a few on one row of holes.

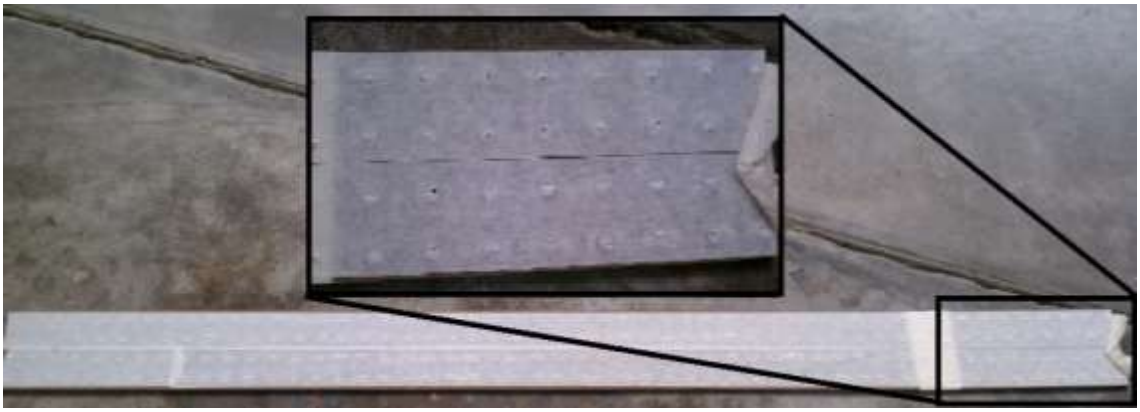

Figure 34. The pegboard used in velocity and flux testing wrapped in tape to create "reduced sized" holes

Again the quantity and location of the pegboards were varied. Various types of obstructions were also used for multiple tests. Table 13 shows the list of test runs as well as how to the read the table captions for the velocity profiles in this section.

Some of the tests need more clarification. For case 1, for both the hot and cold box, pegboard was placed over the inlet and exit of the outer box. This configuration reduced the airflow through the outer box by increasing the pressure through it. Increasing the pressure through the outer box allowed more air to flow through the inner box.

The obstruction called "tear drop" was a thin piece of metal that was bent into an arc, and secured over the wall in between the two exits on the inner hot box. It was completely sealed. The combination of the metal arc and the triangle shape of the entrance form the shape of a tear drop. The idea of the tear drop was that if the air was pushed around an arc, instead of hitting a flat wall, the air would leave the exits, instead of deflecting down the sides. The results of Configuration E, Hot Side, Case 2 are shown below in Table 14.

Description	Box	Case	Fan	Inner Box	Outer Box	Voltage	Obstructions	Locations
E Peg-board	Hot	1	FanTech 12xL	damper open	pegboard	120		2" From the Top and Bottom
		2	Soler And Palau TD250x	damper open	damper open	120	Pegboard with 1 Row of Reduced Holes Reduced Hole Tear Drop Pegboard	Flush with the entrance 1/2" From Bottom Top Between The Exits 1/2" Below the Tear Drop
		3		damper open	damper open	120	2 Reduced Hole Pegboard Reduced Hole Pegboard	First is 1/2" From Bottom, Second is 3" From First Flush on Top
	Cold	1	FanTech 10xL	damper open	pegboard	120		2" From the Top and Bottom

Table 13. List of velocity profile tests run using the pegboard configurations.

	1	2	3	4	5
A					
B					
C	142 15	175 28	70 51	60 32	490

	1	2	3	4	5
A					
B					
C	160 25	215 56	126 60	85 43	530

	1	2	3	4	5
A					
B					
C	13% 67%	23% 100%	80% 18%	42% 34%	8%

	1	2	3	4	5
A					
B					
C	15% 85%	49% 68%	25% 58%	45% 71%	288%

Table 14. Velocity profile of configuration E, hot box, case 2

This velocity of a single location varied up to 100%. The velocity of the bottom row varied nearly 300%. The velocities were higher in locations not typical of the other tests indicating that pegboard was actually creating nozzles, which the mesh screens had not.

Case 3, which can be seen in Appendix 2: Qualifying Tests on page 99, was slightly more uniform, but much less steady. These tests failed the velocity profile test. Case 1, for both the hot and cold box was selected as the final choice, although it did not quite meet standards either.

PVC Pipe Configuration

In order to eliminate the nozzle effect seen by the pegboard configurations, a PVC pipe had slits over 1" long, cut into it every ½" spanning the entire length of the specimen and the inner box. The idea is that the slits are cut small enough that the air flow will reach terminal velocity at each hole, and as a result this will evenly distribute the flow. The pipes are then pointed at the bottom of the box so that the air will diffuse as it comes up around the pipe eliminating the nozzles. Figure 35 below shows the PVC pipe configuration.

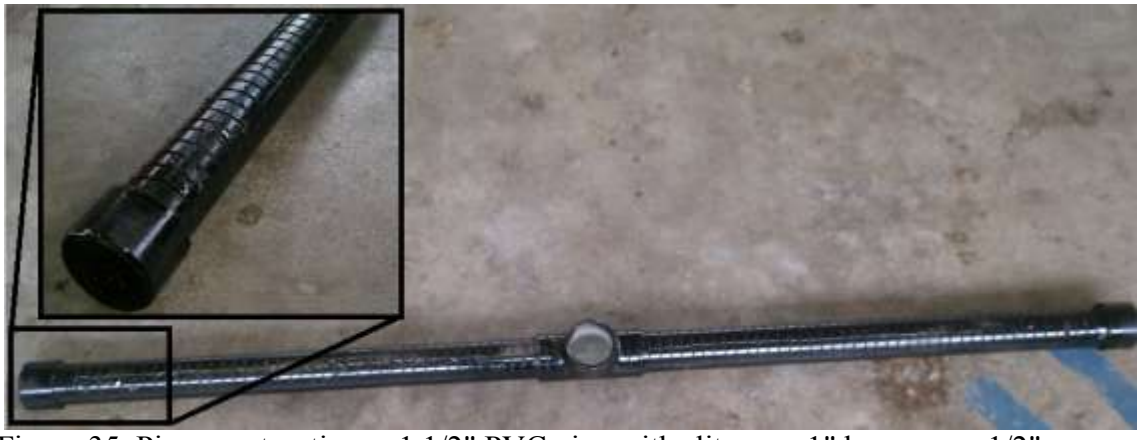

Figure 35. Pipe construction: a 1 1/2" PVC pipe with slits over 1" long every 1/2" spanning the entire length of the box

Several tests were performed using the PVC pipe configuration. With this configuration, not many obstructions could be used, but tape was used to seal the axial cut used in only the first test, and to even the length of each slit in the pipe. In some tests, the ends, where a cap is shown in Figure 35, was left unsealed. The table below, Table 15, shows all of the tests that were performed using this configuration and how to read the velocity profile captions for each table.

Description	Box	Case	Fan	Inner Box	Outer Box	Voltage	Conditions
F PVC Pipe Config-uration	Hot	1	Soler And Palau TD250x	damper open	damper open	120	Ends Unsealed, Axial Cut instead of Traditional Cuts, Bottom Only
		2		damper open	damper open	120	Ends and Axial Cut Unsealed, Bottom Only
		3		damper open	damper open	120	Sealed Ends, Axial Cut Untaped, Bottom Only
		4		damper open	damper closed	120	Sealed Ends Untaped, Bottom Only
		5		damper open	disconnected	120	Ends Sealed and Cuts Taped so Slots are Even, Bottom Only, Axial Cut Untaped
		6		damper open	disconnected	120	Ends Sealed, Completely Untaped, Bottom Only
		7		damper open	disconnected	120	Ends Sealed, Axial Cut is Taped, Cuts are Taped so Slots are Even, Bottom Only
		8		damper open	disconnected	120	Ends Sealed and Configuration on Top and Bottom Only

Table 15. List of velocity profile tests run using the PVC pipe configuration

The best case of these configurations is the final case, case 8. For this case, the ends are sealed and the PVC pipe configuration is on both the top and the bottom. The results for this test can be seen in Table 16.

	1	2	3	4
A	46	94	108	60
B	191	205	113	114
C	205	230	31	78

	1	2	3	4
A	65	133	149	98
B	220	240	142	159
C	220	250	50	94

	1	2	3	4
A	41%	41%	38%	63%
B	15%	17%	26%	39%
C	7%	9%	61%	21%

	1	2	3	4
A	41%	21%	37%	16%
B	19%	29%	26%	21%
C	47%	66%	72%	41%

Table 16. Velocity profile of configuration F, hot box, case 8

The remaining cases using this configuration, shown on pages 99-102, have nearly twice the non-uniformity of the velocity per given row as case 8. One possible reason is that case 8 is the only test run using the 12 hole cover panel, and the bottom row was too close to the pipe to read a steady velocity. The other reason is the best case of the PVC pipe configurations is due to the pipe on top eliminates the overall back flow effects of hitting the top wall between the exits and flowing back down.

The steadiness, although not terrible, was well over 100% for all other cases. The test results make sense considering the following. High velocity air is blown directly at a smooth surface. The air is then deflected back up and is forced to flow around the pipe. Since the air is already turbulent and flowing around a smooth pipe, the back pressure on the opposite side of the pipe causes eddies of all sizes, which causes the velocity to be unsteady.

Throughout the pipe tests, the velocity was low. This pipe configuration created a large pressure drop that resulted in minimal air flow through the inner box. The outer damper was closed, but too much of the air is still allowed through the outer box, so the entrance was disconnected and sealed off. This configuration seemed to result in a pressure built up in the inner box, so the exit had to be disconnected and sealed off as well.

Since the outer box had to be disconnected, a nearly equal pressure drop had to be added to the outer box to distribute air evenly between the inner and outer box. The pegboard was taped over the entrance and the exit of the outer box, and the fan was changed to the Fan Tech 12XL.

Combinations

The final configuration used is actually combinations of any of the previous configurations. Several different obstructions were also used. The tear drop configuration used in the pegboard configurations was also used in these, as well as multiple variations of pegboards. Table 17 shows all of the combinations used during the velocity testing.

There were several tests performed that used pegboards and mesh. The main reason for these combinations was that the peg board created little nozzles, so the mesh screen was used to attempt to eliminate the nozzle effect. Case 4 actually showed the smallest fluctuations and variations. These test results can be seen below, in Table 18.

Description	Box	Case	Fan	Inner Box	Outer Box	Voltage	Obstructions	Locations
DE Combinations of Pegboard and Mesh Screens	H (hot)	1	Soler And Palau TD250x	damper open	damper open	80	Pegboard Mesh Screen	1/2" From Top and Bottom 1/2" From Bottom Pegboard
		2		damper open	damper open	80	Pegboard Mesh Screen	1/2" From Top and Bottom 1/2" From Each Pegboard
		3		damper open	damper open	80	Pegboard with 12 holes in a row Pegboard Mesh Screen	1/2" From Top and Bottom 1/2" From Each Previous Pegboard 1/2" From Each Previous Pegboard
		4		damper open	damper open	120	Pegboard with 12 holes in a row Pegboard Mesh Screen	1/2" From Top and Bottom 1/2" From Each Previous Pegboard 1/2" From Each Previous Pegboard
		5		damper open	damper open	120	3 Reduced Holes Pegboards Mesh Screen Tear Drop 2 Pegboards	First 3" From Bottom, Next two 1/4" From Previous 1/4" From Pegboard on Bottom Top Between The Exits 1/4" From Tear Drop and Eachother
		6		damper partially closed	damper open	120	3 Reduced Holes Pegboards Mesh Screen Tear Drop 2 Pegboards	First 3" From Bottom, Next two 1/4" From Previous 1/4" From Pegboard on Bottom Top Between The Exits 1/4" From Tear Drop and Eachother
		7		damper open	damper open	120	Pegboard with 12 holes in a row Reduced Hole Pegboard Mesh Screen	1/2" From Top and Bottom 1/2" From Previous Pegboard 1/2" From Previous Pegboard
		8		damper open	damper open	120	3 Reduced Holes Mesh Screen Tear Drop 2 Pegboards	First is 1/4" From Bottom, Next two are 1/4" From First and Eachother 1/4" From Previous Pegboard Top Between The Exits 1/4" From Tear Drop and Eachother
		11	FanTech 12XL	damper open	damper open	120	Pegboard Mesh Screen	2" From Top and Bottom Flush on Pegboard
EF Pipe Configuration with Pegboard			FanTech 12XL	damper open	pegboard	120	Pegboard in between the Pipe Configurations	

Table 17. List of velocity profile tests run using multiple configurations

	1	2	3	4	5
A					
B					
C	162	98	255	187	255

	1	2	3	4	5
A					
B					
C	220	137	300	225	310

	1	2	3	4	5
A					
B					
C	36%	40%	18%	20%	22%

	1	2	3	4	5
A					
B					
C	11%	45%	29%	4%	31%

Table 18. Velocity profile of configuration DE, hot box, case 4

The velocity profile is within 45%, and the velocity at any given point varied up to 40%. These case results are significantly better than most of the tests that have been seen, but this test still does not meet standards. The remainder of these tests can be seen in Appendix 2: Qualifying Tests on pages 103-106.

Another combination involved trying to steady the eddies created by the PVC pipe configuration by placing pegboard over it. Only one test was performed with this combination. The results of this test are shown below in Table 19.

	1	2	3	4
A	69	445	270	209
B	520	425	790	325
C	530	435	71	380

	1	2	3	4
A	79	470	280	210
B	560	435	840	350
C	560	445	78	395

	1	2	3	4
A	14%	6%	4%	0%
B	8%	2%	6%	8%
C	6%	2%	10%	4%

	1	2	3	4
A	71%	80%	8%	18%
B	2%	19%	54%	36%
C	51%	22%	79%	7%

Table 19. Velocity profile of configuration EF, hot box, case 1

The velocity was relatively steady for this test, which shows that the pegboard definitely minimized the eddies that PVC pipe configurations created. Although this test is relatively steady (compared to the other tests performed), the velocity profile still varies up to 80%. This test fails to meet the standards and takes up more than the allotted 3" on the top and the bottom that the specimen does not take up.

Final Decisions

The pegboard alone was selected as the best choice of all of the tests performed. For each side, pegboard was placed 2" away from the top and the bottom. Final velocity profile testing was performed twice, for both the cold and the hot side to ensure stability. For the hot side and cold side, the FanTech 12XL and FanTech 10XL, respectively, were used. The final velocity tests are shown below in Table 20, Table 21, Table 22, and Table 23.

	1	2	3	4
A	182	129	57	135
B	300	114	72	290
C	375	173	215	325

	1	2	3	4
A	205	140	68	159
B	315	140	82	315
C	410	185	235	385

	1	2	3	4
A	13%	9%	19%	18%
B	5%	23%	14%	9%
C	9%	7%	9%	18%

	1	2	3	4
A	44%	0%	53%	9%
B	51%	38%	62%	49%
C	36%	38%	22%	23%

Table 20. Velocity profile of configuration E, hot box, case 1

	1	2	3	4
A	178	113	58	147
B	300	110	72	320
C	385	163	215	315

	1	2	3	4
A	200	131	67	175
B	335	125	85	335
C	395	185	240	370

	1	2	3	4
A	12%	16%	16%	19%
B	12%	14%	18%	5%
C	3%	13%	12%	17%

	1	2	3	4
A	41%	9%	53%	20%
B	51%	44%	63%	56%
C	38%	39%	20%	21%

Table 21. Velocity profile of configuration E, hot box, case 1

	1	2	3	4
A	188	149	205	147
B	111	104	210	112
C	150	47	36	162

	1	2	3	4
A	220	200	235	183
B	143	133	270	125
C	175	64	70	205

	1	2	3	4
A	17%	34%	15%	24%
B	29%	28%	29%	12%
C	17%	36%	94%	27%

	1	2	3	4
A	7%	9%	15%	14%
B	16%	22%	59%	22%
C	43%	51%	53%	61%

Table 22. Velocity profile of configuration E, cold box, case 1

	1	2	3	4
A	195	196	186	161
B	122	130	360	94
C	175	73	41	164

	1	2	3	4
A	220	230	205	191
B	153	170	400	127
C	190	88	61	205

	1	2	3	4
A	13%	17%	10%	19%
B	25%	31%	11%	35%
C	9%	21%	49%	25%

	1	2	3	4
A	5%	8%	1%	11%
B	29%	23%	95%	43%
C	46%	35%	59%	48%

Table 23.Velocity profile of configuration E, cold box, case 1

The tests still show that there is a relatively unsteadiness. The hot side velocity varied up to 23% and the velocity profile varied up to 63%. This configuration was chosen because of these results

The cold side, on the other hand, has a velocity variance of 94% and the velocity profile was up to 95% non-uniform. The same results that were seen on the hot side were obviously not seen on the cold side. This configuration was chosen anyway in order to keep the same configuration between the two sides.

CHAPTER V
QUALIFYING TESTS

Mass Flow Rate

In order to obtain the mass flow rate into the inner box, the velocity needed to be determined through the inlet duct. Initially the same Alnor velocity sensor that was used in the velocity testing was used for determining the velocity through the ductwork. The velocity was measured at the entrance to the inner box, the entrance to the outer box, and at a location were the two air streams are combined in one run of ductwork, so that a mass balance could be performed.

The velocity in the main stream of the ductwork was higher than the top range of the Alnor velocity sensor, 2000fpm. Also, the velocity inside the ducts was not uniform, making a hand held sensor an inaccurate method of testing the velocity. A pitot tube was purchased and a wooden structure shown in Figure 21 with pegs to determine the exact location of the velocity measurement was built to sit on top of the run of duct. Ten velocities along two axes within the duct were measured, giving a total of twenty velocity measurements at any given location.

Two Dwyer 616 Weatherproof pressure transmitters with a digital read-out and a top range of 10" of H_2O, were used in conjunction with the pitot tubes to measure the velocity pressure, which could be used to determine the velocity. The sum of the mass flow rates of the inlet and outlet ducts did not add up to the mass flow rate of the 5" duct. This inconsistency was likely due to the fact that the velocity pressure was consistently between 0.01" and 0.2" of H_2O and the uncertainty of the pressure transducer is 0.025" of H_2O, double the smallest measurement.

Two Dwyer 616-00 pressure transmitters that have a top range of 1" of H_2O, replaced the Dwyer 616 Weatherproof pressure transmitters. These pressure transmitters required a data acquisition system to read the data. LabVIEW was used to collect and record the velocity pressure readings every second for 120 seconds. The average velocity pressure and standard deviation are shown in Appendix 2: Qualifying Tests on pages: 107, 108, 114, and 115 respectively. Although the range was still greater than the

velocity pressure, the uncertainty was low enough that the velocity could be measure within 5%.

The velocities and uncertainties were approximated using a constant density, these are shown on pages 109, 110, 116, and 117 to determine the velocity profile which was graphed to ensure that using the average velocity of the pipe was a feasible method of calculating the mass flow rate through the ductwork. The velocity profiles are shown on pages 111-120. The actual velocity of each test run was calculated using average velocity pressure and the density as a function of the temperature of the air within the duct for each run.

Temperature Corrections

The original results of the flux calculations showed that heat was actually being added to the cold side to maintain the temperature and compensate for the heat being added through the specimen. Obviously, these results do not make sense thermodynamically, so it was concluded that the current set up of the RTD was not measuring the correct temperature within the pipe. The original construction set up shown below in Figure 36, was the reason for the error.

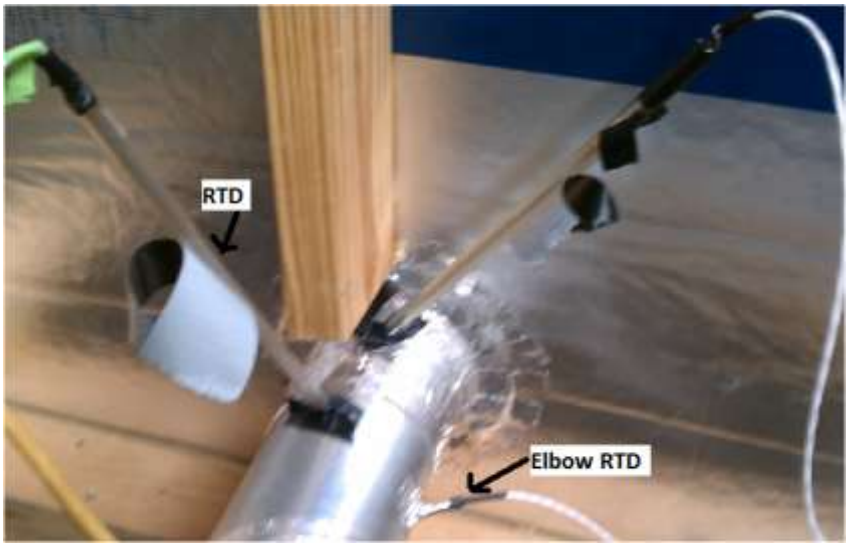

Figure 36. The original and elbow RTD configurations

Originally, about 3.5” of the 14” RTD was inserted and sealed in the pipe, leaving over a foot subjected to the room temperature. This configuration means that the RTD was actually measuring an average of the inlet and room temperature. Rather than rerunning every test, a few calibration tests were run using the following three sensors simultaneously; using a 90° elbow RTD to measure the actual temperature, using the original RTD to get the reading shown in the tests, and using the same RTD to measure room temperature.

The same configuration as the specimen testing with the addition of the elbow RTD was set up to run for a two days collecting data six times over the course of the two days. The tests were run at various times of day to ensure that there was a large range of room temperatures for hot and cold tests. Then the average and standard deviation were taken for each temperature and recorded so the error can be determined.

The difference between the actual temperature and the temperature read by the straight RTD was plotted against the room temperature to determine trends. Each plot including the error in each measurement can be seen in Appendix 2: Qualifying Tests on pages 121-124. As seen from the tables, the cold inner box inlet temperature recorded for each tests are anywhere from 1-8°C different from the actual temperature.

Once the temperature corrections were made, the results showed that heat was removed from the inner box to compensate for the heat being added through the specimen. Unfortunately this correction was not sufficient for every tests, there were still two were there was an undiscovered problem.

CHAPTER VI

DATA ANALYSIS

Temperature Uncertainties

The temperature at each location was taken 120 seconds. The average temperature at each location was taken, and the uncertainty of the temperature at each location was calculated using the following equation.

(1) $$U_{T_i} = \sqrt{\left(B_{T_i}\right)^2 + \left(P_{T_i}\right)^2}$$

The T type thermocouple used had an accuracy of 1°C. This accuracy meant that bias at each thermocouple is 0.5°C. P is the precision limit, which was calculated by the standard deviation multiplied by a zeta factor. The zeta factor used was 1.98 based on a 95% confidence level and 120 points.

For various locations nine different thermocouples were used. The following equation was used to determine the uncertainty for the temperature of that location.

(2) $$U_{T_{average}} = \sqrt{\sum_{i=1}^{9}\left(\frac{U_{T_i}}{9}\right)^2}$$

Velocity Calculations

For the velocity calculations, a pitot tube and a pressure transducer were used to measure the velocity pressure at twenty different locations along two axes at three different locations along the heat sink and the heat source side. The pressure transducer was read by LabVIEW, which recorded 160 seconds of data at each location. Initially, the average and the standard deviation at each point were taken. The uncertainty of the velocity pressure at each location was calculated using the following equation.

(3) $$U_{P_i} = \sqrt{\left(B_{p_i}\right)^2 + \left(P_{p_i}\right)^2}$$

$B_{p,}$ the accuracy of the pressure transducer was ±0.25% of 1" H_20, or 0.0025" H_2O. P_p was the standard deviation times 1.98, which was the zeta value associated with a 95% confidence level and 120 points.

For the more accurate analysis, the average velocity pressure was calculated by averaging the velocity pressure of the twenty points. The uncertainty of the average velocity pressure was calculated using the following equation.

(4) $$U_{p_{average}} = \sqrt{\sum_{i=1}^{20}\left(\frac{U_{p_i}}{20}\right)^2}$$

Then the average velocity pressure was converted to the velocity, using density which depended on temperature. Three points from a standard air temperature table were used to determine the equation for density.

(5) $$\rho = -0.004T + 1.291$$

The temperatures at the three locations for both the heat sink and the heat source were used to calculate the velocity at each location using an accurate density for each test. The actual uncertainty of the temperature at each location was used for the calculation of the velocity and the mass flow rate. The following equations were used for the velocity and uncertainty of velocity calculations.

(6) $$V = 1096.2 * 0.84\sqrt{\frac{P}{\rho}}$$

(7) $$U_V = \sqrt{\left(\frac{1096.2*0.84*0.5}{\sqrt{\frac{P}{\rho}}}\frac{U_P}{\rho}\right)^2 + \left(\frac{1096.2*0.84*0.5}{\sqrt{\frac{P}{\rho}}}\frac{P}{\rho^2}(-0.004U_T)2.2(0.0254*12)^3\right)^2}$$

Since the velocity pressure was in inches of H_2O, the density was in lb_m/ft^3, the equation for density in kg/m^3, so the uncertainty of the density was also converted to

lb_m/ft^3. The velocity given was in ft/min, and was converted to be m/s. The velocity was then converted to mass flow rate by the equation given below.

(8) $$\dot{m} = \rho V \frac{\pi}{4} D^2$$

The uncertainty for the mass flow rate was calculated by the following equation. For both the mass flow rate and the uncertainty of the mass flow rate, the density was a function of temperature. The uncertainty of the diameter of the ductwork was assumed to be 1/64".

(9) $$U_{\dot{m}} = \sqrt{\left(\frac{\pi}{4} D^2 \rho U_V\right)^2 + \left(V \frac{\pi}{4} D^2 (-0.004 U_T)\right)^2 + \left(V \frac{\pi}{4} \rho 2 U_D\right)^2}$$

The velocity profiles were graphed as a method of ensuring that the velocity was uniform enough to calculate an average velocity. For the velocity profiles, the inlet box temperature for the hot side was used to calculate the density for the hot side calculations and the inlet box temperature for the cold side was used to calculate the density of the cold side calculations. An error of 7% was used for the temperature in the density calculations.

Heat Transfer Calculations

The heat transfer through each of the walls was calculated first. The heat transfer through the walls and the corresponding uncertainty were calculated using the following equations. The accuracy of the R-value was assumed to be 5%.

(10) $$Q_{wall_i} = \frac{kA(T_{outer} - T_{inner})}{R}$$

(11) $$U_{Q_{wall_i}} = \sqrt{\begin{array}{c}\left(\frac{U_A}{R}(T_{outer} - T_{inner})\right)^2 + \left(\frac{-AU_R}{R^2}(T_{outer} - T_{inner})\right)^2 \\ + \\ \left(\frac{A}{R} T_{outer}\right)^2 + \left(\frac{A}{R} T_{inner}\right)^2\end{array}}$$

The uncertainty of the area for each wall, given in Table 24 was based off of each dimension that was cut assuming $^1/_8$" accuracy. The area of the inner frames and the uncertainty associated used the same assumptions, also shown in the table below. The k of the polyisocyanurate was calculated based on the thickness of the board. The uncertainty was assumed to be a thickness of $^1/_{64}$".

	Value	Error [%]
R-Value	17.8189	5%
Bottom Wall Area [m^2]	0.1148	4%
Top Wall Area [m^2]	0.1129	5%
Side Wall Area [m^2]	0.1065	2%
Back Wall Area [m^2]	1.0064	0%
Frame Area [m^2]	0.2632	11%
kvalue [W/m °C]	0.0021	5%

Table 24. The error associated with each wall area, the R-Value, and the thermal conductivity

The next heat transfer calculation was the heat transferred from the outer box to the inner box through the inner and outer frames surrounding the specimen, also called the flanking loss through the frame. The heat transfer and its uncertainty were calculated based on the equations shown below.

(12) $$Q_{fl,frame} = \frac{(T_{H,avg} - T_{C,avg})}{\#\ of\ frames}\frac{A}{R}$$

(13) $$U_{Q_{fl,frame}} = \sqrt{\left(\frac{U_A}{R}\frac{(T_{H,avg}-T_{C,avg})}{\#\ of\ frames}\right)^2 + \left(\frac{AU_R}{R^2}\frac{(T_{H,avg}-T_{C,avg})}{\#\ of\ frames}\right)^2 + \left(\frac{A}{R}\frac{T_{H,avg}}{\#\ of\ frames}\right)^2 + \left(\frac{A}{R}\frac{T_{C,avg}}{\#\ of\ frames}\right)^2}$$

The heat transfer through the inner frames from the outer edges of the specimen to the surrounding air, also called the flanking loss to the air, was calculated next using the equation below. It was determined that the heat transfer from the edges of the specimen through the outer frames was negligible because it was significantly thicker than any of the specimen. Consequently, heat transfer would not occur through two of the inner frames because they are insulated by the outer frames. For specimen with only two inner frames, this heat loss was assumed to be 0.

(14) $$Q_{fl,air} = 2 * 1.5 * 0.0254^2 k \left(\frac{48}{3} + \frac{30}{2}\right)(T_{spec,avg} - T_{room})$$

where n was the number of inner frames. $T_{spec, avg}$ was the average of the average hot and cold temperatures of the specimen and T_{room} was the room temperature. This equation was the same as equation 1, but with the area and length plugged into the equation. The uncertainty was calculation using the equation shown.

(15) $$U_{Q_{fl,air}} = sqrt\left(\left(2 * \left({}^{1}/_{64}\right) * 0.0254^2 (n-2) k \left(\frac{48}{3} + \frac{30}{2}\right)(T_{spec,avg} - Troom)2 + 2*1.5*0.02542(n-2)k318(Tspec, avg - Troom)2 + 2*1.5*0.02542n-2k*483218(Tspec, avg - Troom)2 + 2*1.5*0.02542(n-2)k218(Tspec, avg - Troom)2 + 2*1.5*0.02542n-2k*302218(Tspec, avg - Troom)2 + 2*1.5*0.02542n-2k483+302UTspec, avg2 + 2*1.5*0.02542n-2k483+302UTroom2 + 2*1.5*0.02542n-2Uk483+302(Tspec, avg - Troom)2$$

The uncertainty of the k value was calculated using the assumed uncertainty of 5% of the given R-value for the insulation board and the assumed accuracy of $^{1}/_{64}$" for its thickness.

The final heat transfer calculation that was performed was the amount of heat removed from the heat sink and the added to the heat source. This calculation was perfomed using the same equation shown below.

(16) $$Q_{duct} = \dot{m}Cp(T_{inlet} - T_{exit})$$

Equation 16 gave a positive number for the heat source and a negative number for the heat sink. The uncertainty of this heat transfer was given by the equation below. The specific heat of air is 1007J/kgK. The accuracy of the specific heat was assumed to be 10%.

(17) $$U_{Q_{duct}} = \sqrt{(U_{\dot{m}}Cp(T_{inlet} - T_{exit}))^2 + \left(\dot{m}U_{C_p}(T_{inlet} - T_{exit})\right)^2 + \left(\dot{m}CpU_{T_{inlet}}\right)^2 + \left(\dot{m}CpU_{T_{exit}}\right)^2}$$

The overall heat transfer through the specimen was calculated by summing all of the heat transfers. For calculating the heat transfer through the specimen and its uncertainty using the hot side, the following equations were used to calculate the heat transfer through the specimen.

(18) $$Q_{hot,specimen} = Q_{duct} + \sum_{i=1}^{5} Q_{wall_i} - Q_{fl,frame} + Q_{fl,air}$$

(19) $$U_{Q_{hot,specimen}} = \sqrt{\left(U_{Q_{duct}}\right)^2 + \sum_{i=1}^{5}\left(U_{Q_{wall_i}}\right)^2 + \left(U_{Q_{fl,frame}}\right)^2 + \left(U_{Q_{fl,air}}\right)^2}$$

The overall heat transfer through the specimen was also be calculated by summing all of the heat transfers for the heat sink, shown in the following equation. Technically the heat was being transferred to the cold side from the specimen so this number was

negative, but the absolute value should have been equal to the calculations from the cold side.

(20) $$Q_{cold,specimen} = Q_{duct} + \sum_{i=1}^{5} Q_{wall_i} + Q_{fl,frame}$$

(21) $$U_{Q_{cold,specimen}} = \sqrt{\left(U_{Q_{duct}}\right)^2 + \sum_{i=1}^{5}\left(U_{Q_{wall_i}}\right)^2 + \left(U_{Q_{fl,frame}}\right)^2}$$

The flux sensor was also measuring the same values calculated in equations 18 and 20. Since it recorded the same amount of time as all of the temperature sensors, the uncertainty of it follows the same format with the exception that B_{Flux} was based on 5% accuracy.

Overall R-Value

The overall R-value calculation was the same for all three methods of calculating the flux. In order to calculate the R-value and its uncertainty the following equations were used. Use the absolute value of the overall heat flux for these calculations.

(22) $$R = \frac{(T_{H,avg} - T_{C,avg})}{Q_{specmen}}$$

(23) $$U_R = \sqrt{\left(\frac{(T_{H,avg} - T_{C,avg})U_{Q_{specimen}}}{Q_{specmen}{}^2}\right)^2 + \left(\frac{U_{T_{H,avg}}}{Q_{specmen}}\right)^2 + \left(\frac{U_{T_{C,avg}}}{Q_{specmen}}\right)^2}$$

CHAPTER VII

RESULTS

All of the temperature measurements were recorded every second for two minutes. Pages 82-85 in the Appendix 1: Raw Data shows the average and the standard deviation of each surface and air temperature at each location for the hot and cold side of the hot and cold test for each sample. For most readings a thermocouple grid, a grid of nine thermocouples in parallel, was used resulting in one reading that was an average of nine readings. For the air and specimen measurements, nine individual thermocouple readings were used, so the error, which is calculated based on the standard deviation of all nine thermocouple readings, is shown instead of the standard deviation.

The ASTM standards required that the air temperature profile not vary more than 2K, or 2°C. Tables on pages 84 and 85show the overall temperature range calculated in the last column. The air temperature variance for the heat source side of the box was under 1°C for every test. For the cold side, there were two tests where the air temperature range was over 2°C. This standard was met in twenty of twenty two tests.

Although the mass flow rate was calculated for each specimen individually from the average velocity in the inner box air duct and the temperature of the inlet to the inner box, the temperature is relatively constant making the mass flow rate constant. The uncertainty is based off of the error in the velocity measurement and the error in the inner box inlet temperature. The average mass flow rate for the inner box for the hot and cold side for both hot and cold tests are shown in the table below, Table 25.

	Hot Box Inner Inlet			Cold Box Inner Inlet		
	$\dot{m}$ [kg/s]	Error [kg/s]	Error [%]	$\dot{m}$ [kg/s]	Error [kg/s]	Error [%]
Hot Test	0.071	0.0016	2%	0.057	0.0015	3%
Cold Test	0.068	0.0021	3%	0.056	0.0020	3%

Table 25.The average mass flow rate for the hot and cold inlets for the hot and cold tests

The mass flow rate and the inner box inlet and outlet temperatures were used to calculate the heat input into the hot box and the heat removed from the cold box at steady state conditions. The table on page 88 of Appendix 1: Raw Data Tables shows the inner box inlet and outlet temperatures for the heat source and the heat sink, for a hot and cold test. This table also shows the average and standard deviation of the room temperature, which was used to calculate the flanking loss to the surrounding air.

The inner and outer temperatures of each wall of the inner box, shown on pages 86and 87 in Appendix 1: Raw Data Tables, were used to calculate the heat transfer from the inner box to the outer box for the cold and the hot side. These heat transfers were added together and subtracted from the heat added or removed from the inner box by the ductwork. Flanking losses were estimated from the surface temperatures of the specimen and the room temperature and were also subtracted from the heat added or removed by the ductwork. The table showing the heat flux calculated using the heat sink and heat source calculations and the flux sensor is shown below in Table 26. The calculated R-value corresponding to these three methods of determining the flux are shown in SI units in Table 27 and in English units in Table 28.

Test	Specimen	Hot Box Flux [W/m^2]	Hot Box Error [W/m^2]	Hot Box Error [%]	Cold Box Flux [W/m^2]	Cold Box Error [W/m^2]	Cold Box Error [%]	Flux Sensor Flux [W/m^2]	Flux Sensor Error [W/m^2]	Flux Sensor Error [%]
Hot	Uncoated 1	431	138	32%	207	221	107%	119	26.97	23%
	Uncoated 2	509	125	25%	82.7	60.2	73%	123	27.63	22%
	Coated 1	474	127	27%	106	64.4	61%	107	24.04	22%
	Coated 2	437	140	32%	170	311	183%	29.3	61.87	211%
	Shiny	397	75.1	19%	83.6	121	144%	119	26.70	22%
	Uncoated 2x4 R13	369	122	33%	0.2	47.7	23387%	20.9	4.74	23%
	Coated 2x4 R13	341	120	35%	3.2	64.8	2052%	11.8	4.24	36%
	Coated 2x4 R13 w/o Studs	306	121	40%	34.5	54.6	158%	10.6	2.59	24%
	Uncoated Spray	273	123	45%	50.8	56.1	110%	13.9	3.36	24%
	Coated Spray	241	132	55%	41.5	60.4	146%	10.1	4.10	40%
	Uncoated 2x6 R13	262	122	47%	-14.3	63.8	447%	13.6	5.18	38%
Cold	Uncoated 1	144	104	72%	264	82.2	31%	116	26.35	23%
	Uncoated 2	158	145	92%	206	69.7	34%	107	24.20	23%
	Coated 1	128	132	103%	102	67.6	66%	98.7	22.91	23%
	Coated 2	146	177	121%	70.5	56.8	81%	108	24.58	23%
	Shiny	123	200	162%	264	65.5	25%	95.9	22.34	23%
	Uncoated 2x4 R13	152	115	76%	-163	58.5	36%	10.2	3.51	34%
	Coated 2x4 R13	88.1	66.0	75%	104	59.9	57%	10.0	3.41	34%
	Coated 2x4 R13 w/o Studs	53.3	66.7	125%	135	62.4	46%	13.8	5.46	40%
	Uncoated Spray	127	117	92%	110	54.7	50%	9.9	2.94	30%
	Coated Spray	96.5	119	123%	103	56.4	55%	11.2	3.75	34%
	Uncoated 2x6 R13	121	113	93%	38.1	60.3	158%	9.3	3.84	41%

Table 26. Flux and error, as calculated by the heat sink, heat source, and the flux sensor

		Hot Box			Cold Box			Flux Sensor		
Test	Specimen	R-Value [Km^2/W]	Error [Km^2/W]	Error [%]	R-Value [Km^2/W]	Error [Km^2/W]	Error [%]	R-Value [Km^2/W]	Error [Km^2/W]	Error [%]
Hot	Uncoated 1	0.0270	0.0087	32%	0.0562	0.0600	107%	0.0977	0.0222	23%
	Uncoated 2	0.0232	0.0057	25%	0.1430	0.104	73%	0.0961	0.0216	23%
	Coated 1	0.0243	0.0065	27%	0.1088	0.0663	61%	0.107	0.0242	23%
	Coated 2	0.0247	0.0080	32%	0.0637	0.117	183%	0.369	0.778	211%
	Shiny	0.0307	0.0058	19%	0.146	0.210	144%	0.102	0.0231	23%
	Uncoated 2x4 R13	0.0607	0.0200	33%	110	25702	23387%	1.07	0.244	23%
	Coated 2x4 R13	0.0665	0.0235	35%	7.19	148	2052%	1.93	0.694	36%
	Coated 2x4 R13 w/o Studs	0.0755	0.0300	40%	0.669	1.059	158%	2.18	0.533	24%
	Uncoated Spray	0.0825	0.0372	45%	0.443	0.489	110%	1.62	0.392	24%
	Coated Spray	0.0954	0.0521	55%	0.554	0.806	146%	2.26	0.915	40%
	Uncoated 2x6 R13	0.0876	0.0409	47%	-1.61	7.18	-447%	1.68	0.640	38%
Cold	Uncoated 1	0.0838	0.0608	73%	0.0457	0.0142	31%	0.104	0.0237	23%
	Uncoated 2	0.0715	0.0658	92%	0.0547	0.0185	34%	0.105	0.0239	23%
	Coated 1	0.0880	0.0910	103%	0.110	0.0727	66%	0.114	0.0266	23%
	Coated 2	0.0746	0.0901	121%	0.155	0.125	81%	0.101	0.0229	23%
	Shiny	0.0916	0.149	162%	0.0428	0.0106	25%	0.118	0.0276	23%
	Uncoated 2x4 R13	0.157	0.119	76%	-0.146	0.0526	-36%	2.33	0.803	34%
	Coated 2x4 R13	0.265	0.198	75%	0.223	0.128	57%	2.34	0.801	34%
	Coated 2x4 R13 w/o Studs	0.462	0.577	125%	0.183	0.0847	46%	1.79	0.710	40%
	Uncoated Spray	0.186	0.171	92%	0.215	0.107	50%	2.39	0.712	30%
	Coated Spray	0.246	0.302	123%	0.231	0.127	55%	2.12	0.713	34%
	Uncoated 2x6 R13	0.197	0.184	93%	0.625	0.989	158%	2.57	1.07	41%

Table 27. R-Value and the error of the R-Value, as calculated by the heat sink, heat source, and the flux sensor

Test	Specimen	Hot Box			Cold Box			Flux Sensor		
		R-Value [hft²°F/BTU]	Error [hft²°F/BTU]	Error [%]	R-Value [hft²°F/BTU]	Error [hft²°F/BTU]	Error [%]	R-Value [hft²°F/BTU]	Error [hft²°F/BTU]	Error [%]
Hot	Uncoated 1	0.153	0.0492	32%	0.319	0.341	107%	0.555	0.126	23%
	Uncoated 2	0.132	0.0326	25%	0.812	0.591	73%	0.546	0.123	23%
	Coated 1	0.138	0.0369	27%	0.618	0.377	61%	0.610	0.138	23%
	Coated 2	0.140	0.0452	32%	0.362	0.663	183%	2.09	4.42	211%
	Shiny	0.174	0.0332	19%	0.828	1.19	144%	0.581	0.131	23%
	Uncoated 2x4 R13	0.345	0.114	33%	624	145941	23387%	6.10	1.39	23%
	Coated 2x4 R13	0.378	0.133	35%	40.8	838	2052%	10.9	3.94	36%
	Coated 2x4 R13 w/o Studs	0.429	0.170	40%	3.80	6.01	158%	12.4	3.03	24%
	Uncoated Spray	0.468	0.211	45%	2.52	2.78	110%	9.21	2.23	24%
	Coated Spray	0.542	0.296	55%	3.15	4.58	146%	12.9	5.20	40%
	Uncoated 2x6 R13	0.497	0.232	47%	-9.12	40.8	-447%	9.56	3.63	38%
Cold	Uncoated 1	0.476	0.345	73%	0.259	0.0809	31%	0.590	0.135	23%
	Uncoated 2	0.406	0.374	92%	0.310	0.105	34%	0.597	0.136	23%
	Coated 1	0.500	0.517	103%	0.625	0.413	66%	0.647	0.151	23%
	Coated 2	0.424	0.511	121%	0.878	0.707	81%	0.571	0.130	23%
	Shiny	0.520	0.845	162%	0.243	0.060	25%	0.669	0.156	23%
	Uncoated 2x4 R13	0.889	0.675	76%	-0.830	0.299	-36%	13.2	4.56	34%
	Coated 2x4 R13	1.50	1.13	75%	1.27	0.729	57%	13.3	4.55	34%
	Coated 2x4 R13 w/o Studs	2.62	3.28	125%	1.04	0.481	46%	10.2	4.03	40%
	Uncoated Spray	1.05	0.97	92%	1.22	0.607	50%	13.6	4.04	30%
	Coated Spray	1.39	1.71	123%	1.31	0.719	55%	12.1	4.05	34%
	Uncoated 2x6 R13	1.12	1.04	93%	3.55	5.62	158%	14.6	6.06	41%

Table 28. The R-Value and its error converted into English units

The R-Value was converted into English units as a method of checking the accuracy of all three calculations. Since R-13 was used in four of the specimen tested, there should be four cases with an R-value near 13[hr ft^2°F/BTU], but instead all of the R-values are at least one order of magnitude smaller. In addition to being inaccurate, the hot and cold side R-Value calculations are not in agreement, for some cases even within the high error margins. This disagreement implies that there either is a heat transfer unaccounted for, or the measuring devices for the inlet and outlet of each inner box needs to be recalibrated.

The flux sensor does show that the specimens containing R-13 or spray foam insulation have R-values in the range of 9-14, which are two orders of magnitude greater than that of the OSB, but there still appear to be errors with the flux sensor. Although the R-value of the OSB can be definitively determined to be 0.57hr ft^2°F/BTU ± 23%, the R-value for every other run is less definitive. For the coated OSB, the R-value could said to be 0.61 hr ft^2°F/BTU ± 23%, but there was clearly an error in the second hot test. For the remaining tests the accuracy of the flux sensor is less certain. For the Uncoated 2x4 R-13 the calculated R-value for the hot and cold test are not within the uncertainty.

One factor affecting the accuracy of the flux sensor is the building material itself. Since each specimen in not homogeneous the flux through the specimen at one 5mm location could be significantly different than the flux at another 5mm location. Although the argument could be made that the OSB should have different locations that have the same R-Value, the wall segments have lumber separating insulation. Therefore the heat flux through the lumber connecting the OSB to the drywall will be higher than the section where the insulation is in place. Basically, if the flux sensor is not in the exact same location, the readings could be significantly different. In order to obtain an overall R-value the test must be run multiple times with the flux sensor in a different location each time.

The R-value of the paint cannot be determined due to the inaccuracy of the testing facility. Since the hot and cold side calculations in some cases were orders of magnitude away from the actual R-value of the specimen, it can be determined that the testing

facility does not function properly and further testing needs to be performed to improve the testing apparatus before it can be used to accurately determine the R-value of building materials.

In order to improve the testing facility differential thermocouples are recommended to reduce the error in the inlet and outlet temperatures to the inner box. Although the heat flux through the inner box walls is less than1% of the heat flux through the specimen, the temperature difference between the inside and outside surface temperatures of the inner box walls is sometimes less than 1°C, differential thermocouples could be used in this application as well, or it could be considered 0, and its uncertainty neglected.

CHAPTER VIII
CONCLUSIONS

The goal of this project was to design a testing apparatus to test the thermal conductivity of non-homogeneous materials. ASTM-C1363 gives specifications for the guarded hot box apparatus designed; so thus, numerous tests were performed to try to meet these standards.

The box design consisted of two sides, a heat source and a heat sink, each surrounded by a guard box that is maintained at the same temperature. The standard also had multiple specifications pertaining to the types of measuring devices and the number of measurements taken. The main restrictions were the number and size of the thermocouples. The proper number of thermocouples were built to standards and calibrated accordingly.

The next specification that required testing was that the velocity profile needed to be within 10% of the average velocity. Various types of flow straightening techniques were attempted, but these conditions were never achieved. The dampers added turbulence that made the air flow unpredictable. The single layer of pegboard 2” away from the top and the bottom of the inner box was the best case scenario of the damper configurations. This configuration was used for all of the tests despite its unsteady flow and the results would be below standards.

The second specification was that the air temperature profile could not range more than 2K. This velocity profile was recorded per standards and was met for most tests. There were two tests where the cold side that did not meet this requirement. No further testing was performed to understand why these two tests failed, but the remaining twenty did meet this requirement.

Since the mass flow rate needed to be known to calculate the heat transfer into and out of each box, the velocity of the inner and outer box needed to be accurate. The velocity profile of the inner box was calculated using a pitot tube using 1” pressure transmitter. The velocity was recorded 20 times at 10 different locations along two different axes for 120 seconds allowing an error of up to 4% for the inner box air flow.

The testing of all of the samples was conducted and the results have high errors, some well over 100%. The main culprit of these errors appears to be temperature differences where the error of each measurement is larger than the difference between the two measurements. To fix this problem with error, future studies will involve differential thermocouples, which will be used to measure the difference between the inlet and exit temperatures. Also, these will be recorded by grids with nine or more differential thermocouple so that the error will be reduced.

In addition to the high error, the results show that the heat transfer from the hot to the cold side and the heat transfer to the cold side from the hot side were not the same. Since both quantities represent the same heat transfer, the fact that they are not equal implies that something is wrong in the testing. This error is due to the measurements of the inlet and exit temperature difference, but is uncertain until further testing is performed.

In the testing a flux sensor was also used as a triple check for above calculations and measurements. Although the flux sensor only measures a 5mm diameter area, it can be used to approximately determine which specimen has the highest R-Value. Using the flux sensor is not ideal since all of the building materials are non-homogeneous and the 5mm diameter area is not representative of the entire area.

Since the R-value of each specimen was inconsistent, no appreciable difference could be determined from the tests performed. The testing facility does not function properly, and gives inaccurate R-values for specimen of known thermal resistance. There are some improvements that would hopefully increase the accuracy of the testing facility.

Looking Forward

In order to obtain better results from the flux sensor, multiple locations of the no homogeneous material should be measured. The error in the flux sensor measurements at the one location is due to the temperature difference between the thermocouples. Turning the inlet and outlet thermocouples into the differential thermocouples could

reduce the error in this calculation. Using differential thermocouples to measure the temperature difference across the face of the specimen could also improve the error and will not violate standards in any way.

If the improvements listed above do not improve the accuracy of the testing facility in calculating the R-value of specimen with known thermal resistances, the testing facility needs to be examined more closely. Perhaps there is a heat transfer occurring that is not currently being accounted for due to error in construction. Another possible explanation is that there are unknown air leaks causing a direct heat transfer, or the air circulation through the outer box is blocked in some way.

REFERENCES

[1] K. Daryabeigi, G. R. Cunnington and J. R. Knutson , 2011. "Combined Heat Transfer in High-Porosity High-Temperature Fibrous Insulation: Theory and Experimental Validation," *Journal of Thermodynamics and Heat Transfer,* pp. 536-546.

[2] B. Hallsted, 2010. "Eximaning Motivational Factors in Selecting Spray Polyurethane Foam Insulation in Residential Construction," ProQuest Dissertations and Theses, Prescott Valley, Arizona.

[3] D. Appelfeld and S. Svendsen, 2011. "Experimental analysis of energy performance of a ventilated window for reat recovery under controlled conditions," *Energy and Buildings,* pp. 3200-3207.

[4] A. Cooperman, J. Dieckmann and J. Brodrick, 2011. "Superinsulated Homes," *ASHRAE Journal,* pp. 66-72.

[5] P. E. Nelson and P. E. Totten, 2011. "Improving the Condensation Resistance of Fenestration by Considering Total Building Enclosure and Mechanical System Interaction," *Journal of Testing and Evaluation,* p. 6.

[6] E. Moreno, 1996. "Detailing That Weathers Better," *Architectual Record,* p. 42.

[7] J. Kosny, T. Petrie, D. Yarbrough, P. Childs, A. M. Syed and C. Blair, 2007. "Nano-Scale Insulation at Work," *ASHRAE,* p. 6.

[8] D. Kamman, 2011. *Building the Future,* The Science Channel.

[9] Thermablok, 2011. *Phone Price Quote,* Houston, Texas: Thermablok Aerogel Insulation.

[10] B. G. Schellinger, 2011. *Spaceloft Flexible Insulation Blanket,* Wisconsin: Proactive Technology.

[11] J. Xaman, L. Lira and J. Acre, 2009. "Analysis of temperature distribution in a guarded hot plate apparatus for measuring thermal conductivity," *Applied Thermal*

Engineering, pp. 617-623.

[12] ASTM, "ASTM-C-177-10, 2010. " *Standard Test Method for Steady-State Thermal Properties by Means of the Guarded-Hot-Plate Apparatus ,* p. 24.

[13] F. Asdrubali and G. Baldinelli, 2011. "Thermal transmittance measurements with the hot box method: Calibration experimental proceudres, and uncertainty analyses of three different approaches," *Energy and Buildings,* pp. 1618-1626.

APPENDIX 1

RAW DATA TABLES

Specimen	Length [in]	Error [in]	Height [in]	Error [in]	Width [in]	Error [in]
Uncoated 1	48.00	0.0156	23.56	0.0156	0.44	0.0156
Uncoated 2	48.00	0.0156	23.56	0.0156	0.44	0.0156
Coated 1	48.00	0.0156	24.06	0.0156	0.44	0.0156
Coated 2	48.00	0.0156	24.06	0.0156	0.44	0.0156
Shiny	47.94	0.0156	24.13	0.0156	0.44	0.0156
Uncoated 2x4 R13	48.00	0.0156	24.06	0.0156	4.25	0.0156
Coated 2x4 R13	48.00	0.0156	24.00	0.0156	4.25	0.0156
Coated 2x4 R13 w/o Studs	48.00	0.0156	24.06	0.0156	4.25	0.0156
Uncoated Spray	47.94	0.0156	24.00	0.0156	4.25	0.0156
Coated Spray	48.13	0.0156	24.06	0.0156	4.25	0.0156
Uncoated 2x6 R13	48.00	0.0156	24.13	0.0156	6.31	0.0156

Table 29. The dimensions and the error of each dimension for each specimen

		Hot Side of Specimen																		
	Location	1		2		3		4		5		6		7		8		9		Range
Test	Specimen	Temp [°C]	Stdev	Temp [°C]	Stdev	Temp [°C]	Stdev	Temp [°C]	Stdev	Temp [°C]	Stdev	Temp [°C]	Stdev	Temp [°C]	Stdev	Temp [°C]	Stdev	Temp [°C]	Stdev	
Hot	Uncoated 1	39.4	0.0971	38.7	0.0601	38.9	0.0755	39.0	0.0900	39.7	0.0807	40.9	0.1359	39.8	0.1266	41.4	0.1616	40.1	0.1179	2.7
	Uncoated 2	37.4	0.0801	37.5	0.0557	38.0	0.1133	37.8	0.1117	37.6	0.0715	39.0	0.1033	37.8	0.0771	39.7	0.1385	39.3	0.1380	2.3
	Coated 1	38.3	0.0893	38.3	0.0760	38.6	0.0608	38.9	0.1031	39.0	0.0790	39.6	0.1031	38.8	0.0787	39.7	0.0996	39.6	0.1237	1.5
	Coated 2	40.4	0.1575	39.8	0.1059	37.6	0.0713	37.4	0.0659	38.6	0.0750	39.7	0.0922	37.7	0.0618	38.8	0.0660	38.8	0.1163	3.0
	Shiny	37.3	0.0424	37.2	0.0430	37.6	0.0343	37.4	0.0550	37.7	0.0317	38.6	0.0290	38.7	0.0832	40.4	0.0726	38.3	0.0305	3.2
	Uncoated 2x4 R13	44.4	0.0627	44.5	0.0822	43.8	0.0897	45.0	0.0803	44.8	0.1393	44.7	0.1155	44.8	0.1132	44.8	0.1299	45.1	0.1697	1.3
	Coated 2x4 R13	44.8	0.0873	44.6	0.0895	45.0	0.0867	45.0	0.1256	44.7	0.0867	45.0	0.1099			44.8	0.1094	45.1	0.0887	0.5
	Coated 2x4 R13 w/o Studs	44.8	0.0947	44.6	0.0607	44.8	0.1078	45.0	0.1196	44.8	0.0898	44.8	0.0946	44.9	0.0927	44.9	0.0962	45.1	0.1422	0.5
	Uncoated Spray	44.5	0.0806	44.4	0.0628	44.5	0.0824	44.7	0.1062	44.6	0.0815	44.7	0.0915	44.7	0.1149	44.6	0.0897	44.6	0.1137	0.4
	Coated Spray	45.0	0.0839	45.0	0.0737	44.9	0.0864	45.3	0.2056	45.1	0.1045	45.2	0.1439	45.3	0.1158	45.2	0.1156	45.2	0.1156	0.4
	Uncoated 2x6 R13	45.4	0.1171	45.4	0.0766	45.5	0.2039	45.3	0.1190	45.5	0.0963	45.3	0.1369	45.3	0.1023	45.3	0.1007	45.6	0.1415	0.3
Cold	Uncoated 1	24.8	0.0507	24.0	0.0147	23.5	0.0210	23.7	0.0275	24.8	0.0207	26.2	0.0472	25.0	0.0333	26.7	0.0484	25.4	0.0473	3.2
	Uncoated 2	23.3	0.0734	23.5	0.0790	23.2	0.0334	23.0	0.0528	23.4	0.0344	24.4	0.0513	23.6	0.1186	25.9	0.2143	25.1	0.0567	2.9
	Coated 1	23.5	0.0837	23.9	0.1005	23.7	0.1025	23.0	0.1192	23.7	0.0720	24.4	0.0820	23.9	0.0725	24.7	0.0752	24.2	0.0658	1.7
	Coated 2	22.8	0.0761	23.3	0.0685	23.1	0.0661	23.2	0.0818	23.9	0.0711	24.5	0.0882	23.7	0.1113	25.2	0.1634	23.9	0.1055	2.4
	Shiny	22.8	0.0497	23.4	0.0341	23.2	0.0328	23.0	0.0772	24.0	0.0566	23.8	0.0397	24.1	0.2330	24.8	0.1632	25.2	0.1436	2.3
	Uncoated 2x4 R13	29.9	0.0793	29.8	0.0644	29.8	0.0934	30.1	0.1090	29.9	0.0909	30.1	0.1157			30.1	0.1005	30.2	0.1137	0.4
	Coated 2x4 R13	29.2	0.0108	29.1	0.0148	29.4	0.0000	29.3	0.0171	29.4	0.0028	29.5	0.0144	29.6	0.0142	29.4	0.0000	29.5	0.0125	0.4
	Coated 2x4 R13 w/o Studs	31.5	0.0155	31.5	0.0048	31.7	0.0154	31.6	0.0061	31.6	0.0000	31.7	0.0135	31.8	0.0147	31.8	0.0239	31.8	0.0068	0.3
	Uncoated Spray	29.8	0.0894	29.8	0.0637	30.0	0.1365	29.9	0.1220	30.0	0.1368	30.1	0.1295	30.1	0.1268	29.9	0.0963	30.2	0.1134	0.3
	Coated Spray	29.8	0.0786	29.8	0.0700	29.9	0.0979	29.8	0.1015	29.9	0.0782	30.0	0.0991	30.1	0.1130	30.0	0.0948	30.2	0.1126	0.4
	Uncoated 2x6 R13	29.9	0.0662	30.0	0.0893	30.1	0.1447	29.9	0.0945	30.1	0.0973	30.2	0.0934	30.0	0.0925	30.1	0.1026	30.4	0.1284	0.5

Table 30. The average and standard deviation of each surface temperature on the heat source side for hot and cold tests for each specimen, as well as the overall temperature range

		Cold Side of Specimen																		
	Location	1		2		3		4		5		6		7		8		9		Range
Test	Specimen	Temp [°C]	Stdev	Temp [°C]	Stdev	Temp [°C]	Stdev	Temp [°C]	Stdev	Temp [°C]	Stdev	Temp [°C]	Stdev	Temp [°C]	Stdev	Temp [°C]	Stdev	Temp [°C]	Stdev	
Hot	Uncoated 1	28.4	0.0392	27.8	0.0420	28.5	0.0338	29.0	0.0405	27.1	0.0518	26.8	0.0482	28.3	0.0352	28.4	0.0542	28.9	0.0350	2.3
	Uncoated 2	26.5	0.0720	26.1	0.0935	25.0	0.0881	25.2	0.0282	26.2	0.0484	27.2	0.1298	27.2	0.0192	26.4	0.0729	27.7	0.0287	2.6
	Coated 1	27.1	0.0555	27.3	0.0382	27.0	0.0506	26.2	0.0434	26.9	0.0494	27.3	0.0370	28.4	0.0387	28.2	0.0676	28.8	0.0277	2.6
	Coated 2	30.6	0.0461	30.6	0.0284	27.3	0.0967	27.5	0.1021	26.2	0.0669	24.3	0.0629	28.2	0.0777	27.7	0.0521	29.1	0.0270	6.3
	Shiny	26.5	0.1288	26.1	0.0895	25.1	0.0746	24.7	0.0475	25.7	0.0471	26.1	0.0998	27.2	0.0411	26.3	0.0730			2.6
	Uncoated 2x4 R13	22.9	0.0220	22.5	0.0236	22.2	0.0147	22.3	0.0179	22.2	0.0190	22.0	0.0338	21.6	0.0152	22.1	0.0224	22.5	0.0148	1.3
	Coated 2x4 R13	22.5	0.0269	22.3	0.0195	21.9	0.0187	22.0	0.0190	22.3	0.0145	22.3	0.0177	22.2	0.0196	21.9	0.0352	22.1	0.0199	0.6
	Coated 2x4 R13 w/o Studs	21.9	0.0158	21.9	0.0305	21.6	0.0279	21.6	0.0142	21.8	0.0281	21.8	0.0316	21.6	0.0158	21.7	0.0403	21.9	0.0384	0.3
	Uncoated Spray	22.2	0.0144	22.2	0.0141	21.9	0.0246	21.7	0.0172	22.0	0.0165	22.1	0.0310	22.1	0.0078	21.7	0.0161	22.5	0.0150	0.8
	Coated Spray	22.3	0.0526	22.4	0.0346	21.8	0.0138	22.0	0.0150	22.4	0.0254	22.0	0.0201	22.1	0.0281	22.1	0.0159	22.4	0.0611	0.6
	Uncoated 2x6 R13	22.6	0.0378	22.7	0.0307	22.2	0.0234	22.2	0.0110	22.3	0.0212	22.8	0.0454	22.5	0.0254	22.0	0.0213	22.9	0.0171	0.9
Cold	Uncoated 1	12.1	0.0765	12.4	0.0442	13.2	0.0408	13.9	0.0352	12.0	0.0554	11.6	0.0477	13.4	0.0442	13.3	0.0437	13.8	0.0252	2.3
	Uncoated 2	12.4	0.2118	12.0	0.1111	11.8	0.0881	11.8	0.0643	12.6	0.0357	13.2	0.0501	13.9	0.0380	12.6	0.0574	13.6	0.0647	2.1
	Coated 1	12.8	0.1897	12.2	0.0637	12.0	0.0700	12.1	0.0543	12.4	0.0479	11.8	0.0537	13.9	0.0549	12.8	0.0680	13.7	0.0560	2.1
	Coated 2	12.0	0.1114	12.6	0.0319	12.6	0.0571	12.3	0.0430	13.5	0.0434	11.5	0.0683	13.4	0.1240	13.4	0.0525	14.2	0.0611	2.7
	Shiny	12.6	0.0522	11.9	0.1006	12.3	0.0527	11.6	0.0544	12.3	0.1019	12.4	0.0453	13.3	0.0193	12.5	0.1236	13.7	0.0465	2.1
	Uncoated 2x4 R13	6.3	0.0392	6.2	0.0333	6.0	0.0499	5.9	0.0581	6.2	0.0371	6.0	0.0489	6.2	0.0290	6.6	0.0512	6.5	0.0351	0.7
	Coated 2x4 R13	6.1	0.0292	6.1	0.0366	6.0	0.0500	5.9	0.0482	5.9	0.0547	6.0	0.0425	6.0	0.0385	6.4	0.0237	6.1	0.0306	0.5
	Coated 2x4 R13 w/o Studs	6.9	0.0685	6.8	0.0586	6.9	0.0582	6.3	0.0677	6.8	0.0288	6.8	0.0464	7.1	0.0452	8.8	0.0421	7.1	0.0530	2.4
	Uncoated Spray	6.5	0.0151	6.5	0.0325	6.4	0.0140	6.0	0.0195	6.5	0.0149	6.3	0.0203	6.4	0.0440	6.6	0.0264	6.4	0.0193	0.6
	Coated Spray	6.3	0.0537	6.4	0.0335	6.0	0.0636	5.8	0.0615	6.3	0.0367	6.1	0.0605	6.3	0.0235	6.5	0.0224	6.4	0.0358	0.7
	Uncoated 2x6 R13	6.2	0.0514	6.2	0.0400	6.0	0.0339	5.8	0.0344	6.1	0.0463	6.1	0.0373	6.0	0.0566	7.2	0.0303	6.3	0.0404	1.4

Table 31. The average and standard deviation of each surface temperature on the heat source sink for hot and cold tests for each specimen, as well as the overall temperature range

Hot Air Profile																			
	Location	1		2		3		4		5		6		7		8		9		Range
Test	Specimen	Temp [°C]	Stdev	Temp [°C]	Stdev	Temp [°C]	Stdev	Temp [°C]	Stdev	Temp [°C]	Stdev	Temp [°C]	Stdev	Temp [°C]	Stdev	Temp [°C]	Stdev	Temp [°C]	Stdev	
Hot	Uncoated 1	44.2	0.2235	44.0	0.3179	44.4	0.2796	44.5	0.2979	44.5	0.3574	44.5	0.3129	44.8	0.2692	44.6	0.3468	44.4	0.2730	0.8
	Uncoated 2	43.8	0.2221	43.4	0.3217	43.6	0.2308	44.0	0.2630	43.7	0.3260	43.6	0.3024	44.1	0.2751	43.9	0.3310	43.6	0.2154	0.7
	Coated 1	43.9	0.2232	43.7	0.3233	43.9	0.2708	44.2	0.3166	44.1	0.3699	44.0	0.3035	44.4	0.3060	44.2	0.3739	44.0	0.2585	0.7
	Coated 2	43.6	0.2467	43.6	0.3261	43.6	0.2199	43.7	0.2480	43.5	0.2989	43.8	0.2575	43.8	0.2379	43.3	0.2778	43.8	0.2567	0.5
	Shiny	42.8	0.0171	42.5	0.0528	42.4	0.0332	42.6	0.0170	42.7	0.0408	42.5	0.0351	42.7	0.0160	42.5	0.0219	42.4	0.0228	0.4
	Uncoated 2x4 R13	45.2	0.2327	45.2	0.3381	45.2	0.2390	45.3	0.2693	45.4	0.3518	45.1	0.3230	45.3	0.2825	45.2	0.3199			0.2
	Coated 2x4 R13	45.6	0.2595	45.5	0.3647	45.3	0.2881	45.5	0.3185			45.3	0.3072	45.7	0.2480	45.5	0.2960	45.3	0.2128	0.4
	Coated 2x4 R13 w/o Studs	45.5	0.2550	45.4	0.3423	45.4	0.2629	45.4	0.2922	45.6	0.3480	45.3	0.3066	45.5	0.2529	45.3	0.3088	45.1	0.2395	0.5
	Uncoated Spray	45.4	0.2374	45.3	0.3292	45.3	0.2520	45.4	0.2917	45.4	0.3599	45.2	0.3169	45.4	0.3222	45.3	0.3157	45.1	0.2489	0.4
	Coated Spray	45.7	0.2784			45.6	0.3146	45.6	0.3578	45.7	0.4644	45.5	0.3914	45.8	0.3726	45.6	0.3811	45.5	0.2865	0.3
	Uncoated 2x6 R13	45.7	0.2250	45.5	0.3395	45.6	0.2466	45.4	0.2330	45.6	0.3507	45.3	0.2654	45.6	0.3163	45.4	0.2979	45.3	0.2375	0.4
Cold	Uncoated 1	29.3	0.0235	29.1	0.0346	29.3	0.0312	29.4	0.0172	29.4	0.0305	29.3	0.0150	29.5	0.0143	29.4	0.0128	29.3	0.0154	0.4
	Uncoated 2	28.8	0.1580	28.5	0.1997	27.9	0.0596	28.3	0.0403	28.6	0.0622	28.5	0.0700	29.0	0.3342	28.8	0.3691	28.5	0.0889	1.0
	Coated 1	28.9	0.2566	28.5	0.3134	28.3	0.3447	28.9	0.4179	28.7	0.3786	28.5	0.3011	28.9	0.1086	28.6	0.1099	28.5	0.1193	0.6
	Coated 2	28.7	0.2621	28.4	0.3468	28.4	0.2037	28.8	0.2118	29.0	0.3056	28.8	0.2541	29.1	0.3215	28.8	0.3319	28.8	0.2861	0.7
	Shiny	29.1	0.1698	28.7	0.2162	28.6	0.1428	28.8	0.1412	28.7	0.0994	28.6	0.0876	29.1	0.3732	28.9	0.3940	28.8	0.2562	0.5
	Uncoated 2x4 R13	30.2	0.2227	30.2	0.2959	30.1	0.2477	30.2	0.2730	30.4	0.3307	30.1	0.3010	30.3	0.2931	30.2	0.3419	30.1	0.2391	0.3
	Coated 2x4 R13	29.5	0.0088	29.4	0.0204	29.4	0.0000	29.6	0.0000	29.7	0.0131	29.4	0.0225	29.6	0.0000	29.5	0.0028	29.5	0.0062	0.3
	Coated 2x4 R13 w/o Studs	31.8	0.0000	31.8	0.0090	31.8	0.0062	31.9	0.0028	32.0	0.0000	31.7	0.0083	31.9	0.0241	31.8	0.0155	31.7	0.1366	0.3
	Uncoated Spray	30.3	0.2765	30.2	0.3575	30.0	0.2812	30.1	0.3519	30.4	0.4174	30.0	0.2892	30.3	0.3503	30.2	0.3056	30.1	0.2408	0.4
	Coated Spray	30.2	0.2672			30.1	0.2721	30.2	0.3281	30.3	0.3592	30.0	0.3060	30.2	0.3106	30.1	0.2949	30.1	0.2379	0.3
	Uncoated 2x6 R13	30.2	0.2726	30.1	0.3964	30.1	0.2999	30.2	0.2877	30.3	0.3688	30.0	0.2689	30.2	0.3706	30.0	0.3128	30.1	0.2380	0.3

Table 32.The average and standard deviation of each heat source air temperature for hot and cold tests for each specimen, as well as the overall temperature range

		Cold Air Profile																		
	Location	1		2		3		4		5		6		7		8		9		Range
Test	Specimen	Temp [°C]	Stdev	Temp [°C]	Stdev	Temp [°C]	Stdev	Temp [°C]	Stdev	Temp [°C]	Stdev	Temp [°C]	Stdev	Temp [°C]	Stdev	Temp [°C]	Stdev	Temp [°C]	Stdev	
Hot	Uncoated 1	23.8	0.1040	23.7	0.0559	23.1	0.0476	23.1	0.0213	23.1	0.0540	23.3	0.0604	23.7	0.0370	23.1	0.0403	23.1	0.0218	0.8
	Uncoated 2	21.1	0.0493	21.6	0.0319	21.0	0.0448	20.8	0.0647	20.9	0.0508	21.1	0.0852	21.0	0.0644	20.9	0.0364	20.7	0.0412	0.9
	Coated 1	22.8	0.0677	23.2	0.0316	22.4	0.0559	22.0	0.0437	22.5	0.0213	22.6	0.0236	22.2	0.0284	22.4	0.0243	22.6	0.0276	1.2
	Coated 2	27.0	0.0356	27.2	0.0182	22.5	0.0367	22.1	0.0597	22.4	0.0502	22.8	0.0320	22.7	0.1106	22.7	0.0738	22.4	0.0404	5.1
	Shiny	20.8	0.0612	21.1	0.0364	20.8	0.0476	20.5	0.0657	20.6	0.0411	20.9	0.0562	20.5	0.0683	20.5	0.0295	20.5	0.0366	0.6
	Uncoated 2x4 R13	21.2	0.0310	21.4	0.0238	21.3	0.0260	21.2	0.0180	21.3	0.0173	21.3	0.0188	21.0	0.0194	21.2	0.0159			0.4
	Coated 2x4 R13	21.5	0.0515	21.8	0.0577	21.4	0.0412	21.4	0.0441	21.8	0.0225	21.6	0.0188	21.2	0.0378	21.5	0.0298	21.2	0.0576	0.6
	Coated 2x4 R13 w/o Studs	21.1	0.0124	21.3	0.0156	21.0	0.0794	21.0	0.0593	21.1	0.0196	21.2	0.0303	20.6	0.0400	21.0	0.0144	21.0	0.0224	0.6
	Uncoated Spray	21.4	0.0185	21.5	0.0297	21.4	0.0257	21.1	0.0140	21.4	0.0317	21.5	0.0254	21.1	0.0195	21.4	0.0243	21.3	0.0111	0.5
	Coated Spray	21.8	0.1196	21.8	0.1063	21.4	0.0318	21.4	0.0378	21.8	0.0538	21.7	0.0564	21.3	0.0598	21.5	0.0562			0.5
	Uncoated 2x6 R13	21.4	0.0185	21.5	0.0290	21.6	0.0153	21.4	0.0137	21.5	0.0750	21.6	0.0672	20.9	0.0176	21.2	0.0185	21.4	0.0284	0.7
Cold	Uncoated 1	8.5	0.0774	7.8	0.0498	7.9	0.0386	8.0	0.0640	7.2	0.0667	8.6	0.0462	7.9	0.0575	7.5	0.0826	7.8	0.0461	1.4
	Uncoated 2	8.0	0.0649	7.8	0.0433	7.4	0.0734	7.5	0.1733	7.0	0.0539	8.2	0.0574	7.3	0.0897	7.2	0.0891	7.3	0.1528	1.2
	Coated 1	8.6	0.1476	7.8	0.0884	7.5	0.1277	7.6	0.2143	6.4	0.0510	7.7	0.0802	7.0	0.0798	6.8	0.1017	7.4	0.0811	2.2
	Coated 2	7.9	0.1249	7.6	0.0730	7.5	0.0596	7.1	0.0996	6.4	0.0524	7.8	0.0491	6.8	0.0609	6.7	0.0401	6.8	0.1099	1.5
	Shiny	7.9	0.1568	7.2	0.0484	7.3	0.0683	7.3	0.1193	6.7	0.1015	7.8	0.0546	6.9	0.1749	6.7	0.0781	7.1	0.0544	1.3
	Uncoated 2x4 R13	6.3	0.0667	5.7	0.0328	5.3	0.1116	5.7	0.1133	5.0	0.1046	5.9	0.0949	5.5	0.0675	5.5	0.0721	5.3	0.0653	1.3
	Coated 2x4 R13	6.3	0.0527	5.7	0.0276	5.5	0.0822	5.6	0.0837	5.0	0.1053	6.0	0.0991	5.3	0.0520	5.3	0.0422			1.3
	Coated 2x4 R13 w/o Studs	6.9	0.1188	6.3	0.1062	5.9	0.1382	6.0	0.1557	5.6	0.1282	6.6	0.1123	6.1	0.0895	6.1	0.0662			1.4
	Uncoated Spray	6.5	0.1066	6.0	0.0642	5.7	0.0600	6.0	0.1166	5.6	0.0792	6.4	0.0339	5.7	0.0599	5.9	0.0845	5.7	0.0445	0.9
	Coated Spray	6.3	0.1018	5.9	0.0814	5.6	0.0981	5.7	0.1342	5.3	0.1551	6.1	0.1367	5.4	0.0573	5.5	0.0484	5.3	0.1236	1.1
	Uncoated 2x6 R13	6.3	0.0699	5.7	0.0738	5.5	0.0222	5.7	0.0540	5.2	0.1073	6.1	0.0907	5.3	0.1191	5.4	0.1092			1.1

Table 33. The average and standard deviation of each heat sink air temperature for hot and cold tests for each specimen, as well as the overall temperature range

Hot Box																				
		Back Wall Outer		Back Wall Inner		Top Wall Outer		Top Wall Inner		Bottom Wall Outer		Bottom Wall Inner		Near Side Wall Outer		Near Side Wall Inner		Far Side Wall Outer		Far Side Wall Inner	
Test	Specimen	Avg	St Dev	Avg	St Dev	Avg	St Dev	Avg	St Dev	Avg	St Dev	Avg	St Dev	Avg	St Dev	Avg	St Dev	Avg	St Dev	Avg	St Dev
Hot	Uncoated 1	39.4	0.0257	44.1	0.1759	39.7	0.0480	44.5	0.1832	40.0	0.0372	45.8	0.2017	39.2	0.0255	44.5	0.0766	38.9	0.0160	43.8	0.0943
	Uncoated 2	35.4	0.1202	43.1	0.1648	35.1	0.1345	43.7	0.1645	37.5	0.1065	45.1	0.1832	35.2	0.1064	43.4	0.0688	34.7	0.1583	43.0	0.0721
	Coated 1	37.5	0.0788	43.6	0.1657	37.0	0.0917	43.6	0.1767	37.9	0.0973	45.5	0.1937	37.0	0.0739	43.0	0.0596	36.6	0.0798	43.4	0.0622
	Coated 2	41.3	1.2438	43.5	0.1575	40.8	1.2183	43.4	0.1637	40.7	1.2468	45.6	0.2473	41.9	1.7977	43.6	0.2837	40.9	1.2947	43.3	0.1822
	Shiny	35.3	0.1936	42.1	0.0794	35.3	0.2603	42.6	0.0974	37.5	0.1856	43.9	0.0993	35.1	0.1712	42.3	0.0729	35.0	0.2419	42.1	0.0864
	Uncoated 2x4 R13	37.4	0.1503	44.9	0.1571	37.6	0.0819	44.9	0.1674	38.4	0.1053	45.4	0.1795	37.4	0.1780	44.7	0.0762	36.8	0.1023	44.3	0.0753
	Coated 2x4 R13	37.9	0.0810	45.2	0.1525	38.1	0.0376	45.1	0.1610	39.3	0.0506	45.5	0.1692	37.6	0.1103	44.9	0.0763	37.8	0.0315	44.6	0.0704
	Coated 2x4 R13 w/o Studs	38.2	0.1181	45.3	0.1530	38.3	0.1534	45.3	0.1698	39.6	0.0939	45.9	0.1814	38.4	0.0993	45.0	0.0687	37.7	0.1255	44.7	0.0698
	Uncoated Spray	39.4	0.1184	45.1	0.1650	38.9	0.1370	45.1	0.1721	39.5	0.1111	45.4	0.1955	39.7	0.0945	45.0	0.0737	39.0	0.1472	44.7	0.0762
	Coated Spray	40.2	0.1284	45.5	0.1775	39.6	0.1486	45.5	0.1924	40.0	0.1148	45.7	0.2256	40.5	0.1015	45.4	0.0856	39.9	0.1259	45.1	0.0805
	Uncoated 2x6 R13	39.7	0.0647	45.5	0.1828	39.5	0.0703	45.6	0.1625	40.9	0.0462	45.9	0.1809	39.8	0.0594	45.5	0.0828	39.6	0.0701	45.2	0.0801
Cold	Uncoated 1	30.4	0.0491	29.2	0.0267	30.4	0.0271	29.8	0.0407	29.9	0.0404	30.8	0.0337	29.8	0.0428	29.9	0.0458	30.0	0.0314	29.3	0.0285
	Uncoated 2	29.5	0.0174	28.4	0.2033	29.4	0.0149	29.0	0.1692	29.4	0.0162	30.0	0.2023	28.8	0.0312	29.0	0.1184	29.3	0.0275	28.7	0.1113
	Coated 1	30.2	0.0274	28.5	0.1989	29.7	0.0125	29.1	0.1735	29.7	0.0298	30.1	0.2000	29.5	0.0218	29.1	0.1106	30.1	0.0292	28.9	0.0950
	Coated 2	30.2	0.0163	28.7	0.2030	29.8	0.0294	29.2	0.1706	29.7	0.0275	30.2	0.1951	29.5	0.0178	29.2	0.1078	30.0	0.0150	28.9	0.0887
	Shiny	30.3	0.0158	29.2	0.2035	29.9	0.0178	29.2	0.1524	29.8	0.0178	30.1	0.1862	29.7	0.0215	29.4	0.1206	30.0	0.0206	29.1	0.1118
	Uncoated 2x4 R13	27.9	0.0153	30.2	0.1675	28.1	0.0179	30.2	0.1624	28.1	0.0318	30.4	0.1749	27.3	0.0189	30.1	0.0790	27.6	0.0304	29.8	0.0751
	Coated 2x4 R13	29.2	0.0334	29.7	0.0352	29.2	0.0317	29.6	0.0285	28.9	0.0457	29.7	0.0410	28.6	0.0340	29.7	0.0360	29.0	0.0324	29.4	0.0452
	Coated 2x4 R13 w/o Studs	31.7	0.0313	31.9	0.0124	31.7	0.0244	31.9	0.0160	31.4	0.0163	32.0	0.0144	31.1	0.0332	32.0	0.0307	31.4	0.0318	31.7	0.0164
	Uncoated Spray	29.1	0.0159	30.2	0.1798	28.9	0.0148	30.1	0.1701	29.0	0.0130	30.3	0.1967	28.5	0.0305	30.2	0.0828	29.0	0.0147	30.0	0.0826
	Coated Spray	29.8	0.0303	30.2	0.1862	29.6	0.0113	30.2	0.1665	29.6	0.0180	30.3	0.1941	29.2	0.0259	30.3	0.0869	29.7	0.0158	30.0	0.0834
	Uncoated 2x6 R13	29.0	0.0148	30.2	0.1827	28.7	0.0165	30.1	0.1715	28.9	0.0145	30.2	0.1986	28.4	0.0192	30.2	0.0891	28.8	0.0233	30.0	0.0766

Table 34. The wall temperature average and standard deviation on the heat source side for hot and cold tests for each specimen

Cold Box																				
		Back Wall Outer Temp.		Back Wall Inner Temp. [°C]		Top Wall Outer Temp. [°C]		Top Wall Inner Temp.		Bottom Wall Outer Temp.		Bottom Wall Inner Temp.		Near Side Wall Outer Temp		Near Side Wall Inner Temp.		Far Side Wall Outer Temp.		Far Side Wall Inner Temp.	
Test	Specimen	Avg	St. Dev.	Avg	St. Dev.	Avg	St. Dev.	Avg	St. Dev.	Avg	St. Dev.	Avg	St. Dev.	Avg	St. Dev.	Avg	St. Dev.	Avg	St. Dev.	Avg	St. Dev.
Hot	Uncoated 1	22.0	0.0329	24.5	0.0282	21.7	0.0196	21.4	0.0584	23.8	0.0159	23.4	0.0255	23.0	0.0309	23.3	0.0281	24.9	0.0390	23.5	0.0455
	Uncoated 2	19.7	0.0250	22.2	0.0575	19.4	0.0330	19.3	0.0387	20.7	0.0196	21.2	0.0226	20.3	0.0222	20.8	0.0260	21.4	0.0169	21.2	0.0333
	Coated 1	21.3	0.0652	23.6	0.0520	21.2	0.0325	21.2	0.0377	21.9	0.0374	23.0	0.0160	21.9	0.0168	22.5	0.0162	22.3	0.0359	23.0	0.0271
	Coated 2	22.4	1.5720	24.8	1.4253	22.2	1.4502	22.2	1.7860	24.0	0.2941	23.8	1.4086	23.4	1.0796	23.4	1.6761	25.3	0.0702	23.8	1.5404
	Shiny	19.4	0.0185	21.0	0.0538	19.3	0.0342	19.4	0.0339	21.3	0.0838	21.3	0.0585	20.6	0.0709	20.9	0.0762	22.3	0.1072	21.0	0.0417
	Uncoated 2x4 R13	20.9	0.0339	21.6	0.0493	20.7	0.0381	20.9	0.0475	20.9	0.0892	21.7	0.0354	21.2	0.0391	21.6	0.0314	21.0	0.0539	21.3	0.0557
	Coated 2x4 R13	21.5	0.0665	21.7	0.1009	21.5	0.0663	21.3	0.1244	22.6	0.1446	21.9	0.0986	22.0	0.0711	21.5	0.0889	23.1	0.1099	21.8	0.1060
	Coated 2x4 R13 w/o Studs	21.1	0.0497	21.4	0.0483	21.0	0.0462	21.0	0.0449	22.4	0.0546	21.8	0.0360	21.8	0.0216	21.4	0.0441	22.3	0.0433	21.5	0.0378
	Uncoated Spray	21.4	0.0170	22.0	0.0321	21.0	0.0292	21.0	0.0637	22.9	0.0288	21.9	0.0417	21.7	0.0299	21.6	0.0300	23.1	0.0423	21.8	0.0476
	Coated Spray	21.7	0.0504	21.9	0.1164	21.4	0.0661	21.3	0.1390	23.1	0.0296	22.0	0.1007	22.1	0.0744	21.4	0.1094	24.0	0.0327	22.6	0.0990
	Uncoated 2x6 R13	21.4	0.0820	22.0	0.1147	21.1	0.0683	21.3	0.1406	22.5	0.0433	22.0	0.1092	21.6	0.0707	21.5	0.1208	22.0	0.0564	22.0	0.1223
Cold	Uncoated 1	7.0	0.0418	8.9	0.0867	6.7	0.0425	5.4	0.0939	13.1	0.0535	8.5	0.0620	8.7	0.0524	8.8	0.0603	15.0	0.0235	8.2	0.0640
	Uncoated 2	6.7	0.0294	8.5	0.0879	6.4	0.0429	5.5	0.0916	12.6	0.0407	8.0	0.0621	8.5	0.0548	7.9	0.0727	14.6	0.0199	7.9	0.0762
	Coated 1	7.4	0.0380	8.1	0.1511	6.4	0.0820	5.5	0.1961	14.7	0.0534	7.8	0.1367	9.2	0.1041	7.7	0.1256	18.6	0.0218	8.6	0.1466
	Coated 2	7.3	0.0321	8.0	0.0921	6.3	0.0606	5.3	0.1301	14.7	0.0488	7.7	0.0762	9.0	0.0632	7.6	0.0709	18.2	0.0191	7.9	0.1218
	Shiny	7.4	0.0527	7.9	0.1836	6.5	0.0902	5.5	0.1930	14.9	0.0527	7.7	0.1475	9.0	0.1153	7.5	0.1152	18.7	0.0248	8.3	0.1337
	Uncoated 2x4 R13	6.0	0.0358	5.7	0.0799	5.9	0.0361	5.3	0.1040	10.4	0.0375	6.4	0.0675	7.3	0.0549	6.5	0.0617	11.4	0.0175	6.7	0.0627
	Coated 2x4 R13	6.2	0.0348	5.8	0.0883	6.0	0.0470	5.2	0.1001	11.7	0.0411	6.4	0.0657	7.6	0.0487	6.5	0.0543	13.3	0.0324	6.8	0.0571
	Coated 2x4 R13 w/o Studs	6.9	0.0590	6.4	0.1580	6.6	0.0828	5.5	0.1859	13.6	0.0571	7.1	0.1383	8.5	0.1024	7.2	0.1231	15.6	0.0352	7.5	0.1434
	Uncoated Spray	6.2	0.0323	6.0	0.0579	5.9	0.0241	5.1	0.0668	11.6	0.0322	6.9	0.0507	7.4	0.0410	7.1	0.0519	13.6	0.0398	6.9	0.0498
	Coated Spray	6.4	0.0377	6.0	0.0844	6.0	0.0402	5.1	0.0976	12.0	0.0319	6.8	0.0694	7.9	0.0492	7.4	0.0592	14.3	0.0267	6.8	0.1063
	Uncoated 2x6 R13	6.1	0.0325	5.8	0.1210	5.8	0.0569	5.2	0.1329	11.1	0.0329	6.4	0.1002	7.3	0.0564	6.3	0.0763	12.3	0.0191	6.5	0.0698

Table 35. The wall temperature average and standard deviation on the heat sink side for hot and cold tests for each specimen

				Hot Box								Cold Box							
		Room Temp.		Inner Box Inlet Temp.		Inner Box Outlet Temp.		Avg Air Temp.		Avg Surface Temp.		Inner Box Inlet Temp.		Inner Box Outlet Temp.		Avg Air Temp.		Avg Surface Temp.	
Test	Specimen	Avg.	StDev	Avg	St Dev	Avg	St Dev	Avg	Error	Avg	Error	Avg	St. Dev.	Avg	St. Dev.	Avg	Error	Avg	Error
Hot	Uncoated 1	28.4	0.1147	47.0	0.5481	43.4	0.1402	44.5	0.029	39.8	0.182	22.1	0.0602	23.6	0.0356	23.3	0.019	28.1	0.169
	Uncoated 2	23.4	0.1193	46.4	0.5009	42.1	0.1401	43.7	0.249	38.2	0.180	20.1	0.0691	21.1	0.0396	21.0	0.170	26.4	0.174
	Coated 1	26.0	0.5185	46.8	0.5316	42.7	0.1322	44.1	0.263	39.0	0.177	22.0	0.1585	22.8	0.0317	22.5	0.169	27.5	0.169
	Coated 2	31.1	3.1730	46.9	0.5260	43.2	0.3251	43.6	0.242	38.8	0.178	23.6	1.0512	24.0	1.5541	23.5	0.171	27.9	0.172
	Shiny	25.8	0.2990	44.7	0.0608	41.5	0.1118	42.6	0.168	38.1	0.170	21.0	0.1334	21.5	0.0485	20.7	0.170	26.0	0.186
	Uncoated 2x4 R13	25.4	0.9353	46.6	0.4988	43.6	0.1480	44.0	0.243	44.7	0.183	21.9	0.1036	21.4	0.0754	21.2	0.158	22.3	0.167
	Coated 2x4 R13	26.4	0.5063	46.6	0.4928	43.9	0.1376	45.5	0.239	44.9	0.190	22.5	0.2366	21.8	0.1097	21.5	0.169	22.2	0.167
	Coated 2x4 R13 w/o Studs	36.1	0.4436	46.6	0.5021	44.3	0.1443	45.4	0.255	44.9	0.180	23.9	0.0399	21.5	0.0291	21.0	0.169	21.8	0.168
	Uncoated Spray	30.4	0.2342	46.5	0.5132	44.5	0.1380	45.3	0.259	44.6	0.178	22.7	0.0647	21.7	0.0341	21.3	0.167	22.1	0.167
	Coated Spray	34.4	0.0597	46.7	0.5745	45.1	0.1405	45.6	0.274	45.1	0.185	24.0	0.1370	22.1	0.1168	21.6	0.163	22.2	0.168
	Uncoated 2x6 R13	32.6	0.2527	46.5	0.5101	44.7	0.1498	45.1	0.250	45.4	0.186	24.0	0.1777	21.7	0.1342	21.4	0.169	22.5	0.168
Cold	Uncoated 1	23.1	0.0818	31.3	0.0434	29.9	0.0324	29.3	0.167	24.9	0.168	8.4	0.0959	8.5	0.0758	7.9	0.171	12.9	0.170
	Uncoated 2	23.5	0.0361	30.6	0.4679	29.1	0.1613	28.5	0.210	23.9	0.178	9.1	0.0877	8.4	0.0485	7.5	0.179	12.7	0.178
	Coated 1	22.7	0.0373	30.5	0.5041	29.3	0.1533	28.6	0.251	23.9	0.176	10.9	0.1891	9.0	0.1372	7.4	0.184	12.6	0.176
	Coated 2	22.2	0.0545	30.7	0.5430	29.4	0.1605	28.8	0.251	23.7	0.179	10.4	0.1310	8.3	0.0425	7.2	0.175	12.8	0.173
	Shiny	22.4	0.0449	30.6	0.4816	29.4	0.1476	28.8	0.227	23.8	0.183	9.5	0.1708	9.9	0.1432	7.2	0.180	12.5	0.174
	Uncoated 2x4 R13	18.4	0.0497	31.1	0.4973	29.8	0.1416	30.2	0.252	30.0	0.189	11.1	0.1259	7.0	0.0649	5.6	0.176	6.2	0.169
	Coated 2x4 R13	20.4	0.0501	30.2	0.0295	29.6	0.0372	29.5	0.167	29.4	0.167	8.3	0.1053	7.0	0.0669	5.6	0.164	6.1	0.169
	Coated 2x4 R13 w/o Studs	25.4	0.0372	32.5	0.0339	32.0	0.0473	31.8	0.169	31.7	0.167	9.8	0.1766	7.6	0.1282	6.2	0.173	7.1	0.170
	Uncoated Spray	19.5	0.0682	30.9	0.5075	29.9	0.1283	30.2	0.271	30.0	0.183	7.9	0.0679	7.0	0.0411	6.0	0.174	6.4	0.167
	Coated Spray	20.6	0.1102	30.8	0.5204	30.1	0.1474	30.1	0.244	29.9	0.178	8.2	0.1138	7.0	0.0684	5.7	0.182	6.2	0.169
	Uncoated 2x6 R13	18.6	0.0378	30.8	0.4968	29.9	0.1316	29.9	0.267	30.1	0.180	8.2	0.1311	6.7	0.0680	5.6	0.166	6.2	0.169

Table 36. The average temperature and standard deviation of the inlet and outlet of each inner box as well as the room temperature

APPENDIX 2

QUALIFYING TESTS

FLOW STRAIGHTENING

	1	2	3	4	5
A	43	145	19	60	27
B	57	32	145	110	25
C	67	24	82	101	38

	1	2	3	4	5
A	27%	147%	68%	2%	54%
B	23%	57%	96%	49%	66%
C	7%	62%	31%	62%	39%

Table 37. Velocity profile of configuration A, cold box, case 2

	1	2	3	4	5
A	0	1	5	0	0
B	1	66	13	60	5
C	3	18	0	59	0

	1	2	3	4	5
A	0	1	5	0	0
B	1	66	13	60	5
C	3	24	0	66	0

	1	2	3	4	5
A	N/A	0%	0%	N/A	N/A
B	0%	0%	0%	0%	0%
C	0%	33%	N/A	12%	N/A

	1	2	3	4	5
A	100%	17%	317%	100%	100%
B	97%	128%	55%	107%	83%
C	83%	21%	100%	261%	100%

Table 38. Velocity profile of configuration A, cold box, case 4

	1	2	3	4	5
A	66	315	125	0	155
B	330	154	66	81	9
C	153	220	310	345	74

	1	2	3	4	5
A	70	320	152	0	158
B	370	180	81	99	12
C	169	230	420	440	79

	1	2	3	4	5
A	6%	2%	22%	N/A	2%
B	12%	17%	23%	22%	33%
C	10%	5%	35%	28%	7%

	1	2	3	4	5
A	50%	133%	2%	100%	15%
B	153%	21%	47%	35%	92%
C	34%	8%	50%	61%	69%

Table 39. Velocity profile of configuration A, cold box, case 5

	1	2	3	4	5
A	38	66	35	0	62
B	94	48	66	51	12
C	119	65	98	185	17

	1	2	3	4	5
A	42	73	44	0	62
B	107	65	70	60	15
C	142	79	123	215	23

	1	2	3	4	5
A	11%	11%	26%	N/A	0%
B	14%	35%	6%	18%	25%
C	19%	22%	26%	16%	35%

	1	2	3	4	5
A	5%	65%	6%	100%	47%
B	71%	4%	16%	6%	77%
C	22%	32%	4%	88%	81%

Table 40. Velocity profile of configuration A, cold box, case 6

	1	2	3	4	5
A	35	25	50	1	86
B	270	99	153	134	2
C	210	133	240	285	240

	1	2	3	4	5
A	47	40	62	1	90
B	285	130	156	145	3
C	230	144	260	360	250

	1	2	3	4	5
A	34%	60%	24%	0%	5%
B	6%	31%	2%	8%	50%
C	10%	8%	8%	26%	4%

	1	2	3	4	5
A	6%	26%	28%	98%	101%
B	102%	17%	12%	1%	98%
C	6%	41%	6%	37%	4%

Table 41. Velocity profile of configuration A, cold box, case 7

	1	2	3	4	5
A	0	0	10	0	0
B	0	28	0	1	1
C	0	0	21	0	5

	1	2	3	4	5
A	0	3	13	0	0
B	0	31	0	2	5
C	0	0	27	2	35

	1	2	3	4	5
A	N/A	N/A	30%	N/A	N/A
B	N/A	11%	N/A	100%	400%
C	N/A	N/A	29%	N/A	600%

	1	2	3	4	5
A	100%	42%	342%	100%	100%
B	100%	334%	100%	78%	56%
C	100%	100%	167%	89%	122%

Table 42. Velocity profile of configuration A, hot box, case 1

	1	2	3	4	5
A	0	11	8	7	0
B	0	0	36	0	15
C	29	3	45	0	29

	1	2	3	4	5
A	0	16	10	11	1
B	0	1	42	0	21
C	34	3	54	2	35

	1	2	3	4	5
A	N/A	45%	25%	57%	N/A
B	N/A	N/A	17%	N/A	40%
C	17%	0%	20%	N/A	21%

	1	2	3	4	5
A	100%	111%	41%	41%	92%
B	100%	96%	239%	100%	57%
C	35%	87%	112%	96%	37%

Table 43. Velocity profile of configuration A, hot box, case 2

	1	2	3	4	5
A	0	16	2	9	1
B	0	0	52	2	7
C	45	19	68	10	38

	1	2	3	4	5
A	0	20	6	15	1
B	0	1	57	3	9
C	52	24	72	16	43

	1	2	3	4	5
A	N/A	25%	200%	67%	0%
B	N/A	N/A	10%	50%	29%
C	16%	26%	6%	60%	13%

	1	2	3	4	5
A	100%	157%	43%	71%	86%
B	100%	96%	316%	81%	39%
C	25%	44%	81%	66%	5%

Table 44. Velocity profile of configuration A, hot box, case 3

	1	2	3	4	5
A	0	25	20	25	0
B	0	3	71	4	16
C	65	37	89	20	47

	1	2	3	4	5
A	0	33	30	33	0
B	0	3	75	10	35
C	71	40	100	33	55

	1	2	3	4	5
A	N/A	32%	50%	32%	N/A
B	N/A	0%	6%	150%	119%
C	9%	8%	12%	65%	17%

	1	2	3	4	5
A	100%	75%	51%	75%	100%
B	100%	86%	236%	68%	18%
C	22%	31%	70%	52%	8%

Table 45. Velocity profile of configuration A, hot box, case 4

	1		2		3		4		5
A									
B									
C	102	12	50	27	92	32	43	0	168

	1		2		3		4		5
A									
B									
C	117	17	67	42	110	46	65	0	188

	1		2		3		4		5
A									
B									
C	15%	42%	34%	56%	20%	44%	51%		12%

	1		2		3		4		5
A									
B									
C	67%	78%	11%	47%	54%	40%	17%	100%	172%

Table 46. Velocity profile of configuration A, hot box, case 6

	1		2		3		4		5
A									
B									
C	159	39	67	36	72	42	75	28	107

	1		2		3		4		5
A									
B									
C	184	50	90	54	89	52	109	52	130

	1		2		3		4		5
A									
B									
C	16%	28%	34%	50%	24%	24%	45%	86%	21%

	1		2		3		4		5
A									
B									
C	115%	44%	2%	44%	1%	41%	15%	50%	49%

Table 47. Velocity profile of configuration A, hot box, case 7

	1		2		3		4		5
A									
B									
C	235	38	43	98	91	59	86	7	71

	1		2		3		4		5
A									
B									
C	250	50	55	210	117	79	119	10	95

	1		2		3		4		5
A									
B									
C	6%	32%	28%	114%	29%	34%	38%	43%	34%

	1		2		3		4		5
A									
B									
C	155%	54%	49%	62%	9%	27%	8%	91%	13%

Table 48. Velocity profile of configuration A, hot box, case 8

	1		2		3		4		5
A									
B									
C	330	16	86	35	82	66	94	8	79

	1		2		3		4		5
A									
B									
C	360	21	96	70	107	147	113	24	97

	1		2		3		4		5
A									
B									
C	9%	31%	12%	100%	30%	123%	20%	200%	23%

	1		2		3		4		5
A									
B									
C	239%	82%	11%	48%	7%	5%	2%	84%	13%

Table 49. Velocity profile of configuration A, hot box, case 9

	1	2	3	4	5
A	22	0	64	3	0
B	7	48	30	17	33
C	2	0	29	61	33

	1	2	3	4	5
A	28	4	70	3	0
B	15	56	34	25	37
C	5	0	33	84	37

	1	2	3	4	5
A	27%	N/A	9%	0%	N/A
B	114%	17%	13%	47%	12%
C	150%	N/A	14%	38%	12%

	1	2	3	4	5
A	29%	90%	245%	85%	100%
B	64%	72%	6%	30%	16%
C	88%	100%	9%	155%	23%

Table 50.Velocity profile of configuration B, cold box, case 1

	1	2	3	4	5
A	0	0	1	1	0
B	25	5	10	0	0
C	11	0	0	17	43

	1	2	3	4	5
A	2	0	9	1	0
B	37	12	21	1	0
C	25	0	0	31	48

	1	2	3	4	5
A	N/A	N/A	800%	0%	N/A
B	48%	140%	110%	N/A	N/A
C	127%	N/A	N/A	82%	12%

	1	2	3	4	5
A	29%	100%	257%	29%	100%
B	179%	23%	40%	95%	100%
C	3%	100%	100%	37%	160%

Table 51.Velocity profile of configuration B, cold box, case 3

	1	2	3	4	5
A	5	52	10	6	1
B	77	18	22	23	0
C	14	0	36	43	1

	1	2	3	4	5
A	11	73	33	12	5
B	102	29	44	49	8
C	22	2	48	59	5

	1	2	3	4	5
A	120%	40%	230%	100%	400%
B	32%	61%	100%	113%	N/A
C	57%	N/A	33%	37%	400%

	1	2	3	4	5
A	62%	200%	3%	57%	86%
B	141%	37%	11%	3%	89%
C	22%	96%	83%	122%	87%

Table 52.Velocity profile of configuration B, cold box, case 5

	1	2	3	4	5
A	7	14	3	0	1
B	8	9	7	0	0
C	0	0	1	49	1

	1	2	3	4	5
A	17	36	5	0	1
B	9	13	8	2	0
C	9	0	2	72	2

	1	2	3	4	5
A	143%	157%	67%	N/A	0%
B	13%	44%	14%	N/A	N/A
C	N/A	N/A	100%	47%	100%

	1	2	3	4	5
A	43%	198%	52%	100%	88%
B	52%	96%	34%	82%	100%
C	67%	100%	89%	345%	89%

Table 53. Velocity profile of configuration B, cold box, case 6

	1	2	3	4	5
A	1	0	42	0	2
B	68	51	1	3	0
C	1	1	27	4	24

	1	2	3	4	5
A	1	0	51	0	4
B	80	68	1	8	0
C	24	1	30	11	27

	1	2	3	4	5
A	0%	N/A	21%	N/A	100%
B	18%	33%	0%	167%	N/A
C	2300%	0%	11%	175%	13%

	1	2	3	4	5
A	90%	100%	360%	100%	70%
B	164%	113%	96%	80%	100%
C	17%	93%	90%	50%	70%

Table 54. Velocity profile of configuration B, cold box, case 7

	1	2	3	4	5
A	13	1	38	0	2
B	107	87	7	13	0
C	17	0	99	38	82

	1	2	3	4	5
A	21	1	42	0	36
B	129	114	16	19	0
C	42	1	104	134	86

	1	2	3	4	5
A	62%	0%	11%	N/A	1700%
B	21%	31%	129%	46%	N/A
C	147%	N/A	5%	253%	5%

	1	2	3	4	5
A	10%	94%	160%	100%	23%
B	140%	104%	77%	67%	100%
C	51%	99%	68%	43%	39%

Table 55. Velocity profile of configuration B, cold box, case 8

	1	2	3	4	5
A	1	0	1	1	0
B	0	6	1	0	0
C	2	1	1	25	0

	1	2	3	4	5
A	1	0	1	1	0
B	0	10	1	0	1
C	4	1	2	29	10

	1	2	3	4	5
A	0%	N/A	0%	0%	N/A
B	N/A	67%	0%	N/A	N/A
C	100%	0%	100%	16%	N/A

	1	2	3	4	5
A	67%	100%	67%	67%	100%
B	100%	321%	47%	100%	74%
C	60%	87%	80%	260%	33%

Table 56. Velocity profile of configuration B, cold box, case 9

	1	2	3	4	5
A	2	1	1	1	1
B	33	19	2	1	0
C	1	0	7	25	3

	1	2	3	4	5
A	5	1	15	2	1
B	44	44	19	1	0
C	1	0	13	36	5

	1	2	3	4	5
A	150%	0%	1400%	100%	0%
B	33%	132%	850%	0%	N/A
C	0%	N/A	86%	44%	67%

	1	2	3	4	5
A	17%	67%	167%	50%	67%
B	136%	93%	36%	94%	100%
C	89%	100%	10%	235%	56%

Table 57. Velocity profile of configuration B, cold box, case 10

	1	2	3	4	5
A	5	2	2	5	1
B	54	2	8	8	0
C	8	0	1	38	5

	1	2	3	4	5
A	12	9	5	11	3
B	64	9	18	20	2
C	39	2	7	55	8

	1	2	3	4	5
A	140%	350%	150%	120%	200%
B	19%	350%	125%	150%	N/A
C	388%	N/A	600%	45%	60%

	1	2	3	4	5
A	55%	0%	36%	45%	64%
B	219%	70%	30%	24%	95%
C	44%	94%	75%	185%	60%

Table 58. Velocity profile of configuration B, cold box, case 11

	1	2	3	4	5
A	19	6	3	4	1
B	2	31	1	5	1
C	49	0	2	20	71

	1	2	3	4	5
A	28	17	9	12	5
B	16	42	16	12	7
C	70	7	32	70	77

	1	2	3	4	5
A	47%	183%	200%	200%	400%
B	700%	35%	1500%	140%	600%
C	43%	N/A	1500%	250%	8%

	1	2	3	4	5
A	126%	11%	42%	23%	71%
B	32%	174%	36%	36%	70%
C	49%	91%	57%	13%	86%

Table 59. Velocity profile of configuration B, cold box, case 12

	1	2	3	4	5
A	6	4	15	8	1
B	49	19	3	40	1
C	50	8	17	52	31

	1	2	3	4	5
A	18	26	25	20	3
B	72	27	36	72	6
C	88	26	33	107	36

	1	2	3	4	5
A	200%	550%	67%	150%	200%
B	47%	42%	1100%	80%	500%
C	76%	225%	94%	106%	16%

	1	2	3	4	5
A	5%	19%	59%	11%	84%
B	86%	29%	40%	72%	89%
C	54%	62%	44%	77%	25%

Table 60. Velocity profile of configuration B, cold box, case 13

	1	2	3	4	5
A	19	44	0	46	1
B	35	3	16	13	1
C	16	15	44	9	16

	1	2	3	4	5
A	20	44	1	47	3
B	37	3	19	16	1
C	17	16	45	11	16

	1	2	3	4	5
A	5%	0%	N/A	2%	200%
B	6%	0%	19%	23%	0%
C	6%	7%	2%	22%	0%

	1	2	3	4	5
A	13%	96%	98%	107%	91%
B	150%	79%	22%	1%	93%
C	20%	24%	117%	51%	22%

Table 61. Velocity profile of configuration D, Hot box, case 3

	1	2	3	4	5
A	0	48	6	56	3
B	14	14	4	18	8
C	8	1	21	13	22

	1	2	3	4	5
A	0	49	15	58	5
B	14	16	8	20	12
C	25	16	26	1	9

	1	2	3	4	5
A	N/A	2%	150%	4%	67%
B	0%	14%	100%	11%	50%
C	213%	1500%	24%	-92%	-59%

	1	2	3	4	5
A	100%	102%	56%	138%	83%
B	9%	17%	53%	48%	22%
C	16%	40%	65%	51%	9%

Table 62. Velocity profile of configuration D, hot box, case 4

	1	2	3	4	5
A	5	25	3	27	8
B	23	8	5	10	26
C	1	9	2	8	0

	1	2	3	4	5
A	5	27	5	36	13
B	24	10	9	12	29
C	1	10	4	10	0

	1	2	3	4	5
A	0%	8%	67%	33%	63%
B	4%	25%	80%	20%	12%
C	0%	11%	100%	25%	N/A

	1	2	3	4	5
A	68%	69%	74%	105%	32%
B	51%	42%	55%	29%	76%
C	78%	111%	33%	100%	100%

Table 63. Velocity profile of configuration D, hot box, case 5

	1	2	3	4	5
A	0	42	5	52	0
B	18	4	44	18	25
C	9	10	26	8	3

	1	2	3	4	5
A	0	42	12	53	5
B	21	8	46	21	31
C	10	12	37	11	5

	1	2	3	4	5
A	N/A	0%	140%	2%	N/A
B	17%	100%	5%	17%	24%
C	11%	20%	42%	38%	67%

	1	2	3	4	5
A	100%	99%	60%	149%	88%
B	17%	75%	91%	17%	19%
C	27%	16%	140%	27%	69%

Table 64. Velocity profile of configuration D, hot box, case 6

	1		2		3		4		5
A									
B									
C	205	9	94	25	205	80	123	45	139

	1		2		3		4		5
A									
B									
C	235	25	128	44	235	97	144	57	165

	1		2		3		4		5
A									
B									
C	15%	178%	36%	76%	15%	21%	17%	27%	19%

	1		2		3		4		5
A									
B									
C	93%	85%	3%	70%	93%	22%	17%	55%	33%

Table 65. Velocity profile of configuration E, hot box, case 3

	1		2		3		4		5
A									
B									
C	37	240	39	54	69	75	22	105	113

	1		2		3		4		5
A									
B									
C	43	285	57	74	76	91	38	172	151

	1		2		3		4		5
A									
B									
C	16%	19%	46%	37%	10%	21%	73%	64%	34%

	1		2		3		4		5
A									
B									
C	59%	171%	50%	34%	25%	14%	69%	43%	36%

Table 66. Velocity profile of configuration F, hot box, case 1

	1		2		3		4		5
A									
B									
C	95	0	16	12	14	20	16	26	47

	1		2		3		4		5
A									
B									
C	109	1	26	22	36	32	30	37	57

	1		2		3		4		5
A									
B									
C	15%	N/A	63%	83%	157%	60%	88%	42%	21%

	1		2		3		4		5
A									
B									
C	208%	98%	37%	49%	24%	21%	31%	5%	57%

Table 67. Velocity profile of configuration F, hot box, case 2

	1		2		3		4		5
A									
B									
C	1	7	2	0	10	2	2	1	1

	1		2		3		4		5
A									
B									
C	3	19	9	10	28	12	9	7	3

	1		2		3		4		5
A									
B									
C	200%	171%	350%	N/A	180%	500%	350%	600%	200%

	1		2		3		4		5
A									
B									
C	71%	86%	21%	29%	171%	0%	21%	43%	71%

Table 68. Velocity profile of configuration F, hot box, case 3

	1		2		3		4		5
A									
B									
C	7	32	15	10	42	26	16	27	20

	1		2		3		4		5
A									
B									
C	26	41	29	18	54	38	24	37	37

	1		2		3		4		5
A									
B									
C	271%	28%	93%	80%	29%	46%	50%	37%	85%

	1		2		3		4		5
A									
B									
C	40%	32%	21%	49%	73%	15%	28%	15%	3%

Table 69. Velocity profile of configuration F, hot box, case 4

	1		2		3		4		5
A									
B									
C	63	32	136	13	50	19	18	20	46

	1		2		3		4		5
A									
B									
C	77	70	180	40	56	36	134	37	54

	1		2		3		4		5
A									
B									
C	22%	119%	32%	208%	12%	89%	644%	85%	17%

	1		2		3		4		5
A									
B									
C	17%	15%	163%	56%	12%	54%	27%	53%	17%

Table 70. Velocity profile of configuration F, hot box, case 5

	1		2		3		4		5
A									
B	8	2	18	55	1	0	5	3	24
C	16	122	198	15	23	102	46	49	42

	1		2		3		4		5
A									
B	15	30	32	69	18	16	25	13	38
C	46	149	215	30	32	119	82	59	63

	1		2		3		4		5
A									
B	88%	1400%	78%	25%	1700%	N/A	400%	333%	58%
C	188%	22%	9%	100%	39%	17%	78%	20%	50%

	1		2		3		4		5
A									
B	44%	23%	21%	200%	54%	61%	27%	61%	50%
C	60%	73%	164%	71%	65%	41%	18%	31%	33%

Table 71. Velocity profile of configuration F, hot box, case 6

	1		2		3		4		5
A									
B	153	240	80	220	310	92	56	68	174
C	151	87	170	79	136	69	147	68	260

	1		2		3		4		5
A									
B	185	265	113	252	340	123	68	86	205
C	190	106	210	119	171	91	215	95	325

	1		2		3		4		5
A									
B	21%	10%	41%	15%	10%	34%	21%	26%	18%
C	26%	22%	24%	51%	26%	32%	46%	40%	25%

	1		2		3		4		5
A									
B	0%	50%	43%	40%	93%	36%	63%	54%	13%
C	14%	35%	27%	34%	3%	46%	21%	45%	96%

Table 72. Velocity profile of configuration F, hot box, case 7

	1	2	3	4	5
A	1	12	42	2	37
B	13	11	2	1	11
C	2	1	6	10	26

	1	2	3	4	5
A	2	16	43	6	41
B	21	26	17	21	17
C	8	6	19	27	30

	1	2	3	4	5
A	100%	33%	2%	200%	11%
B	62%	136%	750%	2000%	55%
C	300%	500%	217%	170%	15%

	1	2	3	4	5
A	93%	31%	110%	80%	93%
B	21%	32%	32%	21%	0%
C	63%	74%	7%	37%	107%

Table 73. Velocity profile of configuration DE, hot box, case 1

	1	2	3	4	5
A					
B	19	23	11	30	23
C	32	27	29	67	20

	1	2	3	4	5
A					
B	30	34	22	34	28
C	39	28	35	74	22

	1	2	3	4	5
A					
B	58%	48%	100%	13%	22%
C	22%	4%	21%	10%	10%

	1	2	3	4	5
A					
B	4%	12%	35%	26%	0%
C	5%	26%	14%	89%	44%

Table 74. Velocity profile of configuration DE, hot box, case 2

	1	2	3	4	5
A					
B					
C	85	65	97	45	210

	1	2	3	4	5
A					
B					
C	101	84	129	55	168

	1	2	3	4	5
A					
B					
C	19%	29%	33%	22%	-20%

	1	2	3	4	5
A					
B					
C	10%	28%	9%	52%	82%

Table 75. Velocity profile of configuration DE, hot box, case 3

	1	2	3	4	5
A					
B	120	38	185	20	148
C					

	1	2	3	4	5
A					
B	155	51	225	30	188
C					

	1	2	3	4	5
A					
B	29%	34%	22%	50%	27%
C					

	1	2	3	4	5
A					
B	19%	62%	77%	78%	45%
C					

Table 76. Velocity profile of configuration DE, hot box, case 5

	1	2	3	4	5
A					
B	81	44	132	11	98
C					

	1	2	3	4	5
A					
B	98	63	162	17	105
C					

	1	2	3	4	5
A					
B	21%	43%	23%	55%	7%
C					

	1	2	3	4	5
A					
B	10%	34%	81%	83%	25%
C					

Table 77. Velocity profile of configuration DE, hot box, case 6

	1		2		3		4		5
A									
B									
C	225	8	116	181	39	61	108	16	285

	1		2		3		4		5
A									
B									
C	260	13	136	220	58	90	137	30	325

	1		2		3		4		5
A									
B									
C	16%	63%	17%	22%	49%	48%	27%	88%	14%

	1		2		3		4		5
A									
B									
C	89%	92%	2%	56%	62%	41%	4%	82%	138%

Table 78. Velocity profile of configuration DE, hot box, case 7

	1		2		3		4		5
A									
B									
C	197	56	74	163	76	53	58	41	118

	1		2		3		4		5
A									
B									
C	230	67	87	196	108	63	96	54	137

	1		2		3		4		5
A									
B									
C	17%	20%	18%	20%	42%	19%	66%	32%	16%

	1		2		3		4		5
A									
B									
C	105%	41%	23%	72%	12%	44%	26%	54%	22%

Table 79. Velocity profile of configuration DE, hot box, case 8

	1	2	3	4
A	159	59	85	177
B	265	95	95	174
C	325	40	190	139

	1	2	3	4
A	220	95	112	220
B	310	137	112	315
C	405	250	240	235

	1	2	3	4
A	38%	61%	32%	24%
B	17%	44%	18%	81%
C	25%	525%	26%	69%

	1	2	3	4
A	35%	45%	30%	41%
B	53%	38%	45%	30%
C	60%	36%	6%	18%

Table 80. Velocity profile of configuration DE, hot box, case 9

MASS FLOW RATE

Hot Test Hot Side												
Point	Outer				Inner				Overall			
	Average [in H2O]	Stdev	Error [in H2O]	Error [%]	Average [in H2O]	Stdev	Error [in H2O]	Error [%]	Average [in H2O]	Stdev	Error [in H2O]	Error [%]
1	0.01384	0.00425	0.00900	65%	0.12528	0.01692	0.03462	28%	0.09946	0.02723	0.05442	55%
2	0.01343	0.00440	0.00926	69%	0.16392	0.01916	0.03941	24%	0.10518	0.02747	0.05494	52%
3	0.01315	0.00390	0.00834	63%	0.18714	0.02226	0.04564	24%	0.11012	0.02703	0.05412	49%
4	0.01350	0.00430	0.00909	67%	0.20278	0.02048	0.04248	21%	0.10515	0.02672	0.05347	51%
5	0.01441	0.00422	0.00896	62%	0.22761	0.01882	0.03976	17%	0.09183	0.02628	0.05252	57%
6	0.01588	0.00422	0.00898	57%	0.23450	0.01703	0.03660	16%	0.11362	0.02939	0.05877	52%
7	0.01723	0.00428	0.00912	53%	0.22383	0.01806	0.03829	17%	0.13360	0.02866	0.05748	43%
8	0.01791	0.00471	0.00993	55%	0.20860	0.02120	0.04393	21%	0.13720	0.02892	0.05801	42%
9	0.01743	0.00457	0.00965	55%	0.19552	0.01767	0.03708	19%	0.11853	0.02800	0.05607	47%
10	0.01685	0.00445	0.00942	56%	0.17092	0.01883	0.03888	23%				
11	0.00929	0.00444	0.00928	100%	0.16184	0.01690	0.03511	22%	0.14947	0.02176	0.04423	30%
12	0.01045	0.00441	0.00924	88%	0.19700	0.01954	0.04061	21%	0.15732	0.02032	0.04155	26%
13	0.01038	0.00402	0.00852	82%	0.22452	0.01931	0.04063	18%	0.15224	0.01955	0.04002	26%
14	0.01161	0.00459	0.00960	83%	0.23084	0.01800	0.03831	17%	0.13726	0.02401	0.04846	35%
15	0.01093	0.00462	0.00964	88%	0.23357	0.01367	0.03055	13%	0.12338	0.02910	0.05826	47%
16	0.00957	0.00410	0.00865	90%	0.22858	0.01700	0.03643	16%	0.06119	0.02462	0.04907	80%
17	0.00949	0.00399	0.00845	89%	0.21483	0.02137	0.04433	21%	0.04731	0.02137	0.04260	90%
18	0.00979	0.00417	0.00878	90%	0.19661	0.02318	0.04752	24%	0.03891	0.01774	0.03540	91%
19	0.01038	0.00383	0.00816	79%	0.17254	0.02301	0.04689	27%	0.03434	0.01583	0.03162	92%
20	0.00936	0.00419	0.00881	94%	0.13928	0.02048	0.04165	30%				
Overall	0.01274		0.00202	16%	0.19699		0.00898	5%	0.10645		0.01182	11%

Table 81. The velocity pressure for the inner box, the outer box, and the overall flow for the heat source of a hot test

Hot Test Cold Side												
Point	Outer				Inner				Overall			
	Average [in H2O]	Stdev	Error [in H2O]	Error [%]	Average [in H2O]	Stdev	Error [in H2O]	Error [%]	Average [in H2O]	Stdev	Error [in H2O]	Error [%]
1	0.16549	0.02004	0.04112	25%	0.07608	0.01201	0.02459	32%	0.28016	0.03443	0.07014	25%
2	0.19886	0.02402	0.04917	25%	0.11240	0.01381	0.02853	25%	0.41311	0.02980	0.06339	15%
3	0.23008	0.02729	0.05581	24%	0.13893	0.01304	0.02750	20%	0.40668	0.01304	0.03447	8%
4	0.25900	0.02365	0.04931	19%	0.15128	0.01312	0.02786	18%	0.36644	0.04475	0.09102	25%
5	0.27028	0.01872	0.04038	15%	0.14662	0.01355	0.02858	19%	0.27418	0.01355	0.03135	11%
6	0.27249	0.01464	0.03316	12%	0.12026	0.01477	0.03047	25%	0.10059	0.02956	0.05902	59%
7	0.25130	0.01903	0.04057	16%	0.12370	0.01205	0.02539	21%	0.12935	0.03875	0.07724	60%
8	0.21383	0.02162	0.04479	21%	0.12666	0.01196	0.02527	20%	0.18518	0.04220	0.08437	46%
9	0.17577	0.01873	0.03876	22%	0.11423	0.01284	0.02672	23%	0.17538	0.04412	0.08808	50%
10	0.14204	0.01439	0.03006	21%	0.08936	0.01229	0.02532	28%	0.18131	0.04959	0.09886	55%
11	0.09796	0.01332	0.02740	28%	0.04369	0.00961	0.01960	45%	0.40227	0.03893	0.08033	20%
12	0.12611	0.01728	0.03533	28%	0.08286	0.01270	0.02600	31%	0.40193	0.03113	0.06566	16%
13	0.14080	0.01943	0.03964	28%	0.09456	0.01327	0.02724	29%	0.36140	0.04426	0.09001	25%
14	0.17407	0.02170	0.04441	26%	0.10627	0.01397	0.02874	27%	0.31415	0.05456	0.10955	35%
15	0.23151	0.02213	0.04602	20%	0.12457	0.01625	0.03333	27%	0.23223	0.06040	0.12042	52%
16	0.28537	0.01146	0.02821	10%	0.14757	0.01199	0.02571	17%	0.18809	0.04774	0.09528	51%
17	0.27792	0.01841	0.03997	14%	0.14531	0.01201	0.02570	18%	0.25188	0.05161	0.10329	41%
18	0.25666	0.02505	0.05191	20%	0.14393	0.01297	0.02744	19%	0.30809	0.05873	0.11767	38%
19	0.20909	0.02384	0.04895	23%	0.13023	0.01476	0.03059	23%	0.33152	0.04622	0.09349	28%
20	0.17312	0.01809	0.03752	22%	0.09848	0.01301	0.02681	27%	0.27960	0.04623	0.09301	33%
Overall	0.20759		0.00935	5%	0.11585		0.00608	5%	0.27918		0.01935	7%

Table 82. The velocity pressure for the inner box, outer box, and the overall flow for the heat sink of a hot test

Hot Test Hot Side											
		Outer			Inner				Overall		
	Distance [in]	Velocity [ft/min]	Error [ft/min]	Error [%]	Velocity [ft/min]	Error [ft/min	Error [%]	Distance [in]	Velocity [ft/min]	Error [ft/min]	Error [%]
1	0.063	413	134	33%	1242	172	14%	0.13	1107	303	27%
2	0.250	407	140	34%	1421	171	12%	0.38	1138	297	26%
3	0.500	402	128	32%	1518	185	12%	0.69	1165	286	25%
4	0.875	408	137	34%	1580	166	10%	1.06	1138	289	25%
5	1.313	421	131	31%	1674	146	9%	1.69	1064	304	29%
6	2.563	442	125	28%	1700	133	8%	3.25	1183	306	26%
7	3.063	461	122	26%	1660	142	9%	3.88	1283	276	22%
8	3.375	470	130	28%	1603	169	11%	4.25	1300	275	21%
9	3.625	463	128	28%	1552	147	9%	4.56	1208	286	24%
10	3.875	456	127	28%	1451	165	11%	4.88			
11	0.06	338	169	50%	1412	153	11%	0.13	1357	201	15%
12	0.25	359	159	44%	1558	161	10%	0.38	1392	184	13%
13	0.50	358	147	41%	1663	150	9%	0.69	1369	180	13%
14	0.88	378	156	41%	1686	140	8%	1.06	1300	230	18%
15	1.31	367	162	44%	1696	111	7%	1.69	1233	291	24%
16	2.56	343	155	45%	1678	134	8%	3.25	868	348	40%
17	3.06	342	152	45%	1627	168	10%	3.88	763	344	45%
18	3.38	347	156	45%	1556	188	12%	4.25	692	315	45%
19	3.63	358	141	39%	1458	198	14%	4.56	650	299	46%
20	3.88	340	160	47%	1310	196	15%	4.88			
Overall		393.61	32.01	8%	1552.33	36.59	2%		1122.87	60.64	5%
Overall [m/s]		2.00	0.16	8%	7.89	0.19	2%		5.70	0.31	5%

Table 83. The velocity Calculated from the velocity pressure for the inner box, the outer box, and the overall flow for the heat source of a hot test

Hot Test Cold Side											
		Outer			Inner				Overall		
	Distance [in]	Velocity [ft/min]	Error [ft/min]	Error [%]	Velocity [ft/min]	Error [ft/min]	Error [%]	Distance [in]	Velocity [ft/min]	Error [ft/min]	Error [%]
1	0.06	1377	171	12%	934	151	16%	0.13	1792	224	13%
2	0.25	1510	187	12%	1135	144	13%	0.38	2176	167	8%
3	0.50	1624	197	12%	1262	125	10%	0.69	2159	92	4%
4	0.88	1723	164	10%	1317	121	9%	1.06	2050	255	12%
5	1.31	1760	131	7%	1297	126	10%	1.69	1773	101	6%
6	2.56	1767	108	6%	1174	149	13%	3.25	1074	315	29%
7	3.06	1697	137	8%	1191	122	10%	3.88	1218	364	30%
8	3.38	1566	164	10%	1205	120	10%	4.25	1457	332	23%
9	3.63	1420	157	11%	1144	134	12%	4.56	1418	356	25%
10	3.88	1276	135	11%	1012	143	14%	4.88	1442	393	27%
11	0.06	1060	148	14%	708	159	22%	0.13	2148	214	10%
12	0.25	1202	168	14%	975	153	16%	0.38	2147	175	8%
13	0.50	1270	179	14%	1041	150	14%	0.69	2035	253	12%
14	0.88	1413	180	13%	1104	149	14%	1.06	1898	331	17%
15	1.31	1629	162	10%	1195	160	13%	1.69	1632	423	26%
16	2.56	1809	89	5%	1301	113	9%	3.25	1468	372	25%
17	3.06	1785	128	7%	1291	114	9%	3.88	1699	348	21%
18	3.38	1715	173	10%	1285	122	10%	4.25	1879	359	19%
19	3.63	1548	181	12%	1222	143	12%	4.56	1950	275	14%
20	3.88	1409	153	11%	1063	145	14%	4.88	1790	298	17%
Overall		1528	35	2%	1143	30	3%		1760	61	3%
Overall [m/s]		7.76	0.18	2%	5.80	0.15	3%		8.94	0.31	3%

Table 84. The velocity Calculated from the velocity pressure for the inner box, the outer box, and the overall flow for the heat sink of a hot test

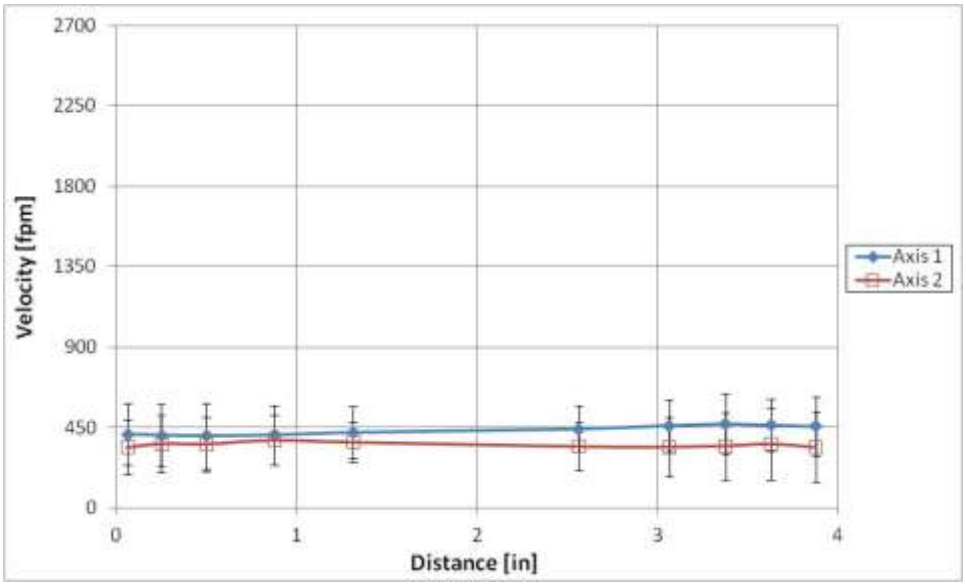

Figure 37. Outer box inlet velocity profile of the heat source for the hot test

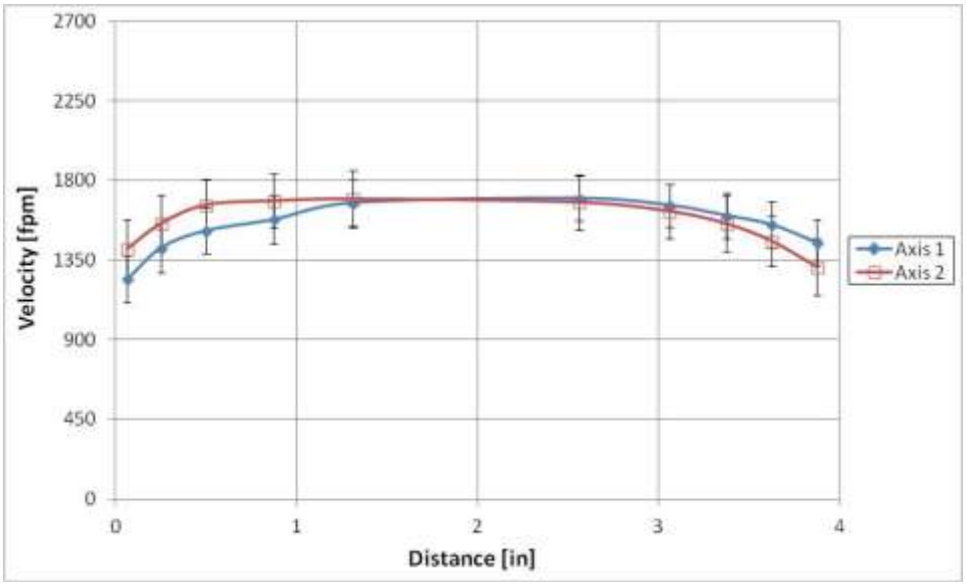

Figure 38. Inner box inlet velocity profile of the heat source for the hot test

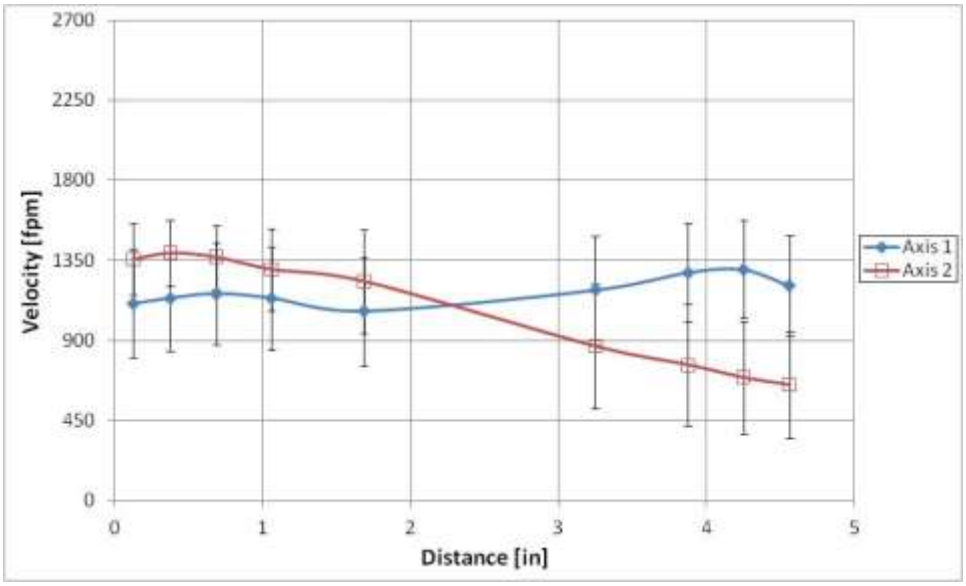

Figure 39. Overall velocity profile of the heat source for the hot test

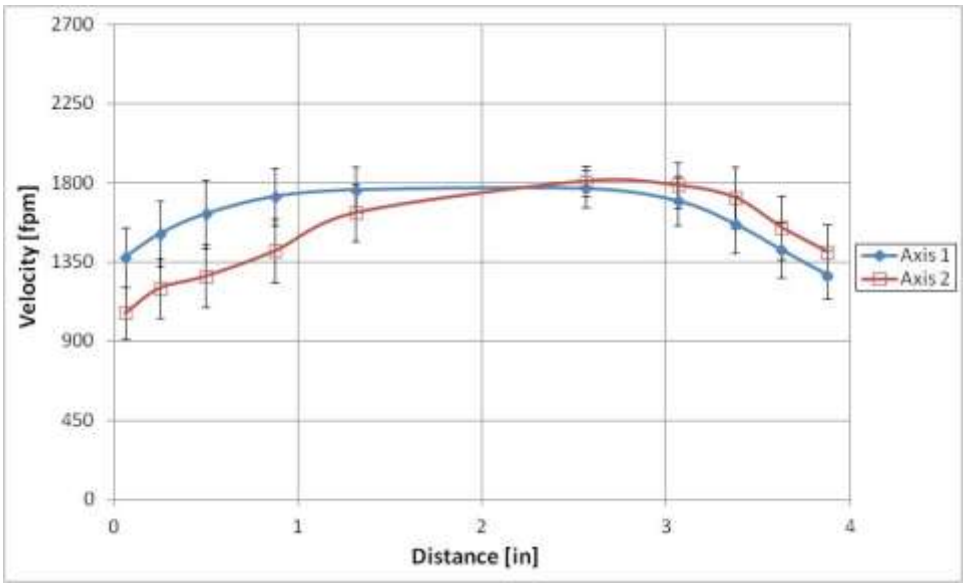

Figure 40. Outer box velocity profile of the heat sink for the hot test

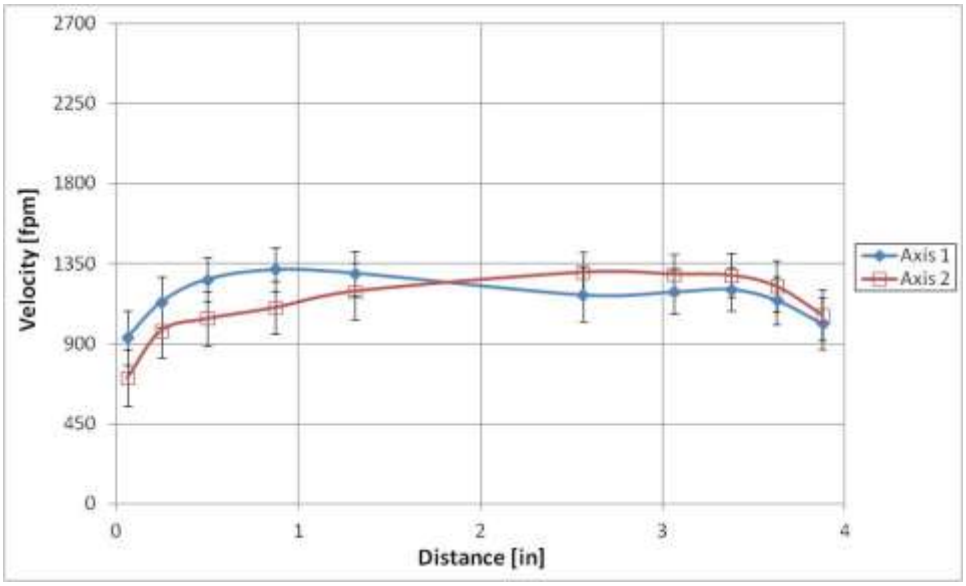

Figure 41. Inner box inlet velocity profile of the hear sink for the hot test

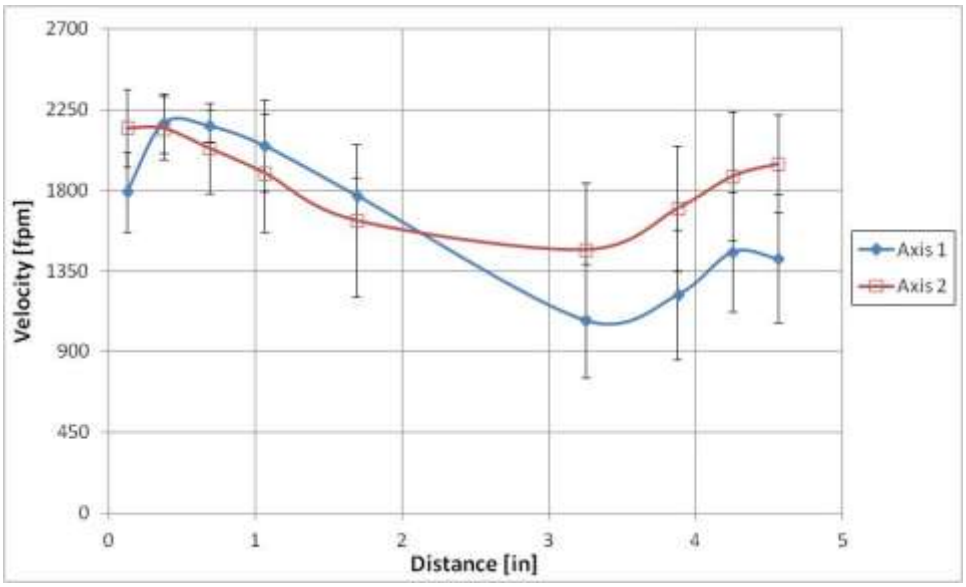

Figure 42. Overall velocity profiles of the heat sink for the hot test

Cold Test Hot Side												
Point	Inner				Outer				Overall			
	Average [in H2O]	Stdev	Error [in H2O]	Error [%]	Average [in H2O]	Stdev	Error [in H2O]	Error [%]	Average [in H2O]	Stdev	Error [in H2O]	Error [%]
1	0.13505	0.01908	0.03889	29%	0.01986	0.00408	0.00880	44%	0.0990	0.02891	0.05773	58%
2	0.16901	0.02036	0.04178	25%	0.02004	0.00424	0.00910	45%	0.1099	0.02633	0.05273	48%
3	0.19695	0.02004	0.04155	21%	0.01991	0.00444	0.00947	48%	0.1052	0.02631	0.05266	50%
4	0.20546	0.01754	0.03701	18%	0.02073	0.00483	0.01020	49%	0.1000	0.02792	0.05578	56%
5	0.20949	0.01454	0.03157	15%	0.01980	0.00438	0.00934	47%	0.0902	0.02866	0.05717	63%
6	0.20126	0.01559	0.03332	17%	0.01996	0.00418	0.00899	45%	0.1175	0.02951	0.05902	50%
7	0.18357	0.02086	0.04293	23%	0.01831	0.00410	0.00881	48%	0.1343	0.03135	0.06275	47%
8	0.17161	0.02386	0.04853	28%	0.01865	0.00412	0.00885	47%	0.1359	0.03032	0.06075	45%
9	0.14859	0.02436	0.04924	33%	0.01958	0.00393	0.00853	44%	0.1071	0.02898	0.05791	54%
10	0.10478	0.01935	0.03908	37%	0.01891	0.00441	0.00939	50%				
11	0.09277	0.01744	0.03527	38%	0.01741	0.00402	0.00865	50%	0.1468	0.02500	0.05047	34%
12	0.13191	0.01888	0.03848	29%	0.01752	0.00411	0.00880	50%	0.1523	0.01943	0.03977	26%
13	0.15440	0.02207	0.04488	29%	0.01745	0.00458	0.00967	55%	0.1522	0.02304	0.04672	31%
14	0.17153	0.01982	0.04078	24%	0.01801	0.00425	0.00908	50%	0.1407	0.02375	0.04797	34%
15	0.19048	0.01817	0.03793	20%	0.01773	0.00452	0.00957	54%	0.1201	0.02470	0.04964	41%
16	0.20729	0.01672	0.03552	17%	0.02075	0.00436	0.00933	45%	0.0529	0.02200	0.04386	83%
17	0.19429	0.01981	0.04109	21%	0.02147	0.00533	0.01114	52%	0.0432	0.02195	0.04371	101%
18	0.18478	0.01850	0.03847	21%	0.02378	0.00452	0.00968	41%	0.0347	0.01821	0.03631	105%
19	0.17405	0.02108	0.04321	25%	0.02204	0.00492	0.01039	47%	0.0271	0.01402	0.02803	104%
20	0.14961	0.01847	0.03792	25%	0.01995	0.00402	0.00869	44%				
Overall	0.16884		0.00897	5%	0.01959		0.00209	11%	0.1038		0.01201	12%

Table 85. The velocity pressure for the inner box, the outer box, and the overall flow for the heat source of a cold test

Cold Test Cold Side												
Point	Inner				Outer				Overall			
	Average [in H2O]	Stdev	Error [in H2O]	Error [%]	Average [in H2O]	Stdev	Error [in H2O]	Error [%]	Average [in H2O]	Stdev	Error [in H2O]	Error [%]
1	0.09028	0.01504	0.03060	34%	0.07454	0.01499	0.03034	41%	0.38569	0.08452	0.16876	44%
2	0.11498	0.01576	0.03227	28%	0.10314	0.01834	0.03711	36%	0.42948	0.02804	0.06047	14%
3	0.13563	0.01743	0.03574	26%	0.12530	0.02397	0.04827	39%	0.42224	0.01743	0.04182	10%
4	0.14635	0.01695	0.03497	24%	0.15313	0.02194	0.04461	29%	0.37651	0.04407	0.08982	24%
5	0.14407	0.01881	0.03849	27%	0.21186	0.02802	0.05700	27%	0.27317	0.01881	0.04060	15%
6	0.11892	0.01489	0.03068	26%	0.26590	0.01385	0.03165	12%	0.09450	0.02636	0.05269	56%
7	0.12341	0.01349	0.02808	23%	0.24974	0.02407	0.04995	20%	0.12473	0.03451	0.06889	55%
8	0.12552	0.01289	0.02699	22%	0.21525	0.03090	0.06261	29%	0.13777	0.04093	0.08159	59%
9	0.11657	0.01303	0.02712	23%	0.16598	0.02784	0.05617	34%	0.10850	0.03671	0.07312	67%
10	0.08060	0.01387	0.02823	35%	0.13148	0.02174	0.04399	33%	0.00842	0.00239	0.00557	66%
11	0.06535	0.01199	0.02444	37%	0.11888	0.02025	0.04097	34%	0.40814	0.03680	0.07639	19%
12	0.08248	0.01057	0.02195	27%	0.15464	0.02516	0.05086	33%	0.40458	0.03507	0.07306	18%
13	0.09382	0.01325	0.02721	29%	0.20158	0.02956	0.05987	30%	0.36920	0.04702	0.09543	26%
14	0.10818	0.01483	0.03042	28%	0.23052	0.03004	0.06110	27%	0.32081	0.05217	0.10494	33%
15	0.12766	0.01918	0.03900	31%	0.24877	0.02370	0.04924	20%	0.25535	0.05978	0.11935	47%
16	0.15062	0.01343	0.02842	19%	0.25377	0.01590	0.03496	14%	0.19341	0.05488	0.10935	57%
17	0.15212	0.01322	0.02806	18%	0.25145	0.01543	0.03406	14%	0.24797	0.06053	0.12077	49%
18	0.15070	0.01269	0.02706	18%	0.21863	0.02402	0.04943	23%	0.29314	0.05874	0.11756	40%
19	0.13995	0.01379	0.02892	21%	0.16457	0.02253	0.04587	28%	0.33340	0.05299	0.10667	32%
20	0.10906	0.01405	0.02893	27%	0.14298	0.02125	0.04316	30%	0.31823	0.05370	0.10791	34%
Overall	0.11881		0.00675	5.7%	0.18411		0.01063	5.8%	0.27526		0.02074	7.5%

Table 86. The velocity pressure for the inner box, the outer box, and the overall flow for the heat sink of a cold test

Cold Test Hot Side											
		Outer			Inner				Overall		
	Distance [in]	Velocity [ft/min]	Error [ft/min]	Error [%]	Velocity [ft/min]	Error [ft/min]	Error [%]	Distance [in]	Velocity [ft/min]	Error [ft/min]	Error [%]
1	0.0625	465.38	175	38%	1289.79	103	8%	0.13	1104.42	303	27%
2	0.25	467.47	168	36%	1442.87	106	7%	0.38	1163.27	263	23%
3	0.5	465.97	155	33%	1557.57	111	7%	0.69	1138.44	268	24%
4	0.875	475.55	135	28%	1590.89	117	7%	1.06	1110.12	291	26%
5	1.3125	464.75	114	25%	1606.39	110	7%	1.69	1054.13	314	30%
6	2.5625	466.55	123	26%	1574.53	105	7%	3.25	1203.09	284	24%
7	3.0625	446.84	165	37%	1503.77	108	7%	3.88	1286.02	283	22%
8	3.375	451.02	193	43%	1453.94	107	7%	4.25	1294.00	272	21%
9	3.625	462.07	211	46%	1352.90	101	7%	4.56	1148.44	292	25%
10	3.875	454.11	199	44%	1136.08	113	10%	4.88			
11	0.0625	435.76	191	44%	1068.99	108	10%	0.13	1344.82	218	16%
12	0.25	437.17	175	40%	1274.74	110	9%	0.38	1369.63	168	12%
13	0.5	436.26	189	43%	1379.12	121	9%	0.69	1369.09	198	14%
14	0.875	443.26	163	37%	1453.62	112	8%	1.06	1316.55	211	16%
15	1.3125	439.73	143	33%	1531.79	119	8%	1.69	1216.12	237	19%
16	2.5625	475.78	129	27%	1597.94	107	7%	3.25	807.00	315	39%
17	3.0625	483.90	154	32%	1547.03	126	8%	3.88	729.83	347	48%
18	3.375	509.23	148	29%	1508.70	104	7%	4.25	653.47	322	49%
19	3.625	490.24	171	35%	1464.24	116	8%	4.56	577.60	281	49%
20	3.875	466.48	162	35%	1357.56	102	7%	4.88			
Overall		461.88	37.02	8%	1434.62	24.75	2%		1104.78	59.56	5%
Overall [m/s]		2.35	0.19	8%	7.29	0.13	2%		5.61	0.30	5%

Table 87. The velocity calculated by the velocity pressure for the inner box, the outer box, and the overall flow for the heat source of a cold test

Cold Test Cold Side											
		Outer			Inner				Overall		
	Distance [in]	Velocity [ft/min]	Error [ft/min]	Error [%]	Velocity [ft/min]	Error [ft/min]	Error [%]	Distance [in]	Velocity [ft/min]	Error [ft/min]	Error [%]
1	0.0625	924	172	19%	1017	188	18%	0.13	2103	460	22%
2	0.25	1087	161	15%	1148	196	17%	0.38	2219	156	7%
3	0.5	1199	164	14%	1247	231	19%	0.69	2200	109	5%
4	0.875	1325	155	12%	1295	193	15%	1.06	2078	248	12%
5	1.3125	1558	172	11%	1285	210	16%	1.69	1770	131	7%
6	2.5625	1746	151	9%	1168	104	9%	3.25	1041	290	28%
7	3.0625	1692	135	8%	1189	169	14%	3.88	1196	330	28%
8	3.375	1571	129	8%	1200	228	19%	4.25	1257	372	30%
9	3.625	1379	134	10%	1156	233	20%	4.56	1115	376	34%
10	3.875	1228	168	14%	961	205	21%	4.88	311	103	33%
11	0.0625	1167	162	14%	866	201	23%	0.13	2163	202	9%
12	0.25	1331	129	10%	972	219	23%	0.38	2154	194	9%
13	0.5	1520	150	10%	1037	226	22%	0.69	2057	266	13%
14	0.875	1626	157	10%	1114	215	19%	1.06	1918	314	16%
15	1.3125	1689	185	11%	1210	167	14%	1.69	1711	400	23%
16	2.5625	1706	124	7%	1314	117	9%	3.25	1489	421	28%
17	3.0625	1698	122	7%	1321	115	9%	3.88	1686	411	24%
18	3.375	1583	118	7%	1314	179	14%	4.25	1833	368	20%
19	3.625	1374	131	10%	1267	191	15%	4.56	1955	313	16%
20	3.875	1280	148	12%	1118	193	17%	4.88	1910	324	17%
Overall		1434	33	2%	1160	43	4%		1708	67	4%
Overall [m/s]		7.29	0.17	2%	5.89	0.22	4%		8.68	0.34	4%

Table 88. The velocity pressure Measured for the inner box, the outer box, and the overall flow for the heat sink of a cold test

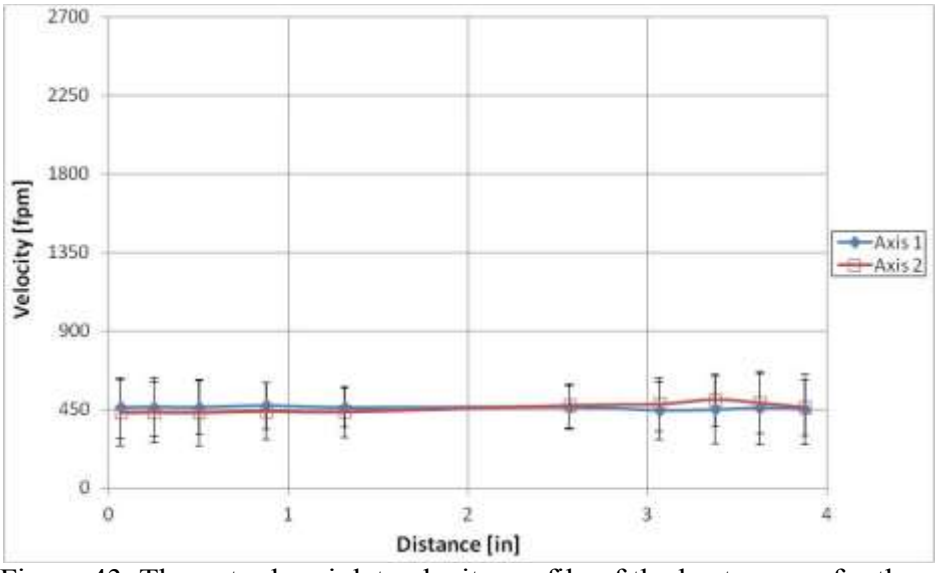

Figure 43. The outer box inlet velocity profile of the heat source for the cold test

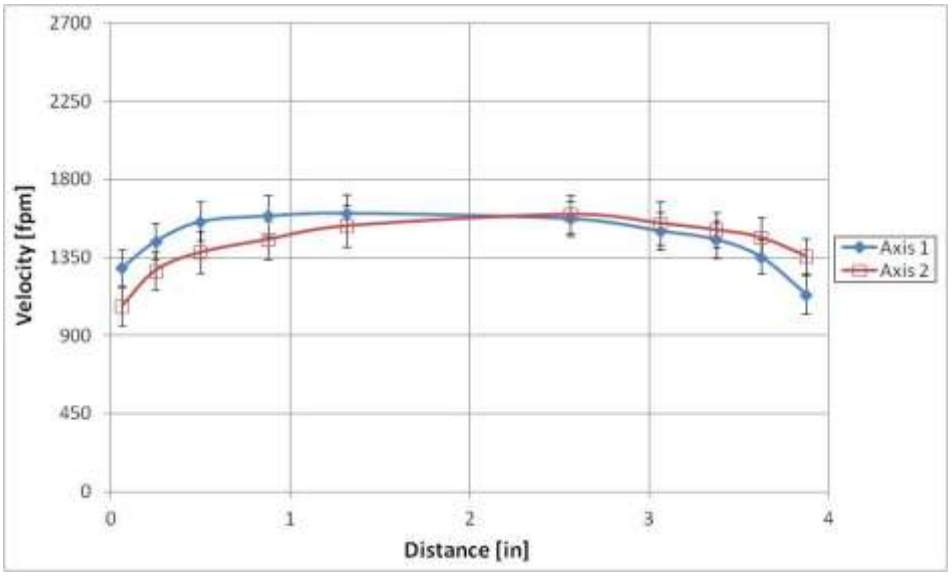

Figure 44. The inner box inlet velocity profile of the heat source for the cold test

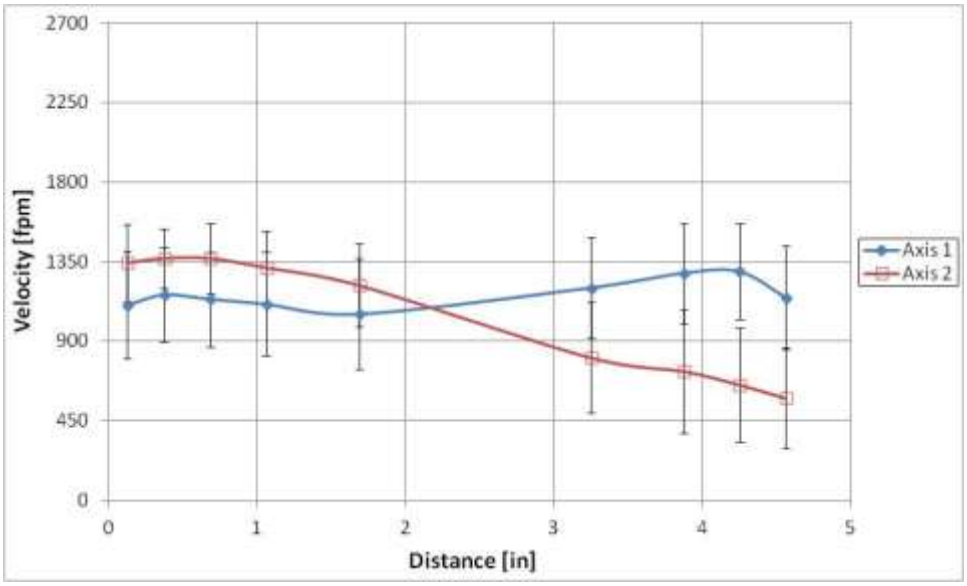

Figure 45. The overall velocity profile of the heat source for the cold test

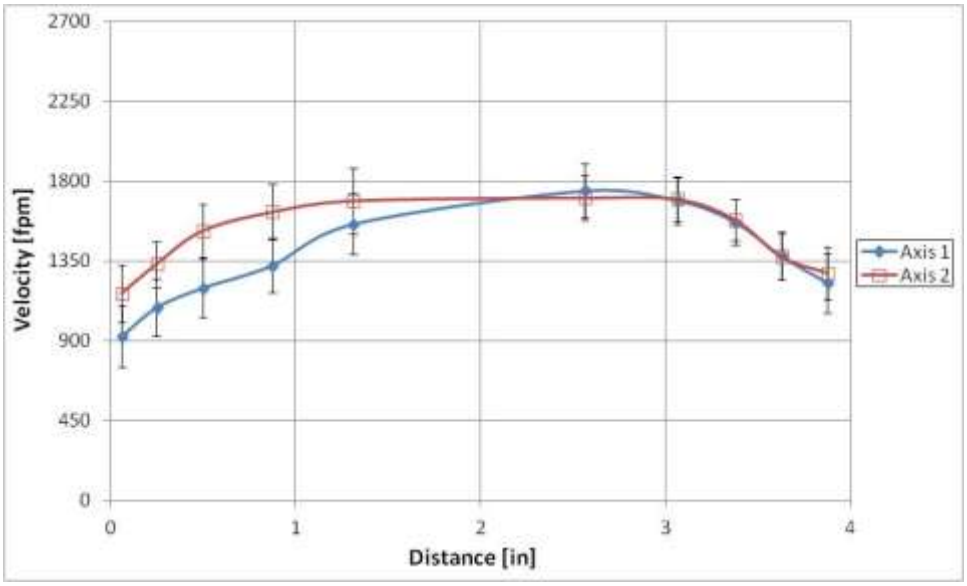

Figure 46. The outer box inlet velocity profile of the heat sink for the cold test

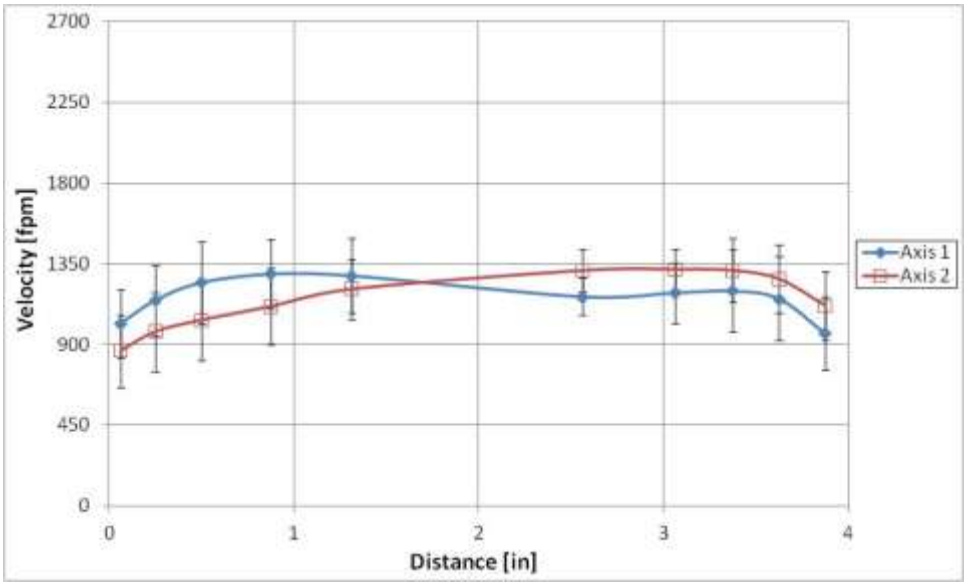

Figure 47. The inner box inlet velocity profile of the heat sink for the cold test

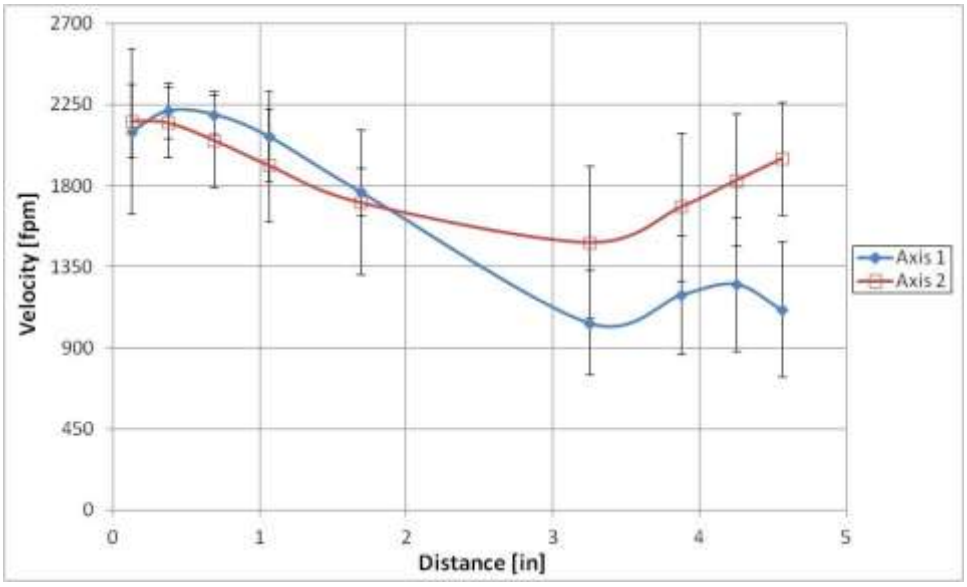

Figure 48. The overall velocity profile of the heat sink for the cold test

TEMPERATURE CORRECTIONS

Hot tests

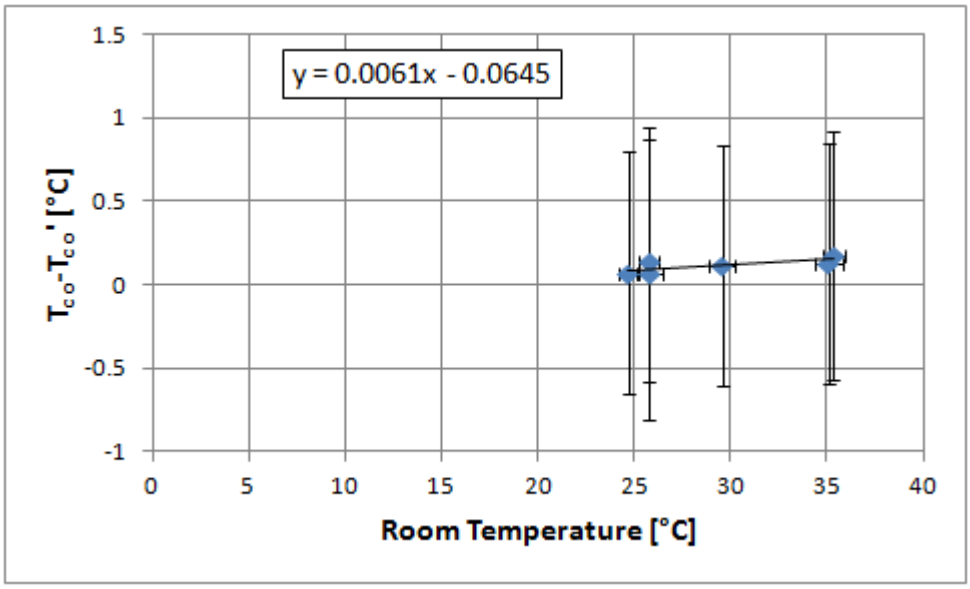

Figure 49. The difference between the recorded and actual temperatures for the heat sink outlet plotted against room temperature for a hot test

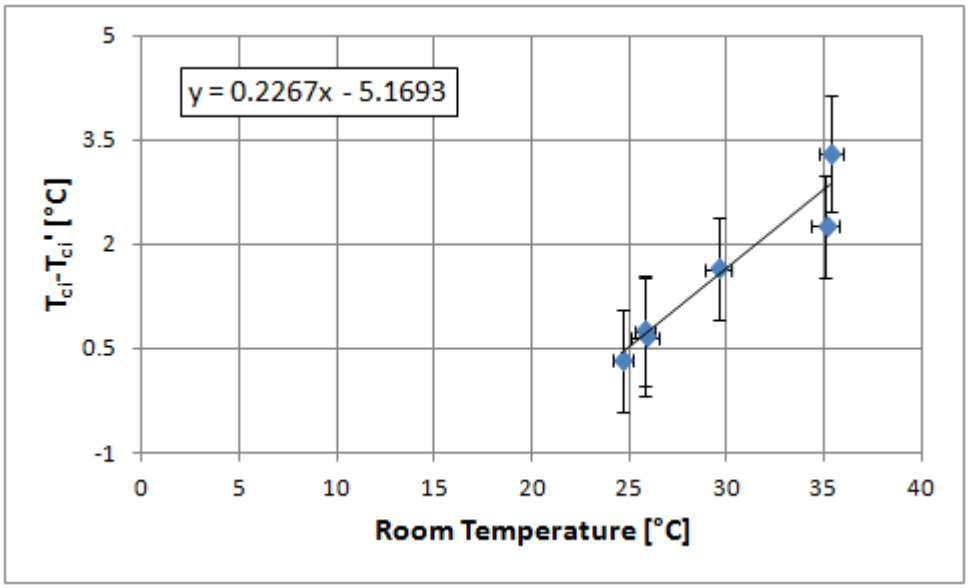

Figure 50. The difference between the recorded and actual temperatures for the heat sink inlet plotted against room temperature for a hot test

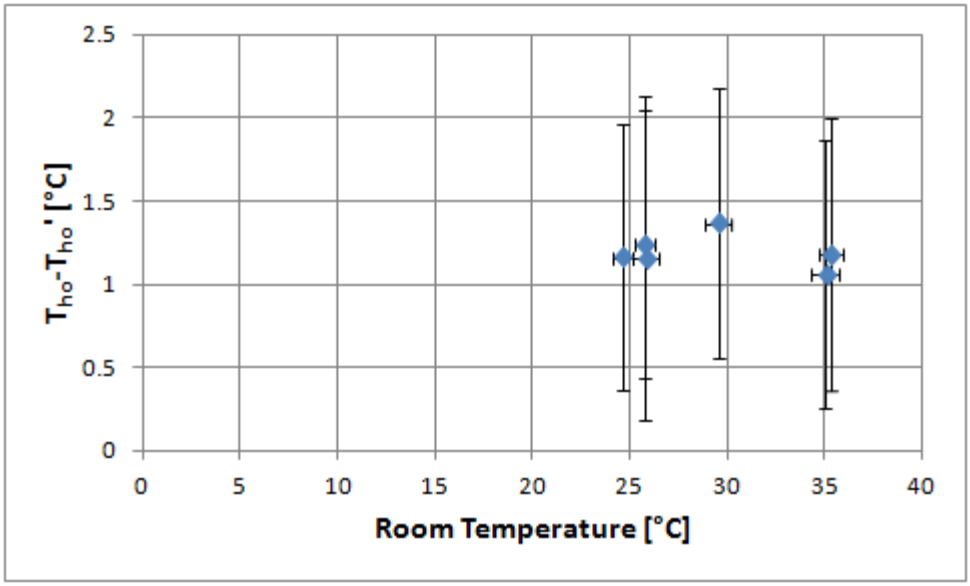

Figure 51. The difference between the recorded and actual temperatures for the heat source outlet plotted against room temperature for a hot test

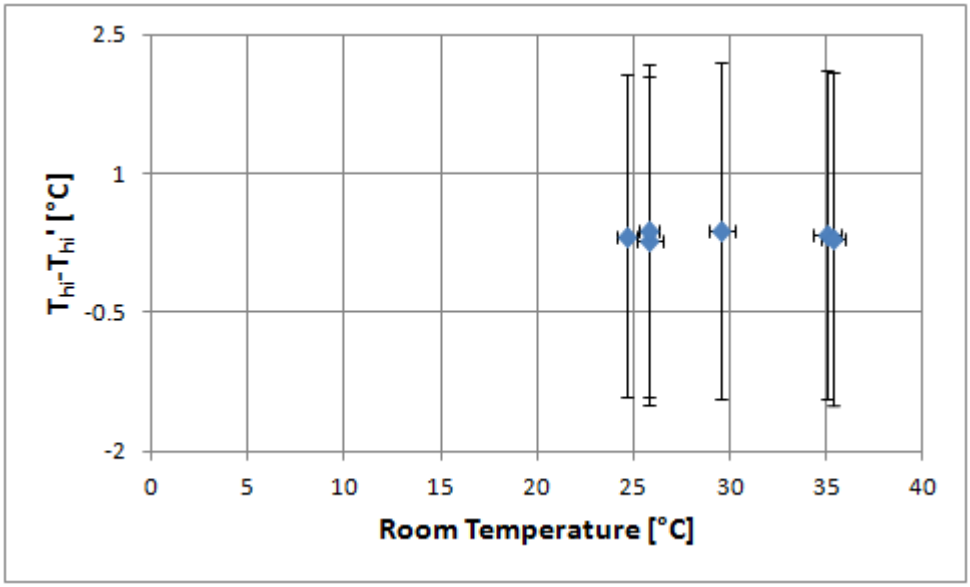

Figure 52. The difference between the recorded and actual temperatures for the heat source inlet plotted against room temperature for a hot test

Cold tests

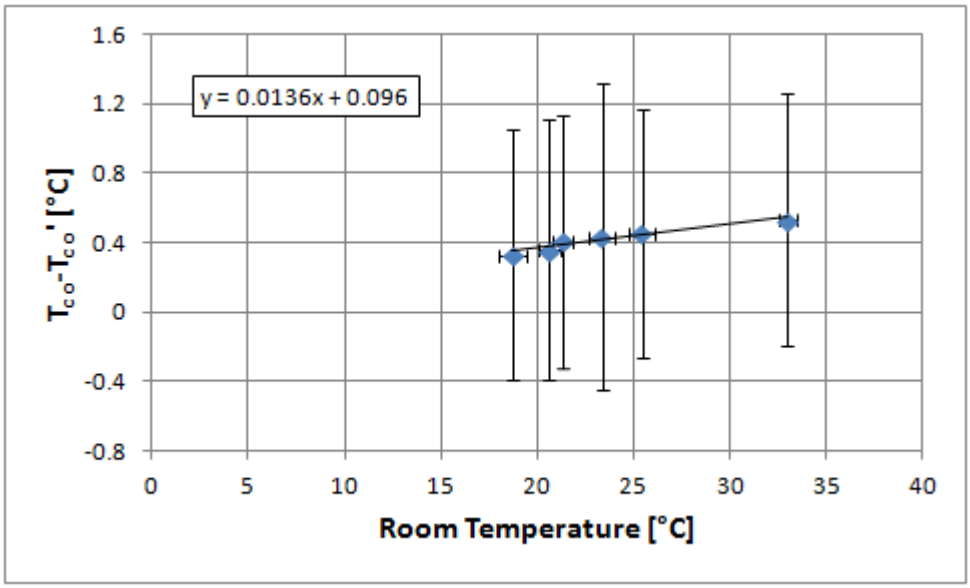

Figure 53. The difference between the recorded and actual temperatures for the heat sink outlet plotted against room temperature for a cold test

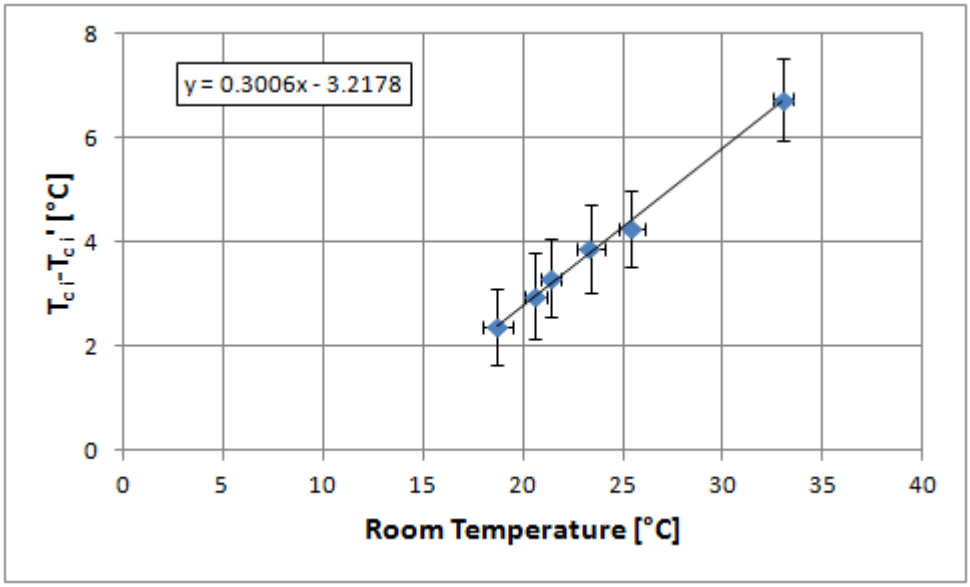

Figure 54. The difference between the recorded and actual temperature for the heat sink inlet plotted against room temperature for a cold test

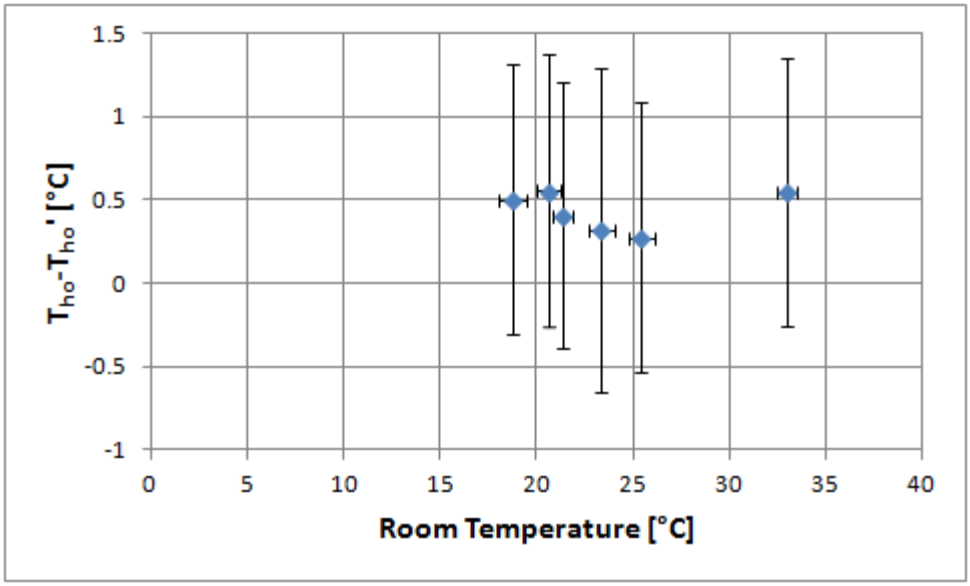

Figure 55. The difference between the recorded and actual temperature for the heat source outlet plotted against the room temperature for a cold test

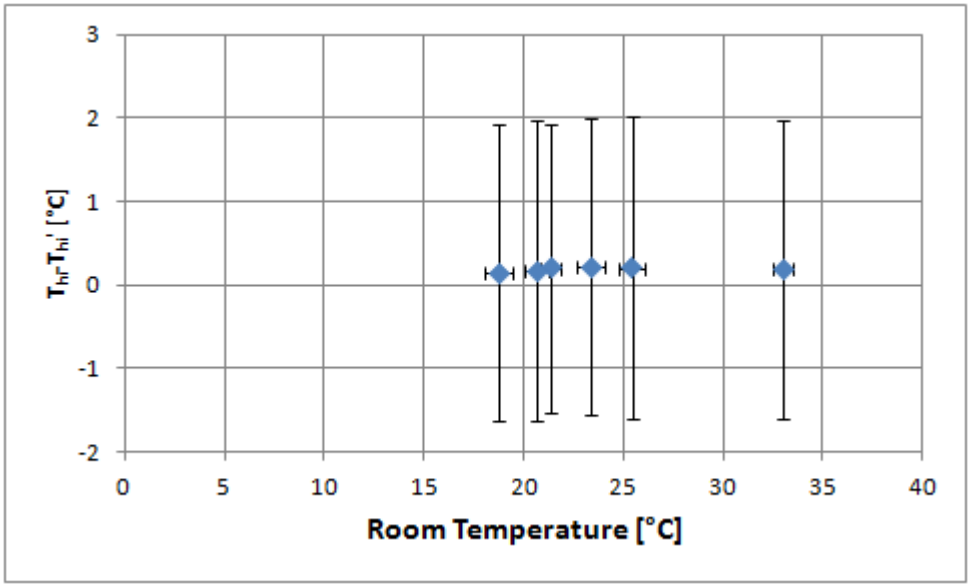

Figure 56. The difference between the recorded and actual temperature for the heat source inlet plotted against the room temperature for a cold test

APPENDIX 3

ASSEMBLY PROCEDURES

Making the Thermocouples

For this project, the temperature difference across each inner box wall needs to be determined so that the heat transfer through these walls can be measured. The inner and outer side of the top, bottom, side walls, and back wall for both the heat sink and heat source need to be measured totaling to twenty needed thermocouple grids. The air temperature of both the heat sink and the heat source, as well as the surface temperature of both sides of the specimen also must be recorded, totaling to 36 individual thermocouples. All of these add up to a required 216 thermocouples that need to measured and created.

- Start by determining the locations of the thermocouples. Since nine thermocouples are used to measure each surface, measure the locations such that all of the thermocouples are equidistant.
- Once the location of each thermocouple is determined, determine the length of thermocouple wire needed. Be sure to consider where the thermocouple grids will meet, and the length considering that the box needs to be able to slide apart.
- Cut the required lengths of 30 gauge T type thermocouple wire, making sure to label each wire indicating the location of each thermocouple. (30 gauges is used because it is required by the ASTM code. Labeling each wire will be useful for the calibration and installation)
- Strip all of the wires about ½” on both sides of each wire. The best way to strip the thermocouple ends is to actually cut the wire axially, splitting the red and blue wires. Then cut off the brown overall insulation, and use a wire stripper to remove the red and blue insulation individually. (The blue wire is the copper which breaks easily.)
- Take one precut and stripped thermocouple wire and twist one end tightly. This end will be the temperature measuring side. Cross, or twist once, the wires of the opposite end. Crossing the wires is done to complete the circuit in the next few steps. Perform this step to each wire.

- Pick up and plug in the thermocouple welder. The thermocouple welder owned by the lab is a wooden structure with a variable transformer underneath and guarded from the person using it. The variable control is above the structure so it can be adjusted without touching the transformer. The active wires power a metal block, and the negative wires go to a clamp. There is no ground. A switch turns on the transformer and a light lets the user know it is live. The picture below shows the thermocouple welder.

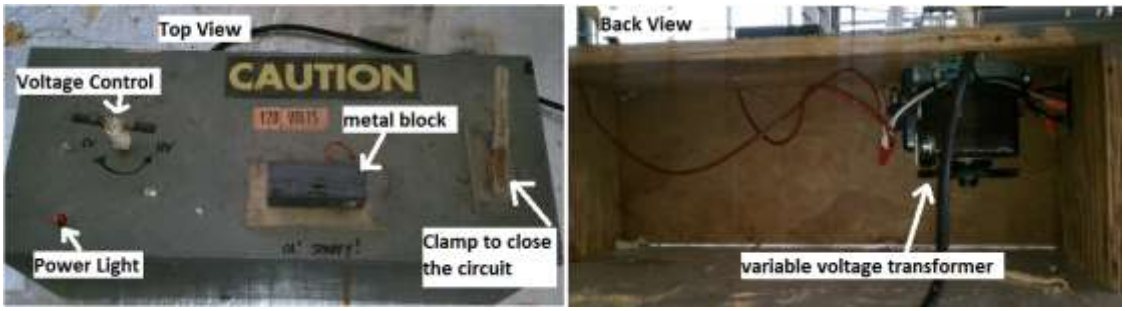

Figure 57. Top and back views of the thermocouple welder.

- Put on safety glasses and turn on the thermocouple welder, making sure the transformer is at the lowest setting. Take the crossed end of the pre-twisted wire and clamp it in the clamp. Take the tightly twisted end and touch it to the block. If nothing happens slightly increase the power and try again. Repeat until the wires are melted together and form a small bulb, no more than twice the diameter of the wire as per ASTM standards.
- Remove the wire from the clamp and continue with the remaining pre-twisted wires until all of the thermocouples have been made.

Calibrating the Thermocouples

- This step must be performed before every set of tests. For example, all tests for this client count as one set.

- Make sure that all of the thermocouples are of the proper length to reach the proper location. Be sure to leave enough wire to travel the proper path and so there will be have plenty of room to install the thermocouples.
- Install the thermocouple wires into the computer system and set up LabVIEW to record the temperatures.
- Place a small bundle of thermocouples in a cold temperature bath maintained at the lowest temperature in the range that will occur in the experiment, for this experiment I chose 0°C. Also place a calibrated measuring device in the bath to serve as the standard.
- Allow all of the temperature measuring devices to reach an equilibrium state with the bath water and then run LabVIEW to collect the data of all of the temperature measuring devices in the bath.
- Switch out the bundle with another bundle of thermocouples that need to be calibrated and repeat the previous step until all of the thermocouple readings have been recorded at that temperature.
- Change the bath temperature by a set increment, in this case 5°C and wait until the bath reaches steady state. Place a small bundle of thermocouples in the bath and record using LabVIEW. Change the bundles until all of the thermocouple readings have been recorded at this set temperature.
- Repeat the previous step until the bath is set to the highest possible temperature that will occur in the experiment. Since 46°C is not in the increment, the test was performed at 45°C and 50°C.
- Import all of the data into Excel and take the average of the temperature readings for each temperature reading device.
- Subtract the average of each individual temperature reading device from the average calibrated temperature reading device.
- Use a linear offset function in LabVIEW and import the temperature and the correction factor so that the temperature correction uses linear interpretations between the set temperatures. This function allows for the correction factor to be

non-linear as well. Be sure that the table is in the correct order so the correction factor corresponds to the correct thermocouple.

Installing Thermocouples on Inner Box Walls

Once all of the thermocouples are calibrated, all of the thermocouple grids need to be installed on the inner boxes.

- Measure and mark the thermocouple location on each wall. These walls include the inside and outside of the top, bottom, side walls, and back wall for both boxes.
- Cut a long T type thermocouple wire to stretch from the location where the bundle meets to the data acquisition system and strip both ends.(I used a much larger gauge here, but that is not necessary) and strip
- Take the thermocouples for one grid and twist together all of the copper wires to the copper wire of the long thermocouple wire in the previous step. Soldering those helps keeps them all in contract. Do the same to the constantan wire. (The soldering was not initially performed on all of the thermocouple wire connections, but as the preliminary tests were performed certain thermocouples were failing. Soldering them together helped.)
- Tape the twisted copper and constantan wires, making sure that no copper and constantan wires touch. The wires crossing will cause an error in the reading. Perform this step and the previous steps until the twenty thermocouple grids are ready to install.
- Cut nine 4” strip of tape with a similar emissivity of the surface the thermocouple will measure the temperature of, as per ASTM standard. (For the polyisocyanurate I used the ducting tape. It has a foil reflective tape like the insulation board.)
- Take one thermocouple from the grid and place it at its designated location.
- Take one of the 4” pieces of tape and tape the thermocouple down without covering the bulb, such that 4” of the thermocouple wire up to the bulb is covered by the tape.
- Continue securing the remaining thermocouples in this grid until the entire thermocouple grid is secured.

- Repeat the previous four steps until all twenty thermocouple grids are in there proper locations.

Installing the Inner Boxes into Guard Boxes

Once all of the thermocouples are installed on the inner box, the inner box can be placed inside of the outer box.

- Obtain 2x4's to stack to the height of the bottom wall of the outer box and place them in front of the outer box preferably centered to the outer box. (Technically anything will work as long as the heights are level.)
- Pick up the inner box for the heat source and place it on the stack of 2x4's. (Two average sized guys should be sufficient.)
- Center the inner box with relation to the outer box.
- Pick up the box again and move it backward into the outer box. Be sure to pick up at least slightly otherwise the foam on the bottom will be torn up.
- Repeat these steps for the heat sink.

Installing the Air Temperature grids

- First build the thermocouple grid out of 2x2. In order to build the grid, take a piece of 2x2 and place it against the bottom of one of the inner box and mark the lumber at the inside of the insulation on both sides. Be sure to label the location of the lumber, for example, "hot bottom" is sufficient to mark its location. Repeat this step for the top and the bottom of both the heat sink and heat source. (Since the box was not perfectly square of symmetric this custom finish is necessary for pressure to hold the frame in place.)
- Use a table saw to cut along the lines marked on the four pieces of lumber and place them in their proper location flush with the top of the insulation board.
- Place another piece of 2x2 alongside the inner box and mark the inside of the top and the bottom pieces lumber across and the inner box. Be sure to label the location of

the lumber, for example, “hot right” should be enough of a label. Repeat for both sides of the heat sink and the heat source.

- Use a table saw again to cut along the lines marked in the previous step.
- Use screws to assemble both frames.
- Make three marks on the outer side of each piece of lumber at exactly, ¼, ½, and ¾ of the length of each piece of lumber. Be sure that the marks on opposite sides of the frame are directly across from each other. Repeat this step to both the frame for the heat sink and the heat source.
- Secure a piece of lumber to a work bench such that the lumber hangs off the side of the table using a clamp. Then place the constructed frame on top of the lumber such that the frame is around the lumber and top is sitting on the lumber. Perform this step for both the frame for the heat sink and the heat source. (Securing the lumber in this fashion is so that the top piece of lumber can be drilled through from the outside without putting pressure on the joints.)
- Use a drill to drill a hole through each hole marked. The hole does not need to be too big, but enough to thread a string through it. Repeat this step for both the frame for the heat sink and the heat source.
- Create the grid: Thread a long string (possibly still on the spool) through the outside of a hole on one of the edges of a frame. Then thread it through the hole directly across from the hole it’s currently going though. Thread the same string through the outside of the middle hole on the same side of the frame. Then thread it through the inside of the hole opposing it and then thread it through the last hole on the side of the piece of lumber. Thread it through the hole directly across from it and tie it so that the knot will not slip through the hole. (Going around the 2x2 helps secure any knot) Cut off the thread from the spool and pull the thread through the frame taught in all three stretches of the thread. Secure the other end of the thread by tying a knot around the lumber.
- Repeat the previous step for the other direction of holes in the frame and the other frame.

- Secure a thermocouple to each intersection of strings in the frame making sure to install them in the proper thermocouple location. Push the thermocouples through the inner box and push each frame into its proper location, flush with the front of the inner box.

Sealing the Guard Box

- Cut out pieces to fit between the frame of the inner box and the polyisocyanurate walls of the outer box.
- Slide each piece in such that the outer box is completely sealed out. It should be difficult to slide the pieces in to ensure that there are minimal air gaps.
- Tape the seams to ensure that no air can leak through.

VITA

Name:	Claire Renee Mero
Address:	3433 Bay Breeze Dr. Seabrook, TX 77586
Email Address:	Claire_Bear_017@yahoo.com
Education:	M.S. Mechanical Engineering, Texas A&M University at College Station, 2012. B.S., Mechanical Engineering, Texas A&M University at College Station, 2010